Spatial Equilibrium, Search Frictions and Dynamic Efficiency in the Taxi Industry

Nicholas Buchholz *

May 12, 2021

Abstract

This paper analyzes the dynamic spatial equilibrium of taxicabs and shows how common taxi regulations lead to substantial inefficiencies as a result of search frictions and misallocation. To analyze the role of regulation on frictions and efficiency, I pose a dynamic model of spatial search and matching between taxis and passengers. Using a comprehensive dataset of New York City yellow medallion taxis, I use this model to compute the equilibrium spatial distribution of vacant taxis and estimate intraday demand given price and medallion regulations. My estimates show that the weekday New York market achieves about $5.7 million in daily welfare or about $27 per trip, but an additional 53 thousand customers fail to find cabs due to search frictions. Counterfactual analysis shows that implementing simple tariff pricing changes can enhance allocative efficiency and expand the market, offering daily consumer surplus gains of up to $227 thousand and up to 49 thousand additional daily taxi-passenger matches, a similar magnitude to the gain in matches generated by adopting a perfect static matching technology.

Key Words: dynamic games, spatial equilibrium, search frictions, dynamic pricing, regulation, taxi industry

JEL classification: C73; D83; L90; R12

*Department of Economics, Princeton University. Email: nbuchholz@princeton.edu. This is a revised version of my job market paper, previously circulated under the title *Spatial Equilibrium, Search Frictions and Efficient Regulation in the Taxi Industry*. Special thanks to Allan Collard-Wexler, Eugenio Miravete and Stephen Ryan. I also benefitted from discussions with Hassan Afrouzi, John Asker, Austin Bean, Lanier Benkard, Laura Doval, Neal Ghosh, Andrew Glover, Kate Ho, Jean-François Houde, Jakub Kastl, Ariel Pakes, Rob Shimer, Can Urgun, Nikhil Vellodi, Emily Weisburst, Daniel Xu, Haiqing Xu, anonymous referees and numerous seminar participants.

1 Introduction

It has been well documented that search frictions lead to less efficient outcomes.[1] One particularly salient reason for the existence of search frictions is that buyers and sellers are spatially distributed across a city or region so that meeting to trade requires costly transportation by one or both sides of the market. When locations are fixed, say between households and potential employers, search frictions arise from the added cost of travel associated with meeting. In some spatial settings, however, every trade involves a future re-allocation of buyers or sellers. This is a prominent feature of transportation markets, where every trade entails a vehicle moving from one place to another. When transportation and search intersect, dynamic externalities arise as each trip affects the search frictions faced by future buyers and sellers at each destination. In this paper I study the regulated taxicab industry in New York City, where a decentralized search process and a uniform tariff leads to distortions in the intra-daily equilibrium spatial patterns of supply and demand. I ask how much spatial misallocation is induced by search externalities in this setting and to what extent simple changes to pricing regulations can enhance allocative efficiency.

The taxicab industry is a critical component of the transportation infrastructure in large urban areas, generating about $23 billion in annual revenues. New York City has long been the largest taxicab market in the United States, accounting for about 25% of industry revenues in 2013. In New York and many other cities the taxi market is distinguished from other public transit options by a lack of centralized control; taxi drivers do not service established routes or coordinate search behavior. Instead, drivers search for passengers and, once matched, move them to destinations. Since different types of trips are demanded in different areas of the city, how taxi drivers search for passengers directly impacts the subsequent availability of service across the city. These movements of capacity give rise to equilibrium patterns that can leave some areas with little to no service while in other areas empty taxis will wait in long queues for passengers.

In this paper, I model taxi drivers' location choices in a dynamic spatial search framework in which vacant drivers choose where to locate given both the time-of-day pattern of trip demand as well as the distribution of rival taxi drivers throughout the day. While the spatial search process under current regulations often generates mis-allocation across locations, I also model frictions within each location to account for a block-by-block search process within small windows of time. I show that spatial frictions are largely attributable to inefficient pricing, as tariff-based prices fail to account for driver opportunity costs and the heterogeneity in consumer surplus that is not

[1] Since the pioneering work of Diamond (1981, 1982a,b), Mortensen (1982a,b) and Pissarides (1984, 1985), the search and matching literature has focused on the role of search frictions in impeding the efficient clearing of markets. The literature frequently examines settings where central or standardized exchange is not possible, including labor markets (e.g., Rogerson et al. (2005)), marriage markets (e.g., Mortensen (1988)), monetary exchange (e.g., Kiyotaki and Wright (1989, 1993)), and financial markets (e.g., Duffie et al. (2002, 2005)).

internalized by drivers. To empirically analyze this model, I use data from the New York City Taxi and Limousine Commission (TLC), which provides trip details including the time, location, and fare paid for all 27 million taxi rides in New York between August and September of 2012. Using TLC data together with a model of taxi search and matching, I estimate the spatial and intra-daily distribution of supply and demand in equilibrium. Importantly, the data only reveal matches made between taxis and customers as a consequence of search activity, but do not show underlying supply or demand; I therefore cannot observe the locations of vacant taxis or the number of customers who want a ride in different areas of the city. Because these objects are necessary for measuring search frictions and welfare in the market, I develop an estimation strategy using the dynamic spatial equilibrium model together with a local matching function. I show that the observed distribution of taxi-passenger matches is sufficient to solve for drivers' policy functions and compute the equilibrium distribution of vacant taxis without direct knowledge of demand. I then invert each local matching function to recover the implied distribution of customer demand up to an efficiency parameter. Finally I estimate matching efficiency using moments related to the variance of matches across days of the month.

I use this model to evaluate demand elasticities, welfare and search frictions in the New York taxi market. Baseline estimates of welfare indicate that the New York taxi industry generates $2.5 million in consumer surplus and $3.3 million in taxi driver variable profits during each 9-hour day-shift and across 211 thousand taxi-passenger matches, implying a combined surplus of about $27 per trip. Despite these surpluses, however, there are on average 53 thousand failed customer searches per day and 5,759 vacant drivers at any point in the day. To what extent can a more sophisticated pricing policy mitigate these costs by better allocating available supply to demand? By simulating market equilibrium over nearly one million potential pricing rules, I am able to solve for a dynamically optimal fare structure and show that a flexible tariff that changes with origin location can provide up to a 7.7% increase in consumer welfare and a 9% improvement in taxi utilization. Alternative policies offering flexible tariffs by location and distance yield slightly smaller benefits to consumers in favor of driver profits and higher utilization rates, but all of the counterfactual policies tested offer unambiguous benefits to both sides of the market even after accounting for search and matching frictions.

I contrast these results with two counterfactual technological improvements. The first simulates ride-sharing technology that offers locally frictionless matching. The second simulates an optimal dispatcher in offering socially efficient search incentives. I show that optimal pricing policies can produce nearly the same number of trips as the matching technology and more trips than the efficient search technology. Optimal prices deliver around 60% of the welfare gains from these technologies, suggesting that tariff-based pricing alone can offer gains that compete with high-tech innovations.

Related Literature

This paper integrates ideas from the search and matching literature with empirical industry dynamics. The key component is a model of dynamic spatial choices that adapts elements from Lagos (2000). Lagos (2000) studies endogenous search frictions using a stylized environment of taxi search and competition, showing how meeting probabilities adjust to clear the market and how misallocation can occur as an equilibrium outcome. Lagos (2003) uses the Lagos (2000) model to empirically analyze the effect of taxi fares and medallion counts on matching rates and medallion prices in Manhattan. I draw elements from the Lagos search model, but make several changes to reflect the real-world search and matching process. Specifically, I add non-stationary dynamics, a flexible and more granular spatial structure, stochastic and price-elastic demand, fuel costs, and heterogeneity in the matching process across different locations. Further, I build a tractable framework for the empirical analysis of dynamic spatial equilibrium by providing tools for estimating and identifying the model. I also model frictional market clearing within each local area via an aggregate matching function. Hall (1979) introduces the aggregate matching function concept, using the urn-ball specification adapted in this paper.[2] The Lagos (2000) framework has been applied more widely in recent work. Brancaccio et al. (2019, 2020a) study the estimation and identification of matching functions in spatial settings and apply a related search model to study endogenous trade costs in the bulk shipping industry. Brancaccio et al. (2020b) study efficiency properties of this model and Rosaia (2020) applies a similar framework to study economies of density in the New York ride-hail industry.[3]

I also draw on literature for estimating dynamic models in the tradition of Hopenhayn (1992) and Ericson and Pakes (1995), which characterize Markov-perfect equilibria in entry, exit, and investment choices given some uncertainty in the evolution of the states of firms and their competitors. Here, each taxi operates as a firm choosing where to search in a city. The state variable is the distribution of taxis across each area of the city, a measure of competition. To facilitate computation, I make a large-market assumption that both taxi drivers and customers are non-atomic. As in Hopenhayn (1992) this allows me to compute deterministic state transitions without the need to integrate over a high-dimensional space of states and future periods. The mass of customers in each location varies from day to day in each location and period. Drivers do not condition on these shocks, which I assume are not observed by individual drivers, but rather the expectation of consumer demand. The equilibrium is therefore similar to an Oblivious Equilibrium (Weintraub et al. (2008b)) in which drivers form their policies with respect to averages taken across many days

[2] Mortensen (1986), Mortensen and Pissarides (1999) and Rogerson et al. (2005) survey the labor-search literature and the implementation of aggregate matching functions.

[3] There is also a literature in empirical industrial organization which studies the allocative distortions induced by search frictions in different industries. This includes work on airline parts (Gavazza (2011) and mortgages (Allen et al. (2014)).

in the market. This notion is also similar to an Experience-Based Equilibrium (Fershtman and Pakes (2012)) in which firms' information set is restricted and agents condition their strategies on repeated experiences with market outcomes.[4]

A related study is Frechette et al. (2019), which models the dynamic entry game among taxi drivers to ask how customer waiting times and welfare are impacted by medallion regulations and dispatch technology. Similar to my paper, Frechette et al. (2019) study the effect of regulations on search frictions and welfare.[5] The key difference is that they focus on the labor supply decision rather than the spatial location decision. Though these research questions and approaches differ substantially, they lead to similar predictions when comparing similar counterfactuals..[6]

Finally, there is a recent literature on the benefits of dynamic pricing for ride-hail services (Hall et al. (2015), Castillo et al. (2017), Castillo (2020)). This paper also highlights the impact of pricing on efficiency, but with two distinct differences. First, I focus on posted tariffs instead of real-time price adjustment. Posted tariffs are a feature of *both* traditional taxis and ride-hail services that affect the search behavior of taxi drivers. Second, I explicitly model the influence of prices on the dynamic path of supply and demand. I use this model to show how posted prices can be used to induce dynamically efficient allocations of supply and demand.

This paper contributes in several ways to the study of the taxi industry and more generally to the methodology of empirical spatial equilibrium models. This is the first empirical analysis of pricing in a taxi market and the first to study how price regulations impact the equilibrium spatial allocation of vacant taxis, profits, consumer welfare, trips and utilization. It also contributes by offering novel evidence for the quantitative impact of frictions in a spatial search market, revealing important sources of value added by modern ride-hail technology. Methodologically, I contribute a framework for estimating supply and demand in a dynamic spatial search model when only matches are observed and where prices are centrally set. This approach may be usefully applied to other transportation markets like ride-hail, global freight and logistics, and private bus and trucking markets. I also demonstrate that the behavioral and information assumptions proposed by Weintraub et al. (2008b) and Fershtman and Pakes (2012) can be leveraged to make such an

[4]This approach also relates to auction models with many bidders (Hong and Shum (2010)) and as an empirical exercise in studying non-stationary firm dynamics (Weintraub et al. (2008a), Melitz and James (2007)).

[5]A diverse literature addresses whether taxi regulation is necessary at all. Both the theoretical and empirical findings offer mixed evidence. Studies point to regulation's ability to reduce transaction costs (Gallick and Sisk (1987)), prevent localized monopolies (Cairns and Liston-Heyes (1996)), correct for negative externalities (Schrieber (1975)), and establish efficient quantities of vacant cabs (Flath (2006)). Other authors assert that regulations restricted quantities and led to higher prices (Winston and Shirley (1998)) and that low sunk- and fixed-costs in this industry are sufficient to support competition (Häckner and Nyberg (1995)).

[6]There is an additional body of literature on taxi drivers' labor supply choices, including Camerer et al. (1997), Farber (2005, 2008), Crawford and Meng (2011), and Thakral and Tô (2017). These studies investigate the labor-leisure tradeoff for drivers. They ask how taxi drivers' labor supply is determined and to what extent it is driven by daily wage targets and other factors. Buchholz et al. (2017) estimate a dynamic labor supply model of taxi drivers to show that behavior consistent with dynamic optimization may appear as a behavioral bias in a static setting.

estimation tractable in a large-scale strategic setting.

In Section 2 I detail taxi industry characteristics relating to search, regulation, and spatial sorting, as well as a description of the data. In Section 3 I present a dynamic model of taxi search, matching and equilibrium. Section 4 outlines my empirical strategy for computing equilibrium and estimating model parameters. I present estimation results in Section 5 and an analysis of counterfactual pricing policies in Section 6. Section 7 concludes.

2 Market Overview and Data

2.1 Regulatory Environment

As with nearly all major urban taxi markets, the New York taxi industry is highly regulated. Two regulations imposed by the New York Taxi and Limousine Commission (TLC) directly impact market function and efficiency. The first is a tariff-based fare pricing structure. Taxi fares are based on a one-time flag-drop fee and a distance-based fee, plus additional fees for idling time, surcharges, taxes and tolls. Except for separate fares for some airport trips, this fare structure does not depend on location, and except for an evening surcharge to the flag-drop fare, the base fare structure is fixed over the day. The second type of regulation is entry restrictions imposed via a limit on the number of legal taxis that can operate. This is implemented by requiring drivers to hold a "medallion" or permit, the supply of which is capped (Schaller (2007)).[7] Medallion cabs can only be hailed from the street and are not authorized to conduct pre-arranged pick-ups, a service exclusively granted to separately licensed livery cars.

In recent years, several ride-hail firms including Uber and Lyft have entered the taxi industry including the New York market. These firms operate mobile platforms to match customers with cabs, greatly reducing frictions associated with taxi search and availability. The precipitous expansion and popularity of ride-hail suggests there are large benefits associated with both the reduced search costs and more flexible pricing technologies compared with traditional taxi markets. My paper aims to understand how price regulation and matching technology impact the equilibrium spatial allocations of supply and demand as well as the corresponding impact on market welfare and efficiency.[8]

[7] These licenses are tradable, and the fact that they tend to have positive value, sometimes in excess of one million dollars, implies that this quantity cap is binding and below the quantity that would be supplied in an unrestricted equilibrium.

[8] The spatial availability of taxis is of evident concern to municipal regulators around the country: a number of cities have introduced policies to control the spatial dimension of service. For example, in the wake of criticism over the availability of taxis in certain areas, New York City issued licenses for 6,000 additional medallion taxis in 2013 with special restrictions on the spatial areas they may service (See, e.g., cityroom.blogs.nytimes.com/2013/11/14/new-york-today-cabs-of-a-different-color/). Specifically, these green-painted "Boro Taxis" are only permitted to pick up passengers in the boroughs outside of Manhattan.[9] Though the city's traditional yellow taxis have always been able to

2.2 Data

In 2009, the New York TLC initiated the Taxi Passenger Enhancement Project, which mandated the use of upgraded metering and information technology in all New York medallion cabs. The technology includes the automated data collection of taxi trip and fare information. I use TLC trip data from all New York City medallion cab rides given from August 1, 2012 to September 30, 2012. An observation consists of information related to a single cab ride. Data include the exact time, date and GPS coordinates of pickup and drop-off, trip distance, and trip time length for approximately 27 million rides.[10] New York cabs typically operate in two separate shifts of 9-12 hours each, with a mandatory shift change between 4–5pm. I focus on the weekday, day-shift period of 7am until 4pm and I assume all drivers stop working at 4pm.

Due to New York rules governing pre-arranged trips, the TLC data only record rides originating from street-hails. This provides an ideal setting for analyzing taxi search behavior since all observed rides are obtained through search. Table 1 provides summary facts for this data set. I provide additional monthly-level statistics in Appendix A.3.

Most of the time, New York taxis operate in Manhattan. When not providing rides within Manhattan, the most common origins and destinations are New York's two city airports, LaGuardia (LGA) and John F. Kennedy (JFK). At the airports taxis form queues and wait in line for next available passengers. Table 2 provides statistics related to the frequency and revenue share of trips between Manhattan, the two city airports, and elsewhere.

Uber began operating in New York City in 2011, but service was minimal. In an October 2012 interview, the CEO reported that 160 drivers had provided trips in the city since the company's entry into New York.[11] This represents about 1% of licensed yellow cab drivers, and likely much less in trip volume as these drivers were not necessarily operating consistently throughout the prior year.

2.3 September 2012 Fare Hike

On September 4, 2012, the TLC increased tariffs from \$2.50 plus \$2.00/mile, to \$2.50 plus \$2.50/mile. The flat rate fare charged for rides between JFK and Manhattan also increased from \$45 to \$52. Average fares increased by about 17%. Although this change provides critical price variation that

operate in these areas, it's apparent that service was scarce enough relative to demand that city regulators intervened by creating the Boro Taxi service. This intervention highlights the potential discord between regulated prices and the location choices made by taxi drivers.

[10] Using this information together with geocoded coordinates, we might learn for example that cab medallion 1602 (a sample cab medallion, as the TLC data are anonymized) picks up a passenger at the corner of Bowery and Canal at 2:17pm of August 3rd, 2012, and then drives that passenger for 2.9 miles and drops her off at Park Ave and W. 42nd St. at 2:39pm, with a fare of \$9.63, flat tax of \$0.50, and no time-of-day surcharge or tolls, for a total cost of \$10.13. Cab 1602 does not show up again in the data until his next passenger is contacted.

[11] Source: `https://www.cnet.com/news/uber-quietly-puts-an-end-to-nyc-taxi-service/`.

Table 1: Taxi Trip and Fare Summary Statistics

Sample	Rate Type	Variable	Obs.	10%ile	Mean	90%ile	S.D.
All Data	Standard Fares	Total Fare ($)	27,475,749	4.90	10.57	19.00	6.95
		Dist. Fare ($)	27,475,749	1.36	5.59	12.00	6.14
		Flag Fare ($)	27,475,749	2.50	2.83	3.50	0.36
		Distance (mi.)	27,475,749	0.82	2.70	6.00	2.74
		Trip Time (min.)	27,475,749	4.00	12.04	22.52	8.23
	JFK Fares	Total Fare ($)	491,689	45	48.32	52	3.58
		Distance (mi.)	491,689	3.02	16.25	20.58	5.95
		Trip Time (min.)	491,689	22.75	39.49	60.00	17.33
Weekdays, Day-Shift, Manhattan & Boro.	Standard Fares	Total Fare ($)	8,122,515	4.50	10.16	17.70	6.39
		Dist. Fare ($)	8,122,515	1.12	4.65	9.60	5.33
		Flag Fare ($)	8,122,515	2.50	2.5	2.5	0
		Distance (mi.)	8,122,515	0.71	2.28	4.66	2.36
		Trip Time (min.)	8,122,515	4.00	12.74	23.8	8.49
	JFK Fares	Total Fare ($)	163,737	45.00	48.30	52.00	3.60
		Distance (mi.)	163,737	6.00	16.41	20.95	5.77
		Trip Time (min.)	163,737	28.00	46.35	67.22	18.40

Taxi trip and fare data come from the New York Taxi and Limousine Commission (TLC). This table provides statistics related to individual taxi trips taken in New York City between August 1, 2012 and September 30, 2012 for two fare types. The first is the standard metered fare (TLC rate code 1), in which standard fares apply, representing 98.1% of the data. The second is a trip to or from JFK airport (TLC rate code 2). Total Fare and Distance are reported for each trip. The two main fare components are a distance-based fare and a flag-drop fare. I predict these constituent parts of total fare using the prevailing fare structure and trip distance. Flag fare calculations include time-of-day surcharges. The remaining fare is due to a fee for idling time plus a $0.50 per-trip tax. The first set of statistics corresponds to the full sample of all New York taxis rides across the two months. The second set concerns the smaller sample used in my analysis: weekday day-shift trips occurring within the regions in Figure 1.

Table 2: Taxi Trips and Revenues by Area

Time	Place	Obs.	Mean Fare	Trip Share	Rev. Share
All Times	Intra-Manhattan Trips	24,704,475	$9.24	90%	75%
	Airport Trips	1,320,091	$34.72	5%	15%
	Other Trips	1,478,992	$21.01	5%	10%
Weekdays, Day-shift	Intra-Manhattan Trips	7,773,214	$9.29	91%	76%
	Airport Trips	497,445	$34.92	6%	18%
	Other Trips	258,198	$20.94	3%	6%

This table provides statistics related to the locations of taxi trips taken in New York City between August 1, 2012 and September 30, 2012. Intra-Manhattan trips begin and end within Manhattan, Airport Trips are trips with either an origin or destination at either LaGuardia or JFK airport. Other Trips captures all other origins and destinations within New York City. Statistics are reported for all times as well as for the day-shift period of a weekday.

I use together with an equilibrium model to identify demand elasticities, a closely related pattern can be directly observed in the number of trips taken. Table 3 separates trips into four distance

categories, and for each shows the post-fare-hike changes in daily trips and average fares for both the morning and afternoon hours. Consistent with the increased distance tariff, fares on longer trips generally increased more than shorter trips.[12] Due to search and matching frictions, trips are not necessarily equivalent to passenger demand. However these patterns do suggest that demand was impacted differentially across trip lengths, and moreover that the impact was not proportional to the price change alone. In Appendix A.4 I show an alternative spatial decomposition of the effects in order to show how the fare hike impacted the average fares and trips across spatial regions of the city.

Table 3: Effect of the September 2012 Fare Hike

Description	**Trip Type**				
	0-2 mi.	*2-4 mi.*	*4-6 mi.*	*>6 mi.*	*Airport Trips*
Mornings: 7:00am-12:00pm					
Change in log fares	0.162	0.208	0.215	0.198	0.124
Change in log trips	−0.039	−0.107	−0.164	−0.163	−0.141
Afternoons: 12:00pm-4:00pm					
Change in log fares	0.162	0.205	0.211	0.194	0.124
Change in log trips	−0.122	−0.163	−0.223	−0.220	−0.111

This table shows the mean change in log fares and log number of trips following the September 4, 2012 fare hike. Fare calculation includes base fares, taxes, surcharges and imputed tips.

2.4 Discretizing time and space

To analyze the spatial and inter-temporal distributions of supply and demand, I discretize time and space across the weekday, day-shift hours in this market. Time is divided into five minutes periods. I divide space into 39 distinct areas that are linked to observed GPS points of origin and destination for each taxi trip. These locations represent 98% of all taxi ride originations, and I depict them in Figure 1. The average observed travel time from one location to a neighboring location is 2 minutes, 45 seconds, or about one-half of a five-minute period. This suggests that the 5-minute period is reasonably well-suited to this geographic partitioning. For additional details on location selection and construction see Appendix A.2.

I further denote five *regions* as disjoint subsets of all 39 locations. I depict regions as shaded sections of Figure 1. Each region is characterized by a unique mix of geographical features and transit infrastructure. I will estimate the efficiency of search for each of these five regions. Region

[12] Trips over six miles are much more likely to include bridge or tunnel surcharges so the average fare increase in this category is slightly lower. The number of trips also declined more on longer routes.

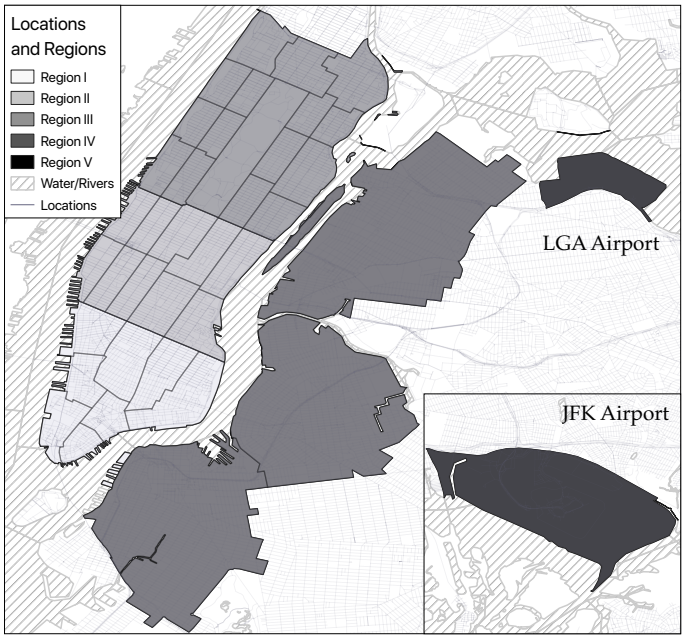

Figure 1: 39-Location Map of New York City

Each of the outlined sections of Manhattan is one of the 39 locations indexed by i in my model. Locations are formed by aggregating census-tracts. Each shaded section depicts a region r, indicated with Roman numerals I–V. Regions are characterized by similarities in transit infrastructure, road layouts, and zoning.

I is Lower Manhattan, an older part of the city where streets follow irregular patterns, and where numerous bridges, tunnels and ferries connect to nearby boroughs and New Jersey. Region II is Midtown Manhattan, with fewer traffic connections away from the island, but denser centers of activity including the major transit hubs Penn Station and Grand Central Station. Region III is Uptown Manhattan, where streets follow a regular grid pattern, but are longer and more spread out. Few bridges, tunnels or stations offer direct connections to other boroughs. Region IV is the large area encompassing Brooklyn and Queens. Region V consists of the two airports, John F. Kennedy (JFK) and LaGuardia (LGA).

2.5 Evidence of Frictions

Search frictions occur when drivers cannot locate passengers even though supply and demand coexist at the same point in time. Frictions in this market manifest as waiting time experienced by drivers looking for a passenger. The TLC data provide evidence of search frictions for drivers that vary across space and time of day. Using driver ID together with the time of pick-up and drop-off, I compute the waiting time between trips. The mean waiting time for different trips is displayed in Figure 2. Panel (a) shows the probability that a driver will find a passenger in each five-minute

period, as well as the expected waiting time to find a passenger in 10-minute units (i.e., a value of 0.5 equals 5 minutes). There is substantial intra-day variation in search times, with the best times of day for finding passengers around 9am to 4pm, with average wait times around six minutes and five-minute finding rates around 50%. The worst times are in early morning and mid-day, when average wait times are nearly 10 minutes and finding rates fall as low as 25%. Panel (b) shows the same driver match probabilities and waiting times by the 37 non-airport locations, taken as an average from 7am-4pm across all weekdays of the month. Again there is heterogeneity across space, with relatively higher match probabilities and lower waiting times in Lower Manhattan (1–8) and Midtown (9–18), declining match probabilities in upper Manhattan (19–34), and even lower match probabilities in Brooklyn (35–37).[13] In aggregate, drivers spend about 47% of their time vacant during the sample period of weekdays during the day-shift. This suggests that among 11,500 active drivers, an average of 5,405 are vacant at any time.[14]

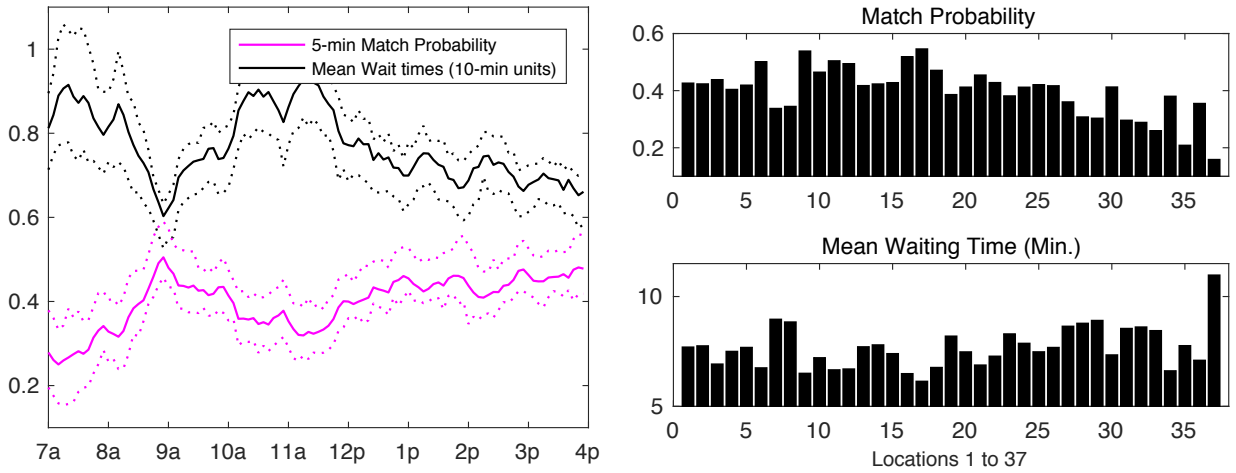

Figure 2: Taxi wait times and match probabilities by time-of-day and location

TLC Data from August 2012, Monday–Friday from 7am until 4pm, within regions indicated on Figure 1. Left Panel: Each series shows taxi drivers' five-minute probability of finding a customer and mean waiting times, averaged across all drivers and all weekdays. Dotted lines depict 25th and 75th percentiles. Right Panel: Each bar shows driver waiting times and matching probabilities by location of drivers' last drop-off. Manhattan locations follow a roughly South-to-North trajectory from index 1–34. Brooklyn locations are indexed 35–36. Queens is location 37.

[13]There is additional evidence that drivers often relocate to find passengers: 61.3% of trips begin in a *different* neighborhood from the neighborhood where drivers last dropped off a passenger. This suggests that there are spatial search frictions for drivers, as finding a customer requires relocation.

[14]The data do not reveal the frictions faced by customers; it is impossible to tell how long a customer has been waiting before pick-up, and it is similarly not possible to tell if a customer arrived to search for a taxi and gave up.

3 Model

A city is a network of L nodes called "locations", connected by a set of routes. A location can be thought of as a spatial area within the city.[15] Time within a day is divided into discrete intervals with a finite horizon, where $t \in \{1, ..., T\}$. At time $t = 1$ the work day begins; at $t = T$ it ends. Model agents are vacant taxi drivers who search for customers within a location $i \in \{1, ..., L\}$. When taxis find passengers, they drive them from origin location i to a destination location $j \in \{1, ..., L\}$. Denote $v_i^t \in \mathbb{R}$ as a measure of vacant taxis and denote $u_i^t \in \mathbb{R}$ as a measure of customers looking for a taxi in each location at each time. The total number of taxis in the city is given by $\sum_i v_i^t = \bar{v}$ for all t. The distance between each location is given by δ_{ij} and the travel time between each location is given by τ_{ij}.

The model has four basic ingredients. First, there is a demand system that describes, for every neighborhood pair ij, how many customers will arrive to the market to search for a taxi as a function of the price of service along that route. Second, there is a payoff vector associated with every route that taxis service. Payoffs include the revenues from each ride minus a service cost due to fuel expenses. Third, there is a model of period-by-period market clearing. Here I use an aggregate matching function to map supply and demand into match probabilities, which adjust payoffs depending on the relative quantities of taxis and customers.[16] Finally, I combine these components in a dynamic model of location choice. In this model vacant drivers make period-by-period location choices accounting for the expected match probabilities and payoffs associated with future locations. These four ingredients are presented in more detail below.

3.1 Demand

In each location i at time t, the measure of customers that wish to move to a new location, u_i^t, is drawn from a Poisson distribution with parameter λ_i^t. Moreover, λ_i^t is a sum of independent Poisson random variables with $\lambda_i^t = \sum_j \lambda_{ij}^t(\pi_{ij}^t)$, where $\lambda_{ij}^t(\pi_{ij}^t)$ represents the destination-j-specific Poisson arrival of customers in location i at time t. The independence of λ_{ij}^t across destinations j entails that there are no aggregate shocks in origin location i. Thus the daily draw of demand for route ij are uncorrelated with that day's demand draw for route ik.[17] The parameters λ_{ij}^t are functions of the price of a taxi ride between i and j, π_{ij}^t. Denote the probability that a customer in i wants to

[15] e.g., a series of blocks bounded by busy thoroughfares, different neighborhoods, etc.

[16] Note that in a setting of ride-hail, in which prices adjust to neighborhood market conditions, we might instead recast this model as one of localized price formation instead of search frictions.

[17] In my application, the average location size is over 0.5 square miles and thus large enough to rationalize such an assumption as they span much more area than any one property. The data do not span major holidays or athletic events and there was no major weather event that would shut down traffic in large areas. Smaller-scaled shocks, say due to demand at a specific property or event, are too granular to model separately given data and computational constraints.

travel to location $j \in \{1, ..., L\}$ at time t by M_{ij}^t, so that $\lambda_{ij}^t(\pi_{ij}^t) = M_{ij}^t \cdot \lambda_i^t(\boldsymbol{\pi})$, where $\boldsymbol{\pi}$ is a vector of prices between all locations.

I assume that taxi drivers face a constant-elasticity demand curve. Demand depends on the origin and destination of the trip, its price, and the time of day, and whether the trip involves an airport (a binary index denoted by ι). Each of these factors shifts demand according to parameters $\beta_{0,i,t,s,\iota}$. Price elasticities, given by parameter $\beta_{1,s,\iota}$ are assumed to vary according to the distance of the trip, indexed by discrete categories s, and airport status ι. Taxi demand is therefore given by the following:

$$ln(\lambda_{ij}^t(\pi_{ij}^t)) = \beta_{0,i,t,s,\iota} + \beta_{1,s,\iota} ln(\pi_{ij}^t) + \eta_{i,t,s,\iota}. \tag{1}$$

In addition, I assume that customers demand taxi services for one period. After this period, consumers use a different method of transit.[18]

Waiting Time I do not observe customer waiting time, but it may be an important determinant of demand for taxi rides.[19] To identify the price elasticity of demand in this specific exercise, I provide evidence that the September price change had a negligible effect on waiting times. There are two primary reasons for this. First, since the estimation of demand parameters λ_{ij}^t does not require knowledge of waiting time or price elasticities, I compute a measure of waiting time using customer match probabilities.[20] I find that the price change lead to an estimated average waiting time change of approximately 21 seconds. Further, the limited empirical evidence for waiting time elasticities suggests that it should be relatively small. Frechette et al. (2019) estimate waiting time elasticity of demand to be about -1.2, while Buchholz et al. (2020) estimate average waiting time elasticity in a large European taxi market to be -0.7. In counterfactuals, however, I study changes to pricing policies that may be large enough to meaningfully impact waiting times. Therefore in all counterfactuals I implement a waiting time elasticity calibrated to -1.0 and allow demand to adjust accordingly.

3.2 Revenue and Costs

Taxis earn revenue from giving rides. At the end of each ride, the taxi driver is paid according to the fare structure. The fare structure is defined as follows: b is the one-time flag-drop fare and π is

[18] In the empirical analysis to follow, I define one period as five minutes.

[19] Many recent studies estimate the value of time in different contexts. See, e.g., Small (2012), Buchholz et al. (2020), Kreindler (2020), and Castillo (2020).

[20] This estimate is premised on the assumption that consumer search takes at most five minutes, after which consumers exit the market. Consumers find a match with probability $q_i^t = m_i^t/\lambda_i^t$ where m_{ij}^t is the observed matches in each i, t cell. I then compute a measure of expected waiting time (in units of minutes) as $5 \cdot (1 - q_i^t)$ assuming any matches are made instantaneously.

the distance-based fare, with the distance δ_{ij} between locations i and j. There is also an additional fee based on waiting time and idling time in traffic, given by $b^t_{2,ij}$ The total fare revenue earned by providing a ride from i to j is $\pi^t_{ij} = b_0 + b_1\delta_{ij} + b^t_{2,ij}$. Note that π^t_{ij} is also the customer price of a trip along route i to j at t.

Drivers have two sources of costs. First, there are fixed costs to a driver for being able to operate a taxi. This cost includes a daily or weekly lease fee for a taxi and medallion license, or alternatively, any financing costs for drivers who own tai and medallion. The opportunity costs of drivers can also be regarded as a part of the fixed cost. The second source of cost is fuel expenses. Denoting per-mile fuel costs as c, the route-specific fuel costs are given by $c_{ij} = c \cdot \delta_{ij}$.

My analysis holds fixed the entry decisions of taxis, so I do not model fixed costs and instead focus on drivers' optimization while working. On any particular day a driver is working, medallion leasing fees and other fixed costs for that day are sunk and therefore independent of the driver's search choices.

The net revenue of any passenger ride is given by

$$\Pi^t_{ij} = \pi^t_{ij} - c_{ij}. \tag{2}$$

This profit function sums the total fare revenue earned net of fuel costs in providing a trip from location i to j at time t.

3.3 Searching and Matching

At the start of each period, taxis search for passengers. The number of taxis in each location at the start of the period is given by the sum of *previously vacant* taxis who have chosen location i to search, plus the *previously employed* taxis who have dropped off a passenger in location i. This sum is denoted as v^t_i. I make the following assumptions about matching: (1) matches can only occur among cabs and customers within the same location, (2) matches are randomly assigned between taxis and customers, and (3) once a driver finds a customer, a match is made and the driver cannot refuse a ride.[21] The expected number of matches made in location i and time t is given by an aggregate matching function $m(\lambda^t_i, v^t_i)$. The ex-ante probability that a driver will find a customer is then given by $p(\lambda^t_i, v^t_i) = \frac{m(\lambda^t_i, v^t_i)}{v^t_i}$. Figure 3 illustrates the within-period search and matching process.

3.3.1 A Model of Neighborhood Search

There are two types of locations, *neighborhoods* and *airports*. Neighborhoods comprise most of a city; they are locations in which cabs drive around to search for passengers. Below I detail how

[21] In New York, the TLC prohibits refusals, c.f. `www.nyc.gov/html/tlc/html/rules/rules.shtml`.

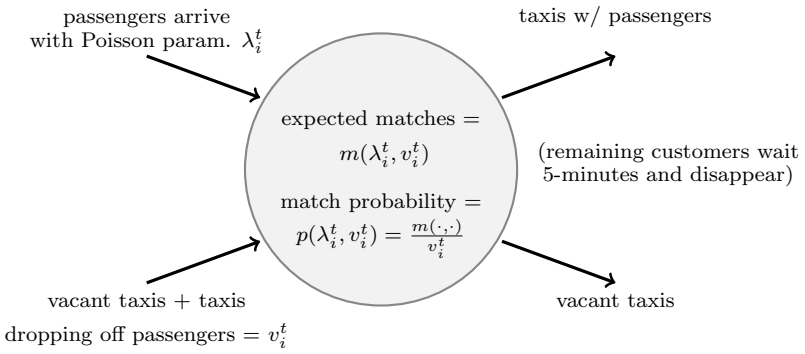

Figure 3: Flow of demand, matches, and vacancies within a location

This illustration depicts the sources of taxi arrivals and departures in location i at time t. At the beginning of a period, all taxis conducting search in location i have either dropped off passengers or were searching from previous periods. In expectation (given randomness in the mass of customers arriving each day), matches are determined by $m(\lambda_i^t, v_i^t)$. At the end of the period, any employed taxis leave for various destinations and vacant taxis continue searching.

matches are formed in neighborhoods. The next subsection discusses airports.

When model locations are specified as spatial areas such as a neighborhood, search within this area will exhibit search frictions even when block-by-block search is nearly frictionless. This design echoes the setup of Lagos (2000) that allows search frictions to arise endogenously from driver behavior. To model search frictions within each location while allowing for the possibility that frictions are not the same in each location, I use the following aggregate matching function.[22]

$$m(\lambda_i^t, v_i^t, \alpha_r) = v_i^t \cdot \left(1 - e^{-\frac{\lambda_i^t}{\alpha_r v_i^t}}\right) \tag{3}$$

Equation 3 is a reduced-form model of intra-location matching. It can flexibly reproduce frictions (i.e. such that $m(\lambda_i^t, v_i^t, \alpha_r) < \min(\lambda_i^t, v_i^t)$), the extent of which are controlled by the search efficiency parameter $\alpha_r > 0$. All else equal, larger values of α_r generate fewer matches. $r = r(i)$ denotes a *region*, or a subset of locations as described in Section 2.4. α_r is region-specific as it reflects the difficulty of search within a region, such as the complexity of the street grid. These are physical characteristics of a region which are assumed to be fixed across the day. I illustrate the aggregate matching function and the role of α_r in Figure 4.

Moreover, this equation is specified in terms of expected demand λ_i^t and not the daily draws u_i^t. It represents the *expected* number of matches produced given demand parameter λ_i^t and vacant taxi

[22]This function is derived from an urn-ball matching problem first formulated in Butters (1977) and Hall (1979). While the original model characterizes matches from discrete (i.e., integer) inputs, my specification characterizes urn-ball matching with a large number (or continuum) of inputs. See, e.g., Petrongolo and Pissarides (2001) and the derivation in Appendix A.9.

supply v_i^t. This is the relevant object from the perspective of taxi drivers' location optimization problem. Hereafter I denote $m_r(\lambda_i^t, v_i^t) = m(\lambda_i^t, v_i^t, \alpha_r)$ to be the location-specific matching function. I adopt the convention that $m_r(\cdot, \cdot)$ refers to the matching function while the scalar m_i^t is a measure of matches that occur in a location i and period t. The probability of a match from a taxi driver's perspective is therefore given by

$$p_r(\lambda_i^t, v_i^t) = \frac{m_r(\lambda_i^t, v_i^t)}{v_i^t} = \left(1 - e^{-\frac{\lambda_i^t}{\alpha_r v_i^t}}\right). \tag{4}$$

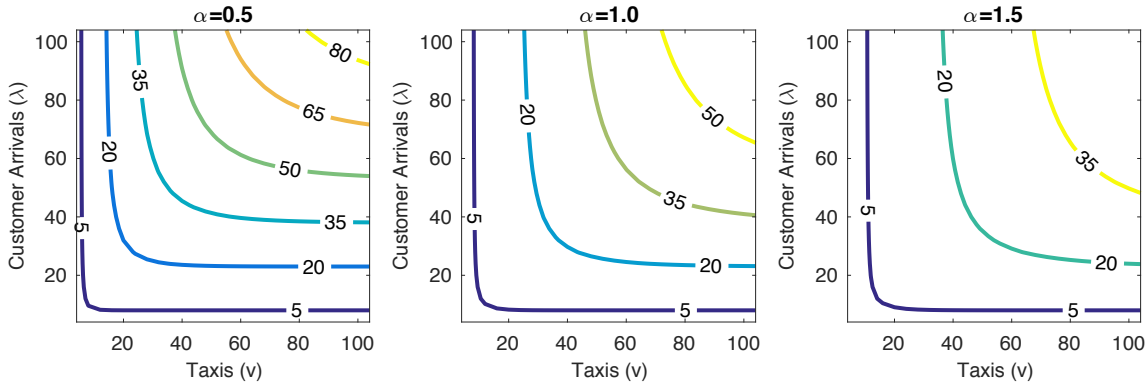

Figure 4: Matching Efficiency and α

This figure shows contour plots of the matching function over three values of α. Contour levels depict the expected number of matches produced in a given location when the level of taxis is v and the expected arrivals of customers is λ, for each level of α.

3.3.2 Airport Queueing

At airports, taxis pull into one of multiple queues and wait for passengers to match with cabs at the front of the queue.[23] Queues may also form on the customer side, for example following a large arrival flight. I interpret demand in the queues as the volume of customers who are granted access to leave the customer queue and enter a taxi, as opposed to the length of the customer queue itself. This interpretation allows for abstracting away from unobserved customer queue lengths and other unobservable factors like traffic congestion which may limit the full queue from clearing in every period even when there are many taxis available. I discuss the implications of this assumption further in Section 4.2. Taxis will therefore face some expectation of waiting time in order for the queue to clear as a function of the length of the taxi queue, which I denote as w_i^t.

[23] In my sample roughly 6% of all taxi trips and 16% of revenues involve one of the two major New York airports. It is important to model airport queueing separately from traditional forms of search because queues reduce the available stock of searching taxis, an important quantity of interest in this study.

3.4 Dynamic Model of Taxi Drivers' Locations, Actions and Payoffs

A taxi driver's behavior depends on his own location, whether he is employed or not at the end of the period, and the market state, $\mathcal{S}^t$. Let e_{ij}^k denote the set of employed taxis in location i who matched in period $k < t$ with a trip to j. The market state $\mathcal{S}^t$ at time t is a measure of vacant taxis v_i^t in each location i and a measure of employed taxis e_{ij}^k that are in-transit between locations.[24] Thus the market state at time t is summarized by

$$\mathcal{S}^t = \{\underbrace{\{v_i^t\}_{i\in\{1,...,L\}}}_{\text{vacant cabs}}, \underbrace{\{e_{ij}^k\}_{i,j\in\{1,...,L\}^2,k<t}}_{\text{hired cabs in-transit}}\}. \tag{5}$$

Denote $\mathcal{S} = \{\mathcal{S}^t\}$ for $t \in \{1, ..., T\}$ so that $\mathcal{S}$ reflects the entire spatial and inter-temporal distribution of vacant and employed taxis. At the beginning of each period, taxi drivers hold beliefs about the current-period state and how it will evolve going forward. Given these beliefs, they assign value V_i^t to each i, t-pair.

I define the drivers' ex-ante (i.e., before observing any shocks and before any uncertainty in passenger arrivals is resolved) value as

$$V_i^t(\mathcal{S}^t) = \mathbb{E}_{\mathcal{S}|\mathcal{S}^1}\Bigg[p_r(\lambda_i^t, v_i^t)\overbrace{\Bigg(\sum_j M_{ij}^t \cdot (\Pi_{ij}^t + V_j^{t+\tau_{ij}}(\mathcal{S}^{t+\tau_{ij}}))\Bigg)}^{\text{Exp. Value of Fare}} + \\ (1 - p_r(\lambda_i^t, v_i^t)) \cdot \underbrace{\mathbb{E}_{\varepsilon_{j,a}}\left[\max_{j\in A(i)}\left\{V_j^{t+\tau_{ij}}(\mathcal{S}^{t+\tau_{ij}}) - c_{ij} + \varepsilon_{j,a}\right\}\right]}_{\text{Exp. Value of Vacancy}}\Bigg]. \tag{6}$$

This expression has two components. Drivers in location i at time t expect to contact a passenger with probability $p_r(\lambda_i^t, v_i^t)$. Drivers' payoff for providing a trip is equal to the net profit of a trip Π_{ij}^t plus continuation values $V_j^{t+\tau_{ij}}$ of being in location j after τ_{ij} periods have elapsed. Therefore the expected value of a trip is simply the value of a trip to each location j weighted by the probability that a passenger picked-up in i chooses j as the destination, which is given by M_{ij}^t.[25]

At the end of the period, any cabs that remain vacant can choose to relocate or stay put to begin a search for passengers in the next period. The set $A(i)$ reflects the set of locations available to vacant taxis and is limited to all *adjacent* locations in the city, where adjacency is defined as

[24] At any moment, employed taxis are not directly competing with vacant taxis for passengers. Accounting for the distribution of employed taxis is an important component of the state variable because the eventual arrival of employed taxis and subsequent transition to vacancy is payoff-relevant when deciding how to conduct future search.

[25] Note that M_{ij}^t has superscript t because passenger preferences change throughout the day.

locations that can be reached in one period, where $\tau_{ij} = 1$. In addition, all trips to and from airports are included in each choice set. In these cases, $\tau_{ij} > 1$.[26]

Vacant drivers choose to search next period in the location that maximizes total expected payoff as the sum of continuation values $V_j^{t+\tau_{ij}}(\mathcal{S})$, fuel costs c_{ij} and a contemporaneous, idiosyncratic shock ε_{ja}^t. ε_{ja}^t is a driver a-specific i.i.d. shock to the perceived value of search in each alternative location j, which I assume to be drawn from a Type-I extreme value distribution. This shock accounts for unobservable reasons that individual drivers may assign a slightly greater value to one location than another. For example, traffic conditions and a taxi's direction of travel may make it inconvenient to search anywhere but further along the road in the same direction.[27]

Vacant drivers in location i move to location j^* by solving the last term in equation 6:

$$j^* = \arg\max_j \{V_j^{t+\tau_{ij}}(\mathcal{S}^{t+\tau_{ij}}) - c_{ij} + \varepsilon_{ja}\}. \tag{7}$$

To compute the drivers' strategies, I define the ex-ante choice-specific value function as $W_i^t(j_a, \mathcal{S}^t)$, which represents the net present value of payoffs conditional on taking action j_a while in location i, before ε_{ja} is observed:

$$W_i^t(j_a, \mathcal{S}^t) = \mathbb{E}_{S^{t+\tau_{ij_a}}}\left[V_{j_a}^{t+\tau_{ij_a}}(\mathcal{S}^{t+\tau_{ij_a}}) - c_{ij_a}\right]. \tag{8}$$

Defining W_i^t allows for an expression of taxi drivers' conditional choice probabilities: the probability that a driver in i will choose $j \in A(i)$ conditional on reaching state $\mathcal{S}^t$, but before observing ε_{ja}, is given by

$$P_i^t[j_a|S^t] = \frac{\exp(W_i^t(j_a, \mathcal{S}^t)/\sigma_\varepsilon)}{\sum_{k\in A(i)} \exp(W_i^t(j_k, \mathcal{S}^t)/\sigma_\varepsilon)}. \tag{9}$$

This expression defines aggregate policy functions $\sigma_i^t = \{P_i^t[j|\mathcal{S}^t]\}_{j\in\{1,\ldots,L\}}$ as the probability of optimal transition from an origin i to all destinations j conditional on future-period continuation values.

Time ends at period T. Continuation values beyond $t = T$ are set to zero: $V_i^t = 0\ \forall t > T, \forall i$. Employed taxi drivers with arrival times beyond period T are assumed to finish en-route trips before quitting.

[26] I assume A(i) is known to drivers. By examining hourly trip time distributions between all pairs of locations, I find that unobserved road blockages between locations, in which minimum travel times on a route increase above the overall mean for that route, occur in less than 1% of all route-hours. This suggests that A(i) is relatively stable over time.

[27] The terms ε_{ja} also ensure that vacant taxis leaving one location will mix among several alternative locations rather than moving to the same location, a feature broadly corroborated by data.

3.5 Intraday timing

There is an exogenous initial distribution of vacant taxis denoted $\mathcal{S}^1$. It is known to all drivers and constant across each weekday. This distribution accounts for the early morning positions of taxis as they leave from garages and arrive to the search regions of the city. Vacant taxis conduct search at the start of each period t. At the end of a period any newly employed taxis disappear from the stock of vacant cabs, transit customers to their destinations, and earn revenue. Vacant taxis earn no revenues but earn the option value associated with each possible move. In the next period, the locations of all vacant taxis are updated based on movement from both employed taxis dropping off passengers and previously vacant taxis' who arrive to new locations.

I assume drivers are unaware of the i.i.d. demand shocks in each location and time, and instead condition policies on long-run market averages (which might, for example, be learned through experience). Taxis hold beliefs $\tilde{v}_i^t$ over the stock of vacant taxis in each i, t that is invariant over all weekdays. Drivers do not update beliefs about the market when they are matched or unmatched, as any subsequent taxi supply is assumed to be unaffected by shocks in any one location. These assumptions are formalized in Section 4.2. Since customer arrivals are Poisson, λ_i^t is the expected demand faced by taxi drivers. Drivers form policies based on forecasting the following intra-day sequence of events:

1. Taxis are exogenously distributed each day according to $\mathcal{S}^1$.
2. $m_r(\lambda_i^1, \tilde{v}_i^1)$ taxis become employed with matched customers in each location.
3. The remaining $\lambda_i^t - m_r(\lambda_i^1, \tilde{v}_i^1)$ expected number of unmatched customers leave the market.
4. The remaining $v_i^t - m_r(\lambda_i^1, v_i^1)$ vacant taxis choose a location to search in next period according to policy functions.
5. Previously vacant and some previously employed taxis arrive in new locations, forming distribution $\tilde{\mathcal{S}}^2 = \{\tilde{v}_i^t\}$.[28]
6. The process repeats from $\tilde{\mathcal{S}}^2$, $\tilde{\mathcal{S}}^3$, etc. until reaching $\tilde{\mathcal{S}}^T$.

3.6 Transitions

Policy functions σ_i^t form a matrix of transition probabilities from origin i to all destinations $j \in L$. Note that only vacant taxis transition according to these policies. Employed taxis will transition according to a different matrix of transition probabilities given by M_i^t denoting the probability

[28] Many hired taxis are in-transit for more than one period. If trips from location i to j will take 3 periods to complete the trip, then only the taxis who were 1 period away at time $t-1$ will arrive in j in period t.

that a matched customer in i will demand transit to any destination $j \in L$. Together, these two transition processes generate a law of motion for the state variable $\mathcal{S}$.

The transition kernel of employed taxis is given by $Q^{employed}(\boldsymbol{e}_i^{t+1}|\boldsymbol{e}_i^t, \boldsymbol{M}^t, \boldsymbol{m}^t)$ where $\boldsymbol{e}_i^t$ is the distribution of employed taxis across locations in period t, $\boldsymbol{M}^t = \{M_{ij}^t\}$ for $i, j = \{1, ..., L\}$ is the set of transition probabilities of each matched passenger at time t and $\boldsymbol{m}^t = \{m_i^t\}$ for $i = \{1, ..., L\}$ is the distribution of matches. $Q^{employed}$ specifies the expected distribution of all employed taxis e_i^t over locations in period $t+1$.

Likewise, the transition kernel of vacant taxis is given by $Q^{vacant}(\boldsymbol{v}_i^{t+1}|\boldsymbol{v}_i^t, \sigma^t)$. As with $Q^{employed}$, Q^{vacant} specifies the expected $t+1$ spatial distribution of period t vacant taxis, given the transitions generated from policies $\sigma^t = \{\sigma_i^t\}$ for $i = \{1, ..., L\}$. The combined set of transitions forms an aggregate transition kernel that defines the law-of-motion, given by $Q(\mathcal{S}^{t+1}|\mathcal{S}^t) = Q^{employed}(\boldsymbol{e}_i^{t+1}|\boldsymbol{e}_i^t, \boldsymbol{M}^t, \boldsymbol{m}^t)$ $+Q^{vacant}(\boldsymbol{v}_i^{t+1}|\boldsymbol{v}_i^t, \sigma^t)$. I provide explicit formulas for the state transitions in Appendix A.6.

3.7 Equilibrium

Taxi drivers' policies in a given period depend on their beliefs about the distribution of their competitors, the policies of competitors when vacant, expected demand across different neighborhoods and the destination preferences of customers across neighborhoods. Beliefs over the current state and competitors' policies enable drivers to infer how the distribution of vacant taxis at time t will update in future periods. Beliefs about demand and customer destination preferences across neighborhoods similarly enable drivers to infer how the distribution of matched cabs and their movement will affect the future distribution of vacant taxis. The net transition of taxis' vacant capacity from one period to the next is denoted as $\tilde{Q}_i^t$.

Definition *Equilibrium is a sequence of state vectors* $\{\mathcal{S}^t\}$*, transition beliefs* $\{\tilde{Q}_i^t\}$ *and policy functions* $\{\sigma_i^t\}$ *over each location* $i = \{1, ..., L\}$*, and an initial state* $\{S_i^0\}_{\forall i}$ *such that:*

(a) In each location $i \in \{1, ..., L\}$*, at the start of each period, matches are made according to equation 3 and are routed to new locations according to transition matrix* $\boldsymbol{M}^t$*. The aggregate movement generates the employed taxi transition kernel* $Q^{employed}(\boldsymbol{v}_e^{t+1}|\boldsymbol{v}_e^t, \boldsymbol{M}^t, \boldsymbol{m}^t)$ *where* $\boldsymbol{v}_e^t$ *is the distribution of employed taxis across locations in period* t *and* $\boldsymbol{m}^t$ *is the distribution of matches across locations.*

(b) In each location $i \in \{1, ..., L\}$*, at the end of each period, vacant taxi drivers (indexed by* a*) follow a policy function* $\sigma_{i,a}^t(\mathcal{S}^t, \tilde{Q}_i^t)$ *that (a) solves equation 7 and (b) derives expectations under the assumption that the state transition is determined by transition kernel* $\tilde{Q}_i^t$*. The aggregate movement generates the vacant taxi transition kernel* $Q^{vacant}(\boldsymbol{v}_v^{t+1}|\boldsymbol{v}_v^t, \tilde{\sigma}^t, \mathcal{S}^t)$ *where* $\boldsymbol{v}_v^t$ *is the distribution of vacant taxis in period* t*.*

(c) State transitions are defined by the combined movement of vacant taxis and employed taxis, defined by $Q(\mathcal{S}^{t+1}|\mathcal{S}^t) = Q^{employed}(\boldsymbol{v}_e^{t+1}|\boldsymbol{v}_e^t, \boldsymbol{M}^t, \boldsymbol{m}^t) \cup Q^{vacant}(\boldsymbol{v}_v^{t+1}|\boldsymbol{v}_v^t, \mathcal{S}^t)$.

(d) Agents' expectations are rational, so that transition beliefs are self-fulfilling given optimizing behavior: $\tilde{Q}_i^t = Q_i^t$ *for all* i *and* t.

Proposition 3.1. *The equilibrium defined above exists and is unique.*

Proof. See Appendix A.7 □

Equilibrium delivers a distribution of vacant taxi drivers such that no driver can systematically profit from an alternative policy: there is no feasible relocation that would, ex-ante, make search more valuable. Vacant taxis are therefore clustered in locations with more profitable customers, but the associated profits are offset by higher search frictions. One implication of this sorting pattern is that equilibrium value functions are nearly identical across locations in each time period. Value functions do not exactly equate, however, because time and fuel make arbitrage costly. See additional details in Appendix A.10.

3.8 Model Notation Summary

Table 4 summarizes the symbols and notation used in the model.

4 Empirical Strategy

In this section I present an estimation strategy that is designed to (1) solve for equilibrium and (2) use this equilibrium to recover model parameters. Estimation is conducted separately for each month. Each parameter, such as those governing demand, matching efficiency, and the travel time and distance between locations, represents a monthly-average. Driver behavior is based on these monthly averages. Below I detail the two main components of estimation.

4.1 Computing Equilibrium

The equilibrium location choices of vacant taxi drivers and their resulting spatial allocations must be computed in order to estimate model parameters. I make the following assumptions about the total supply of taxis and their information set.

Assumption 1 The total supply of cabs $\bar{v}$ for each weekday day-shift during the period studied is equal to 11,500.

Table 4: Notation and Symbol Guide

Description	Symbol	Member Set
Index Variables		
Origin location index	i	{1,...,39}
Destination location index	j	{1,...,39}
Time index	t	{1,...,108}
Region index	$r = r(i)$	$\{1, 2, 3, 4, 5\}$
Driver index	a	$\mathbb{N}$
Market Environment, Prices and Costs		
Vacant taxis	v_i^t	$\mathbb{R}$
Total employed taxis in i	e_i^t	$\mathbb{R}$
Employed taxis from trip i to j	e_{ij}^t	$\mathbb{R}$
Total number of taxis	$\bar{v} = \sum_i v_t^1$	$\mathbb{R}$
Travel time between any two locations	τ_{ij}	$\mathbb{R}$
Distance between any two locations	δ_{ij}	$\mathbb{R}$
Set of locations adjacent to location i	$A(i)$	
Distance fee per mile in USD	b_0	$\mathbb{R}$
Fixed fee per trip in USD	b_1	$\mathbb{R}$
Idling time fee per trip in USD	$b_{2,ij}^t$	$\mathbb{R}$
Fuel cost per mile in USD	c	$\mathbb{R}$
Fuel cost per trip in USD	$c_{ij} = c \cdot \delta_{ij}$	$\mathbb{R}$
Trip price/revenues in USD	π_{ij}^t	$\mathbb{R}$
Driver net revenue	$\Pi_{ij}^t = \pi_{ij}^t - c_{ij}$	$\mathbb{R}$
Demand Model		
Demand for taxi rides from i to j at t	u_{ij}^t	$\mathbb{R}$
Poisson parameter for customer arrivals	λ_{ij}^t	$\mathbb{R}$
Transition probability from i to j at t	M_{ij}^t	$\mathbb{R}$
Aggregated Poisson parameter	$\lambda_i^t = \sum_j M_{ij}^t \cdot \lambda_{ij}^t$	$\mathbb{R}$
Discrete categories of δ_{ij}	s	{<2,2-4,4-6,>6}
Airport trip indicator (i or j is airport)	ι	{0,1}
Demand parameter (mean shifter)	$\beta_{0,i,t,s,a}$	$\mathbb{R}$
Demand parameter (price elasticity)	$\beta_{1,i,t,s,a}$	$\mathbb{R}$
Demand parameter (hourly fixed effect)	ρ_{h_t}	$\mathbb{R}$
Demand parameter (route fixed effect)	$\gamma_{i,j}$	$\mathbb{R}$
Demand parameter (idiosyncratic term)	$\eta_{i,j,t,s,a}$	$\mathbb{R}$
Taxis' Valuations and Behavior		
State space	$\mathcal{S} = \{v_i^t, e_i^t\}\ \forall i, t$	$\mathbb{R}^{108\times39\times2}$
State vector at time t	$\mathcal{S}^t = \{v_i^t, e_i^t\}\ \forall i$	$\mathbb{R}^2$
Search efficiency	α_r	$\mathbb{R}$
Expected number of matches	m_i^t	$\mathbb{R}$
Match probability	p_i^t	$\mathbb{R}$
Number of potential airport rides	w_i^t	$\mathbb{R}$
Driver preference shock	ε_{ij}^t	$\mathbb{R}$
Driver preference shock scale parameter	σ_ε	$\mathbb{R}$
Ex-ante value functions	$V_i^t(\mathcal{S}^t)$	$\mathbb{R}$
Choice-specific value function	$W_i^t(\mathcal{S}^t)$	$\mathbb{R}$
Driver-specific destination choice	j_a	$\{1, ..., 39\}$
Destination conditional choice probability	$P_i^t(j_a\|\mathcal{S}^t)$	$[0, 1]$
Policy functions	$\sigma_i^t = \{P_i^t(j\|\mathcal{S}^t)\}_{j\in\{1,...,39\}}$	$\mathbb{R}^{39}$
Vacant taxi transition kernel	$\mathcal{Q}^{vacant}$	$\mathbb{R}^{39\times39\times108}$
Employed taxi transition kernel	$\mathcal{Q}^{employed}$	$\mathbb{R}^{39\times39\times108}$
Total transition kernel	$\mathcal{Q}$	$\mathbb{R}^{39\times39\times108}$

Assumption 1 satisfies a requirement for an exogenous labor supply necessary to compute the equilibrium level of vacant taxis across time and locations.[29]

Assumption 2 Taxi drivers have knowledge of the initial state vector $\mathcal{S}^1$ and all model parameters including demand parameters $\{\lambda_i^t\}$. Drivers do not observe the specific draws from the distributions of demand across time and locations.

Assumption 2 indicates a behavioral model in which drivers are unable to observe supply or demand beyond the particular streets they drive on in one period. This is not necessarily unrealistic given real-world line-of-sight constraints and, importantly, offers advantages in computational tractability.

To solve for equilibrium I use a two-step procedure where in the first step the set of matches, which I denote by the vector $\mathbf{m} = \{m_i^t\}$, are non-parametrically estimated using trip data. I estimate matches by computing the mean number of trips originating in each i, t cell for each day of the month and further apply a 6th-order polynomial smoothing over time of day t to reduce small sample noise. Equation (4) shows that for any i, t pair, m_i^t is sufficient to determine $p_r(\lambda_i^t, v_i^t)$ solely as a function of the the state variable v_i^t. Given this, the second step is to solve for the equilibrium state vector conditional on a set of parameters σ_ε, M_{ij}^t, τ_{ij}, and Π_i^t. This step is the most involved as it entails solving for equilibrium value functions and policy functions. Hereafter I denote the equilibrium state as $v_i^{t*}(\mathbf{m}, \sigma_\varepsilon)$ to reflect its dependency on these two key parameters.

Computing a dynamic equilibrium in large markets with many states is typically confounded by the curse of dimensionality. In this setting the problem is mitigated by Assumption 2. This assumption gives rise to a limited-information equilibrium similar to that of Weintraub et al. (2008b) and Fershtman and Pakes (2012) in which all agents play strategies and form equilibria without full knowledge of the payoff-relevant state variables. This allows me to compute policy functions without keeping track of which drivers are aware of which shocks, and without history dependence (i.e. 2pm in any particular neighborhood is always valued the same). Drivers therefore play against beliefs over average values of the state vector. By playing the same equilibrium policies each day, these beliefs become self-fulfilling in equilibrium.

State transitions are composed of the combined transitions of vacant and employed taxis. Under the continuum model both of these transitions are deterministic in each period given the prior period's matches and vacancies. Given an exogenous initial allocation of all 11,500 taxis in the market, assumed vacant at time $t = 1$, drivers compute a single, deterministic equilibrium path for the state $\{\mathcal{S}_i^t\}$ for $t = \{1, ..., T\}$. Taxi drivers start the day in garages around the city. When initially arriving to the set of locations in Figure 1, they form an initial distribution of vacant

[29] The number is data-driven; see Section A.5 for details and additional discussion in Section 5.3.

supply. Because these locations are unobserved, I approximate this distribution using the empirical distribution of early morning matches. To compute equilibrium conditional on this initial state, I devise a numerical algorithm that couples backwards induction and value function iteration. See Appendix A.8 for computational details and a robustness analysis on the initial condition.

4.2 Model Estimation and Identification

In this subsection, I show that demand parameters $\{\lambda_i^t\}$, matching efficiency parameters $\{\alpha_r\}$ and the scale parameter σ_ε can be identified given the available data. Identification has three steps.

1. I first estimate several objects relating to destination shares, trip times, trip distances, profits, costs and airport queueing as means over observations in the data. Given these and the expected matches $\mathbf{m} = \{m_i^t\}$ I can solve for the equilibrium state $\{v_i^{t*}(\mathbf{m}, \sigma_\varepsilon)\}$ up to σ_ϵ

2. I resolve for $\{v_i^t(\mathbf{m}, \sigma_\varepsilon)\}$ given different values of σ_ϵ, and choose the value that best matches a set of simulated moment conditions to data.

3. Given estimates of σ_ϵ and $\mathbf{m}$ and the corresponding equilibrium v_i^t, I can identify the ratio $\frac{\lambda_i^t}{\alpha_r}$ by inverting $m_r(v_i^t, \frac{\lambda_i^t}{\alpha_r})$ in its second argument.

I describe each of these steps in more detail below. I then explain how to use the recovered demand parameters from before and after a fare change to estimate the price elasticities of demand along different routes. Finally, I describe how I obtain standard errors on model parameters.

4.2.1 Objects Identified Directly from Data

In addition to estimating expected matches $\{m_i^t\}$ as discussed in Section 4.1 , six additional parameters of the model are identified directly from data:

1. M_{ij}^t is the transition probability of employed taxis in each period and location. In each period, I record the probability of transition from each origin to each destination conditional on a taxi matching with a passenger. The mean of these probabilities over each weekday of the month, computed for each origin i, destination j and hour t, generates expected transition probabilities M_{ij}^t.

2. τ_{ij} is the travel time between each origin and each destination. As above, I record the average of all travel times between each i and j, for each hour t, over all weekdays of the month. I set $min(\tau_{ii}) = 1$, so that within-location trips must take at least 1 period.

3. δ_{ij} is the distance between each origin and each destination, a component of profits Π_{ij}^t With the trip distance variable in TLC data, I record the mean distance between each i and j across all weekdays of the month. Note that $\delta_{ii} > 0$ since trips can occur within a location.

4. $b_{2,ij}^t$ is the idling/waiting time component of the trip price, which is not observed directly. For each trip, first I compute the distance and fixed component of the fee based on trip distance, and then take the final price net of taxes and tolls, both of which are observed, and subtract distance and fixed fees, giving the trip-specific idling time fee. I then take the mean of these fees across all trips in each origin, destination and hour to obtain $b_{2,ij}^t$.

5. To compute the number of periods a taxi driver expects to wait in the airport queue, I compute the mean number of pickups per period ρ_i^t across each day at each airport as the expected queue throughput rate and use this to determine the waiting period length as $w_i^t = \texttt{round}(v_i^t/\rho_i^t)$. This moment is sufficient to determine how drivers value the airport, upon arrival, as a search location. To estimate demand, I treat the mean number of pick-ups in each airport location as direct observations of λ_{38}^t and λ_{39}^t.[30]

6. Finally I compute the cost of fuel per mile c as the average fuel price in New York City in 2012 divided by the average fuel economy in the New York taxi fleet, 29 mpg.[31] Using $c = \$0.124$, I compute the cost of traveling between any origin and destination as $c_{ij} = c \cdot \delta_{ij}$. Note that $\delta_{ii} > 0$ implies $c_{ii} > 0$.

After I record the distances between each origin and each destination, I can derive Π_{ij}^t, the expected profit associated with each possible trip. Recall from equation 2 that $\Pi_{ij}^t = \pi_{ij}^t - c_{ij}$, where the regulated fare structure is given by the set $\{b_0, b_1, b_{2,ij}^t\}$. With these parameters, and given data on expected matches by time and location, I can solve for the equilibrium distribution of taxis up to a scale parameter. Below I describe how solving for equilibrium and using it to solve a simulated moment estimator allows me to recover the scale parameter. With an estimate of the scale parameter in hand, I can further recover estimates for demand and matching efficiency.

[30] Note if airport riders were to wait more than 5 minutes, then due to some per-period constraints on the queue these estimates may be biased. For example if we let $\bar{x}_i^t$ be the maximum number of cabs that can clear the queue and $\lambda_{LGA}^t > \bar{x}_{LGA}^t$, the estimate would be truncated at $\bar{x}_{LGA}^t$. To address this, I hold airport prices fixed in all counterfactuals (and hold the queuing technology fixed). This leaves frictions unchanged from the baseline estimates. The model estimates of λ_{LGA}^t nevertheless continue to capture the maximum number of trips attainable by all airport-located drivers in period t.

[31] Data come from the New York City Taxi and Limousine Commission 2012 Fact Book and the U.S. Energy Information Administration. The taxi fleet is approximately 60% hybrid vehicles. Volatility of fuel prices is low in this period: cost-per-mile fluctuates within a range of $0.01 during the sample period.

4.2.2 Estimating σ_ε

Since the static profit function is observable, it is possible to test how much drivers depend on observed versus unobserved factors in making search choices. This is done through the scale parameter σ_ε, which affects how much drivers' location decisions are explained by trip profits. To estimate this parameter, I search for the value of σ_ε that generates an equilibrium state vector $\{v_i^t(\mathbf{m}, \sigma_\varepsilon)\}$ and corresponding driver-specific moments that are closest to the data.

I rely on four moments to conduct the estimation. The first two moments are the average trip time and average trip distance from 7a–4p. The second two moments are the per-period match probabilities in central (region II in Figure 1) and non-central Manhattan. For the first two data moments I only include drivers whose entire shifts fall within the area of study. Across all of their trips I compute average trip times and distances. The remaining two data moments are constructed using the distribution of waiting times across drivers following a drop-off in each location. The match probability is equal to the proportion of drivers who find a match within five minutes.[32]

To generate the corresponding data moments, I fix a value of σ_ε and compute equilibrium match probabilities and transitions. I then simulate 25,000 driver days worth of trips at equilibrium probabilities and transitions. With the simulated trips I compute the four analogous moments. I then employ a simulated method of moments procedure to recover an estimate of σ_ε.

A high-σ_ε equilibrium leads to drivers that are more spread out spatially, as choice probabilities tend towards a uniform distribution. This leads drivers to choose search patterns that are less centralized in Manhattan as well as longer trip times and distances since more peripheral locations are associated with longer trips. In Appendix A.9 I provide additional detail on computing this parameter.

4.2.3 Estimating λ_i^t and α_r

In order to estimate λ_i^t and α_r, I first recover the ratio $\frac{\lambda_i^t}{\alpha_r}$. In a slight abuse of notation I will denote the equilibrium state vector as $\mathbf{v}^*(\mathbf{m}) = \{v_i^{t*}(\mathbf{m})\}$, omitting the explicit dependency on the scale parameter σ_ε, as this parameter is estimated in the step above. The next proposition shows how to derive the set of ratios $\{\frac{\lambda_i^t}{\alpha_r}\}$ using $\{v_i^{t*}(\mathbf{m})\}$ by inverting equation 3 at $\mathbf{m}$.

Proposition 4.1. *Suppose a vector of expected matches by location and time,* $\mathbf{m}$*, is observed. Further, suppose* $v_i^{t*}(\mathbf{m}) \neq 0 \; \forall i, t$*. Then the ratio* $\frac{\lambda_i^t}{\alpha_r}$ *is identified.*

Proof. Equation (3) is strictly increasing in λ_i^t/α_r given $v > 0$. Since a strictly increasing function is one-to-one, it follows that since $\mathbf{v}^*(\mathbf{m})$ is unique, via Proposition 3.1 then equation (3) can be

[32] For example, if the median waiting time across drivers in a location is five minutes, then the average match probability in one period is 50%.

uniquely inverted for $\frac{\lambda_i^t}{\alpha_r}$:

$$\frac{\lambda_i^t}{\alpha_r} = -v_i^{t*}(\mathbf{m}) \cdot \ln\left(1 - \frac{m_{it}}{v_t^{t*}(\mathbf{m})}\right). \tag{10}$$

□

Since $\mathbf{m}$ is observed and $\mathbf{v}^*(\mathbf{m})$ is uniquely determined upon recovering σ_ϵ, I can compute the right-hand-side of equation 10 to recover $\frac{\lambda_i^t}{\alpha_r}$. The non-zero condition on the state vector is confirmed by the numerically obtained equilibrium.

To separately identify λ_i^t and α_r, I develop an estimator based on the daily variance of matches across days in the sample. Variance in matches will naturally arise from variation in demand each day.[33] To illustrate how match variance can help to identify α_r, suppose that matches were determined by $m(\lambda_i^t, v_i^t) = \frac{\lambda_i^t}{\alpha_r}$. Then for a Poisson parameter λ_i^t we have $Var(m_i^t) = \frac{1}{\alpha_r^2} Var(\lambda_i^t) = \frac{\lambda_i^t}{\alpha_r}\frac{1}{\alpha_r}$. Thus by comparing the recovered $\frac{\lambda_i^t}{\alpha_r}$ and the observed $Var(m_i^t)$, one can uniquely determine α_r.

While the matching function is more complex than the simple example above, the logic is similar; a higher α_r parameter induces lower day-over-day variance in matches. Since match variance is observed, it is possible to form an estimator for the efficiency parameters – one for each region – by choosing α_r to minimize the distance between the variance in matches in the data and that produced by the model. This is accomplished with the following estimator:

$$\hat{\alpha_r} = \arg\min_{\alpha} \left(\sum_{i,t} \mathbb{I}(i \in r(i)) \left(Var(m_i^t(\alpha_r)) - Var(\hat{m}_i^t) \right)^2 \right), \tag{11}$$

where $Var(m_i^t(\alpha_r))$ denotes the model-simulated variances and $Var(\hat{m}_i^t)$ denotes the variances computed from data. To compute $Var(m_i^t(\alpha_r))$, I derive an analytic expression based on the matching function. Recall that the matching function $m_r(\lambda_i^t, v_i^t)$ reports the expected or mean matches given λ_i^t. To recover an expression for the variance of matches, I use the urn-ball matching function $g_r(u_i^t, v_i^t)$ from which the expectation $m_r(\lambda_i^t, v_i^t)$ is derived:

$$g_r(u_i^t, v_i^t) = v_i^t \left(1 - \left(1 - \frac{1}{\alpha_r v_i^t}\right)^{u_i^t}\right). \tag{12}$$

In Appendix A.9 I show that $m_r(\lambda_i^t, v_i^t) = E_u[g_r(u_i^t, v_i^t)]$. I then obtain an analytic expression of $Var(m_i^t(\alpha_r)) = Var(g_r(u_i^t, v_i^t))$ by deriving the variance of $g(u_i^t, v_i^t)$ when $u_i^t \sim Poisson(\lambda_i^t)$ and

[33] While variation in demand is important to this approach, I note that any unobserved sources of variation, say due to local demand shocks or unobserved variation in vacant taxis' supply each day could raise the variance of matches beyond any variation attributable to demand and search frictions. If such unobserved variation exists, my estimates α_r would imply lower frictions than the true value. Therefore any estimated welfare gains to improving search frictions can be viewed as a lower bound.

when v_i^t is constant each day. For this to be credible I require the following assumption:

Assumption 3 The equilibrium level of vacant cabs in each location and time-of-day is invariant across each day of the month, or $Var(v_i^t) = 0$

I substantiate Assumption 3 by simulating the market with and without variance in vacant taxis to show that it yields nearly identical variance in matches (see Appendix A.9.2). This assumption implies that, even when there is variation in matches between any two locations due to the variation in customers, there are enough routes with independent variation that the expected inflow of vacant taxis each period remains constant each day. The benefit of this assumption is that it allows for analytically computing the variance of matches and obviates the need for a much more complicated simulation-based estimator. This assumption together with equation 12 allows me to derive the following expression:

$$Var(m_i^t(\alpha_r)) = \left(v_i^{t*}\right)^2 e^{-2\frac{\lambda_{it}}{\alpha_r}\frac{1}{v_{it}^*}} \left(e^{\frac{\lambda_{it}}{\alpha_r^2}\frac{1}{v_{it}^{*2}}} - 1 \right). \tag{13}$$

Proposition 4.2. *Suppose Assumption 3 and all assumptions of Proposition 4.1 hold, and suppose a vector $\sigma^{\mathbf{2}}_{\mathbf{m}}$ of the variance of matches by time and location across days is observed. Then $\{\lambda_i^t\}$ and $\{\alpha_r\}$ are identified.*

Proof. $\frac{\lambda_i^t}{\alpha_r}$ and v_i^{t*} are obtained as in Proposition 4.1. Denote $\hat{\lambda} = \frac{\lambda_i^t}{\alpha_r}$, and $\hat{\sigma}^{\mathbf{2}}_{\mathbf{m,it}} = \{Var(\hat{m}_i^t)\}$, where the variance of matches in each location and at each time is taken across days. Then inverting equation 21 for α_r gives the following estimate:

$$\hat{\alpha}_r = \frac{\hat{\lambda}_{it}}{v_{it}^*(\hat{\mathbf{m}})} \left(\ln\left(e^{2\hat{\lambda}_{it}} \left(\frac{\hat{\sigma}^{\mathbf{2}}_{\mathbf{m}}}{v_{it}^{*2}(\hat{\mathbf{m}})} \right) + 1 \right) \right)^{-1}. \tag{14}$$

With estimates of α_r and $\frac{\lambda_i^t}{\alpha_r}$, I can recover the demand parameters $\{\lambda_i^t\}$ directly. □

Equation 14 shows that α_r is overidentified as each region r is made up of several locations i and periods t. While α could be treated as i- or t-specific, modeling frictions on the basis of broader regions obtains more credible results for each α_r, as there could be error in the measurement and estimation of the right-hand-side parameters and moments. I estimate α_r by minimizing equation 11 where model variance is determined by equation 13.

4.2.4 Estimating Demand Elasticities

To compute market welfare, I estimate the demand elasticity parameters in equation 1. On September 4, 2012, the distance fee increased by \$0.50 per-mile, and the JFK airport flat-fee increased

by \$7. Using September 2012, data, I re-estimate the model for σ_ε, $\{v_i^{t*}\}$, $\{\lambda_i^t\}$, and $\{\alpha_r\}$.[34] In the analysis that follows, I use the price variation from this regulatory change to estimate demand elasticities across different types of trips, where the demanded quantity is the average number of customer arrivals in each i with destination j at time t given prices π_{ij}^t.[35]

I estimate demand via the following specification:

$$ln(\lambda_{ij}^t(\pi_{ij}^t)) = \beta_{0,s,\iota} + \beta_{1,s,\iota} ln(\pi_{ij}^t) + \rho_{h_t} + \gamma_{ij} + \eta_{i,j,t}. \tag{15}$$

In a slight abuse of notation I define the index $s = s(i,j)$ as a set of the distance categories associated with a trip i, j, such that $s \in \{s_0, s_1, s_2, s_3\} = \{$0–2 mi., 2–4 mi., 4–6 mi., 6+ mi.$\}$, roughly corresponding to trip-distance quartiles. The index ι indicates an airport trip, or $\iota = \mathbb{I}(i \text{ or } j \in \{JFK, LGA\})$. Price elasticities $\beta_{1,s,\iota}$ are different for each distance category among trips without airports, and different for airport trips. I include hourly fixed effects δ_{h_t} and region fixed effects for drop-off location j and pickup location i.

In this demand system, all customers of a given type s, ι have the same price elasticities. Origin, destination and time fixed effects capture the heterogeneity of locations: some have more public transit stations, bus stops, or walkability. Given these fixed effects, identifying variation comes from the differences in prices before and after the September 2012 fare change. To estimate parameters, I estimate an empirical analogue of equation 1 for each s category using OLS. Since prices are fixed within a location and time period, this specification does not suffer from simultaneity bias, unlike traditional non-instrumented demand models.

4.2.5 Standard Errors

The estimation procedure detailed above requires, for each month, first estimating the scale parameter σ_ε as well as a set of simple means on matches, travel times, travel preferences, and fares: $\{m_i^t\}, \{\tau_{ij}\}, \{M_{ij}^t\}, \{\Pi_{ij}\}$. The remaining parameters are then estimated in a second-stage that is conditional on the first stage estimates.

To compute standard errors, I re-sample data from the set of day-long blocks of observations. For example, there are 23 weekdays in the month of August 2012. I draw, at random and with replacement, from each of these complete days, including all taxi trip data for that day until I obtain 23 sampled days that I treat as one bootstrap sample. This process incorporates random

[34] I allow σ_ε and α_r to vary by month, as road conditions, traffic patterns, and seasonal weather may change.

[35] Based on the discussion in Section 3.1, I compute that average waiting times dropped by 21 seconds between August and September, and in Manhattan the largest drop in location-specific waiting time was 31 seconds. I therefore assume the changes in waiting times are sufficiently small to be negligible for the demand estimation. My counterfactuals, however, will incorporate an elasticity of waiting time.

variation that occurs each day, as modeled in the daily draws of arriving demand, but also allows for intra-daily correlations in matches across space and time due to the flow of trips.

For each bootstrap sample, I re-estimate the first stage by computing the above empirical means and by re-estimating σ_ε by simulated method of moments. With first stage estimates, I re-estimate the second stage parameters. Standard errors are produced by computing standard deviations over parameter estimates across 150 samples. I conduct this procedure separately for August and September data.

Table 5: Model Estimates and Equilibrium Results

Panel A: Parameter Estimates Summary

Description	Parameter	Elements	Estimate	Std. Err.	Avg/Min/Max
Demand (August 2012)	$\{\lambda_i^{t,aug.}\}$	4,212	See Figures A7-A8		52.2/0.79/508.5
Demand (September 2012)	$\{\lambda_i^{t,sep.}\}$	4,212	.		48.4/0.60/415.4
Efficiency, Region I (Aug.)	$\alpha_1^{aug.}$	1	0.833	(0.021)	n.a.
Efficiency, Region I (Sep.)	$\alpha_1^{sep.}$	1	0.776	(0.006)	n.a.
Efficiency, Region II (Aug.)	$\alpha_2^{aug.}$	1	0.845	(0.015)	n.a.
Efficiency, Region II (Sep.)	$\alpha_2^{sep.}$	1	0.748	(0.006)	n.a.
Efficiency, Region III (Aug.)	$\alpha_3^{aug.}$	1	1.126	(0.007)	n.a.
Efficiency, Region III (Sep.)	$\alpha_3^{sep.}$	1	1.033	(0.006)	n.a.
Efficiency, Region IV (Aug.)	$\alpha_4^{aug.}$	1	1.069	(0.007)	n.a.
Efficiency, Region IV (Sep.)	$\alpha_4^{sep.}$	1	0.987	(0.006)	n.a.
Driver Shocks (Aug.)	$\sigma_\varepsilon^{aug.}$	1	2.526	(0.132)	n.a.
Driver Shocks (Sep.)	$\sigma_\varepsilon^{sep.}$	1	3.260	(0.111)	n.a.

Panel B: Equilibrium Summary

Estimated Object	Number of Elements	Computed Value	Avg/Min/Max
$\mathcal{S} = \{v_i^t\}$	4,212 (108 × 39)	See Figures A7-A8	158.3 / 3.05 / 539.1
$\{V_i^t\}$ (non-airport i)	3996 (108 × 37)	See Figure A9	\$208.7 / \$3.73 / \$412.31
$\{V_i^t\}$ (airport i)	216 (108 × 2)	See Figure A9	\$214.3 / \$3.77 / \$651.02

Panel A presents a summary of estimation results from both August and September 2012. Point estimates for matching efficiency parameters α_r correspond to Figure 1 sections I–IV, respectively. Panel B shows computed equilibrium objects in the August 2012 sample.

5 Empirical Results

This section presents the results of estimation, quantifies the importance of search frictions and dynamic externalities, and provides estimates of demand elasticities and welfare. Table 5, Panel A shows estimation results for the Poisson demand parameters $\{\lambda_i^t\}$, as well as point estimates by month for additional parameters σ_ε and each α_r. Panel B summarizes the computed equilibrium

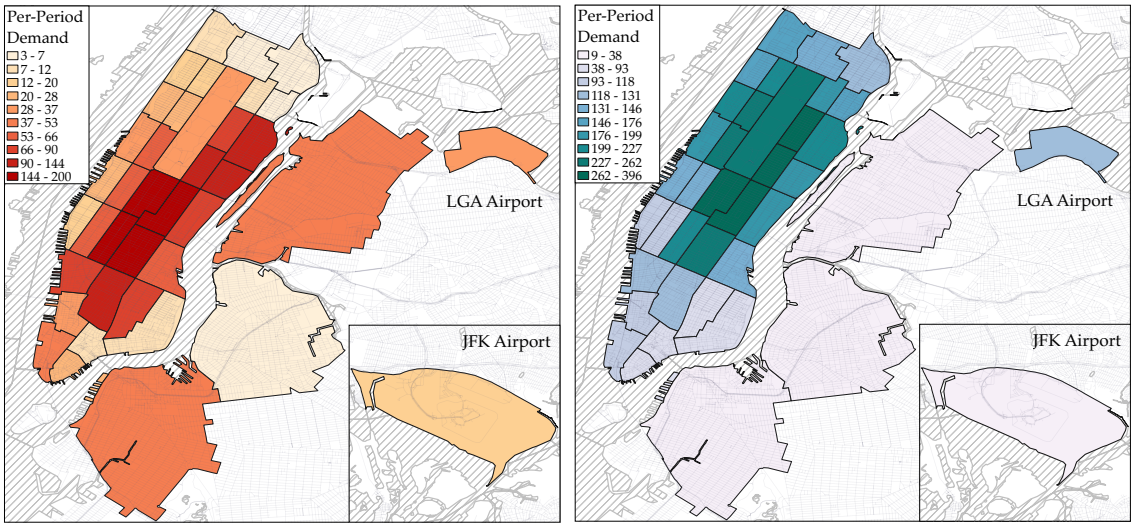

(a) Demand (b) Supply

Figure 5: Map of Estimated Supply and Demand: Mean Across t

This figure shows the supply and demand estimates for August 2012 averaged over time-of-day. The left panel shows the mean estimated per-period customer arrivals and the right panel shows the mean number of vacant taxis.

objects: the supply of vacant taxis across time and locations, $\{v_i^t\}$, and the corresponding value functions $\{V_i^t\}$ at each time and location. Full results are available in Section A.10.

5.1 Spatial Distributions and Intra-day dynamics

Figure 5 depicts supply and demand for taxi rides across all locations, averaged across all periods of the day. Both taxi supply and passenger demand are most highly concentrated in the central part of Manhattan. For the most part, the number of vacant taxis is sufficient to meet demand in the absence of search frictions. The notable exception is in two central regions with very high demand, where average demand exceeds average supply.

Figure 6 provides an inter-temporal view of the results for two busy locations, Greenwich Village/SoHo and Central Midtown. Both graphs depict the equilibrium supply of vacant taxis, the estimated arrival of customers looking for a taxi, the number of matches as observed in the data, and a polynomial-smoothed series of these matches. Each series depicts the day shift in five-minute increments. Panel (a) shows that there are periods of relative oversupply and undersupply (compared to demand) of taxis at different times of day. Panel (b) shows an oversupply of taxis at the same time where there is an undersupply shown in Panel (a). This simultaneous over-supply and under-supply illustrates evidence of spatial misallocation as an equilibrium outcome: there is mismatch across locations, as across Panels 1 and 2. Within-location matching frictions are captured

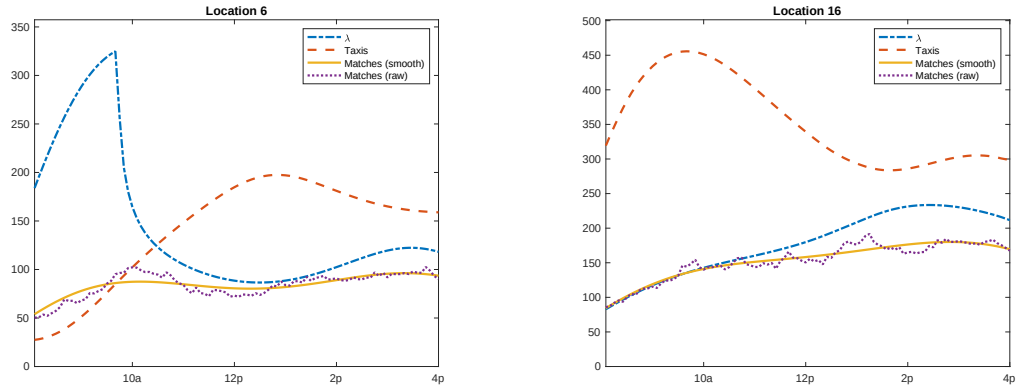

(a) Undersupply: Greenwich Village

(b) Oversupply: Central Midtown

Figure 6: Dynamic Spatial Misallocation Example

This figure shows intra-day results for two example locations. Panel 1 shows the location that encompasses Greenwich Village and SoHo between Canal Street and 14th Street. Panel 2 is Central Midtown from 37th Street to 59th Street. Each figure depicts the equilibrium supply of taxis (red, dashed line) and the estimated arrival of passengers (blue, dot-dash line), compared with the expected number of matches. Matches are shown in two forms: the purple (dotted) line shows the expected number of matches in each minute, for each location, where the expectation is taken over days of the month. The yellow (solid) line fits a sixth-order polynomial to smooth matches over time. Each point depicts the over- or under-supply of taxis relative to demand in each 5-minute interval from 8am until 4pm.

as the vertical space between the minimum of supply and demand at any point (i.e., $\min\{v_i^t, \lambda_i^t\}$) compared with matches (i.e., m_i^t). I present results for more locations in Appendix (A.10).

The movement of hired and vacant taxis alike shifts the spatial distribution of vacant capacity across space. Figure 7 shows how these two types of spatial flows relate to each other. It aggregates taxi supply across all 39 locations into five regions (identical to those in Figure 1) and depicts the *net flow* of matches by region, defined as the sum of drop-offs minus pick-ups in each location, summed across all locations in each region. Panel (b) shows the net flow of taxis due to vacant taxis' location choices by region. In the first half of the day employed taxis are traveling into Midtown and out of most other regions, while at the same time vacant taxis are proportionally exiting Midtown. Across the day, the choices of vacant taxis almost perfectly offset the movement of employed taxis. This pattern arises from drivers' time- and location-specific policy functions which maintain a near-equality of equilibrium value functions across locations in each period.

5.2 Externalities

To demonstrate how the movement of vacant taxis shifts the incidence of matches and welfare across the day, Table 6 computes the expected impact, across a single day, of reallocating a single vacant

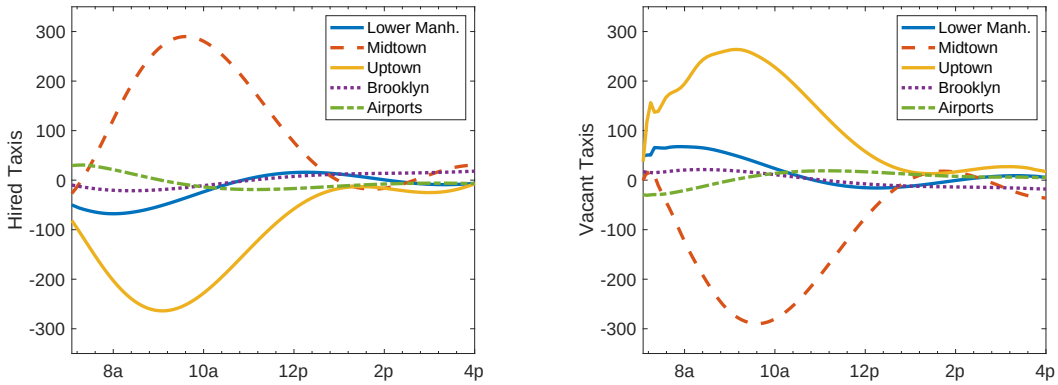

(a) Net Matches

(b) Net Choices

Figure 7: Equilibrium Flow of Matches and Vacant Taxi Choices by Region

This figure shows the net flow of matches and vacant taxis for August 2012. The top panel shows the net flow of matches, defined as the sum of matches with destinations *into* each region minus the sum of pick-ups headed *out of* each region. The bottom panel similarly shows the net movement of vacant taxis into and out of locations within each region. Positive values therefore reflect a net inflow of vacant cabs in each location due to taxis dropping off customers (in Panel I) and previously vacant cabs (in Panel II).

taxi between two regions at 9am. This reallocation is done relative to the baseline equilibrium distribution of vacant taxis. Example 1 shows that swapping one taxi from Brooklyn to Midtown will, on average, generate more matches in Midtown and Uptown regions at the expense of all other regions. The effect is driven not just by changes in the 9am stock but the subsequent movements of the reallocated taxi. Welfare is also impacted; in Example 1, the net effect of this single unit reallocation is around \$50 per day.[36] Example 2 shows a reallocation with a nearly-neutral aggregate impact on matches and welfare, moving one unit from Midtown to Lower Manhattan. Finally, Example 3 shows that a reallocation from Lower Manhattan to JFK airport leads to a net reduction in matches and welfare.

Figure 8 shows the expected change in matches over time due to the same three examples. The top row shows the change in matches by region in the first two hours following each reallocation. The bottom row shows the net impact across the entire day. The expected impact dissipates in about one to two hours. This diffusion is a natural consequence of the period-by-period randomness in both customer destinations and subsequent search patterns. Taken together, this exercise shows that the externality is relatively short lived by up to two or three hours, but that the net effects are not trivial. The existing equilibrium is also not efficient. This result further motivates the question

[36] Welfare definitions and calculations are discussed in detail below.

Table 6: The Effect of Repositioned Vacant Taxis by Region: Examples

Description	**Effect**	*Region I*	*Region II*	*Region III*	*Region IV*	*Region V*	*Overall*
Ex 1: Send 1 Brooklyn (36)	Net Δ in Matches	-2.0	2.3	2.7	-1.3	-0.3	1.3
taxi to Midtown (12)	Net Δ in Welfare ($)	-19.34	23.59	32.03	12.03	0.00	48.32
Ex 2: Send 1 Midtown (11)	Net Δ in Matches	2.3	-0.9	-1.5	0.0	-0.0	-0.1
taxi to Lower Manhattan (5)	Net Δ in Welfare ($)	16.15	-9.73	-18.35	0.24	0.00	-11.69
Ex 3: Send 1 Lower	Net Δ in Matches	-3.6	-3.3	0.6	0.3	1.3	-4.8
Manhattan taxi (5) to JFK	Net Δ in Welfare ($)	-26.30	-31.60	5.76	-0.85	0.00	-52.99

This table shows the marginal effect of switching the location of one taxi between two locations, as indicated, at 9am. The marginal impact on the number of trips and consumer welfare is the sum of all resulting subsequent matches up to 4pm net of the baseline equilibrium.

of how to properly price customer trips accounting for these spillovers and how to incentivize drivers to locate themselves efficiently when vacant.

5.3 Frictions

The estimated results also allow for assessing the impact of search frictions within and across locations. Aggregate excess demand over the course of a day-shift is given by $\sum_{i,t}\left(\lambda_i^t - m_r(\lambda_i^t, v_i^{t*})\right)$. Total daily demand is for 249,552 trips whereas total matches in the data are 196,099, implying that 53,453 demanded customer trips are unmet each day, or an average 494 unmet trips each period. This contrasts with an average of 5,759 taxis that are vacant in each period, suggesting substantial frictions on both sides of the market.

I further decompose search frictions by attributing unmet demand to within-location and across-location frictions. Within-location frictions are due to an imperfect matching technology – in this case, searching on the street. These frictions are measured by $\sum_{i,t}\left(min(\lambda_i^t, v_i^{t*}) - m_r(\lambda_i^t, v_i^{t*})\right)$, where the first term reflects frictionless matching. These are frictions that can be directly mitigated with better technology, for example through app-based ride-hail platforms. Within-location frictions amount to 40,038 unmet passengers, or 75% of the total number of unmatched passengers. The remaining 13,415 unmet trips are due to spatial mismatch between vacant drivers and passengers. Even with better technology, these frictions exist when supply and demand are farther apart and thus not readily matched. This residual mismatch highlights the possibility of pricing inefficiencies, as supply and demand distributions are functions of price. An equilibrium analysis of changes to matching technology is examined in Section 6. In Appendix A.10 I discuss the robustness of these results to Assumption 1, that the aggregate supply of cabs is equal to 11,500.

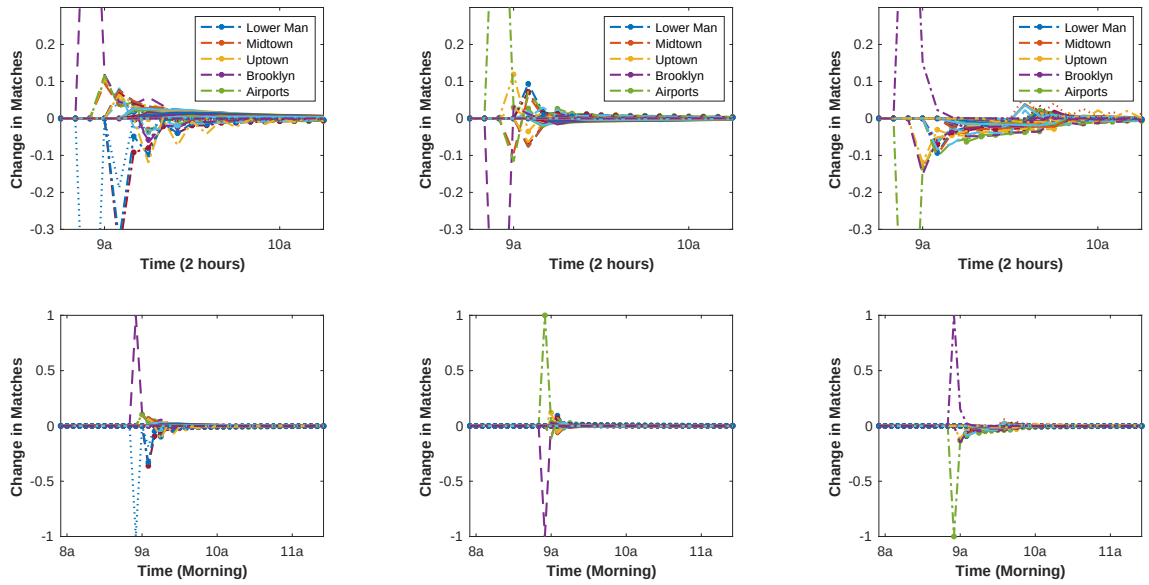

(a) Brooklyn to Midtown (b) Midtown to Downtown (c) Downtown to JFK

Figure 8: Dynamic Response of One Repositioned Vacant Taxi: Examples

This figure shows the dynamic effect of switching the location of one taxi between two locations at 9am. Example 1 captures the effect of moving one vacant Brooklyn taxi (location 36) to Midtown Manhattan (location 11). Example 2 moves one Midtown taxi (location 11) to Lower Manhattan (location 5). Example 3 moves one Lower Manhattan taxi to JFK airpot (location 39). Each example corresponds to those in Table 6. The change in the number of trips is net of the baseline equilibrium.

5.4 Demand Elasticities

As outlined in Section 4.2.4, I first estimate the taxi equilibrium model separately for August 2012 and September 2012 following a change in the regulated tariff. Estimates of location-specific demand λ_i^t and the destination shares M_{ij}^t allow for constructing destination-specific demand parameters as $\lambda_{ij}^t = \lambda_i^t \cdot M_{ij}^t$, where λ_i^t and M_{ij}^t are obtained separately for each month. I then leverage the change in prices over this period to identify price elasticities across trips of differing lengths. By predicting λ_{ij}^t under new prices based on these estimates, I can construct new predictions for both total demand λ_i^t and trip shares M_{ij}^t. Table 7 reports price elasticities of passenger arrivals between -1.07 to -2.22, where shorter trips are more price elastic than longer ones. This is not surprising as short distances tend to be better connected with public transit and more walkable, thereby offering more possible substitutions with taxi service.

I compute welfare by first integrating demand over $q \in [0, \lambda_{ij}^t]$ for each combination of origin,

Table 7: Estimation results: Demand Elasticities for Non-airport Origins

Description	**Trip Type**				
	0-2 mi.	*2-4 mi.*	*4-6 mi.*	*>6 mi.*	*Airport Trips*
Price Elasticity	-2.220^{**}	-1.986^{**}	-1.684^{**}	-1.074^{**}	-1.131^{**}
	(0.082)	(0.104)	(0.149)	(0.222)	(0.055)
Pickup Location FE	X	X	X	X	X
Drop-off Location FE	X	X	X	X	
Time-of-Day FE	X	X	X	X	X
Pickup Region × Hour FE	X	X	X	X	X
Time Trend	X	X	X	X	X
N	99,336	87,012	60,960	48,396	16,848
R^2	0.905	0.860	0.864	0.816	0.919

Standard errors in parentheses, ** p<0.01

Demand data come from model estimates. An observation is an arrival-rate of customers within an origin-location, destination-location, and five-minute period during a weekday from 7a–4p. The dependent variable is $\log(\lambda_{ij}^t)$ and the independent variable of interest is $\log(\pi_{ij}^t)$. Columns 1–4 report estimates for trips within non-airport locations. Column 5 reports estimates for trips that begin in a non-airport location and end at an airport. Standard errors are clustered at the level of origin-location.

destination and hour. From this measure, welfare accrues only to the fraction of customers served, or $m_i^t(\lambda_i^t, v_i^t)/\lambda_i^t$.[37] I illustrate these calculations in Figure 9. The area $A \cup B$ reflects the entire available surplus in this market at price p_i^t . The area B is the lost surplus due to frictions and random matching. A is therefore the realized welfare for each sub-market (i, j, t). Note that A is an equilibrium object due to its dependency on π_{ij}^t and m_{ij}^t. Since elasticity estimates are obtained locally to the price variation, estimating consumer welfare at high prices involves extrapolation far out of sample. To ensure that welfare valuation is not driven by these observations I implement a choke price of $\bar{\pi} = \$100$. Aggregate welfare is then computed as $\sum_{i,j,t} A_{ijt}(\pi_0)$ where π_0 reflects trip prices in each i, j, t sub-market given the observed tariff pricing.

Total estimated welfare for each weekday, day-shift is shown in Table 8. Consumer welfare for New York taxi service is \$2.45M per day-shift. Taxi profits are \$3.27M, or \$284 per driver.[38] There is substantial heterogeneity by time, place and trip length. For example, hourly consumer surplus increases from morning to afternoon. The consumer welfare and profits accrued from trips in Manhattan are vastly higher than those in Brooklyn, and shorter trips make up the bulk of welfare and profits. This variation suggests that if different pricing regimes affect the spatial allocation of supply and demand, then we should expect them to also impact aggregate welfare.

[37] I provide explicit formulas in Appendix A.11.1

[38] Drivers also must pay a leasing fee imposing costs-per-shift of around \$100-125 per day, for which detailed data were not available. Including these fees implies daily profits around \$160 to \$180.

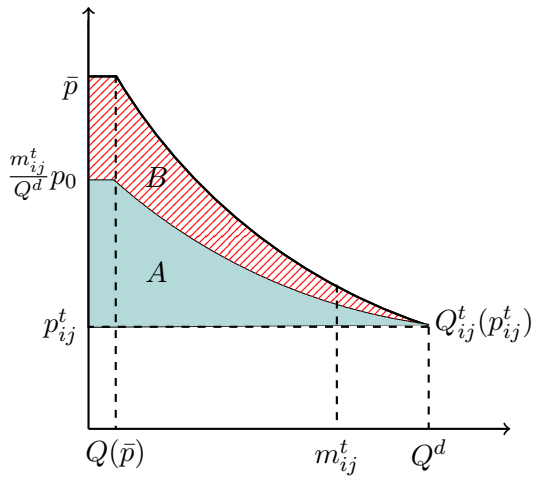

Figure 9: Consumer Surplus with Frictions

This figure illustrates how welfare is calculated in each sub-market (i, j, t) under random matching.

Table 8: Estimated Results: Daily, Single-Shift Welfare Measures

Subset Type	**Subset**	**Cons. Surplus ($, thousand)**	**Taxi Profits ($, thousand)**	**Matches (thousand)**
Aggregate	-	2452.6	3273.6	211.3
By Time-of-day	7a-9a	344.1	561.1	34.7
	9a-11a	604.2	779.2	50.9
	11a-1p	534.8	734.5	48.1
	1p-4p	969.4	1198.8	77.5
By Origin Region	Sec. I	471.1	626.9	36.6
	Sec. II	1164.0	1535.7	100.9
	Sec. III	760.4	1008.6	64.4
	Sec. IV	57.2	102.4	4.6
By Trip-Length	0-2 mi.	1137.9	1481.6	124.0
	2-4 mi.	836.6	1013.2	58.6
	4-6 mi.	292.7	348.8	14.0
	6+ mi.	185.4	430.1	14.7

This table depicts welfare measures decomposed by category. Consumer welfare is summed across all i, j, t in each category. I compute taxi profits from total matches multiplied by prices for each origin, destination, and time-of-day. Profits reflect daily, single-shift revenues net of fuel costs. Sections I–V refer to those in Fig. 1.

6 Counterfactual: Pricing for Dynamic Efficiency

As the above results show, uniform pricing across heterogenous demand will lead to inefficient allocations of service. Mis-pricing inefficiencies may be further amplified by the inter-dependency in allocations from one period to the next. This section studies a set of simple and easily implemented changes to existing tariffs in the New York market with the purpose of generating better welfare

outcomes consistent with the equilibrium dynamics of supply and demand. The changes introduce price flexibility with respect to location, time-of-day, or distance. Flexibility along these dimensions plays two important roles. First, it offers the efficiency of a price mechanism to better clear markets. Second, flexible prices can lead to an endogenous spatial re-allocation of empty capacity to different regions of the city. I show that it is possible to increase both profits and consumer welfare by optimally implementing each type of flexible tariff.

To study flexible tariffs, I create three possible regimes: location-based pricing, time-based pricing and distance-based, or non-linear pricing. In the first regime, I allow prices to vary in segments of 2–3 hours across the day (the four segments are 7a–9a, 9a–11a, 11a–1p, 1p–4p). In the second, I allow prices to vary in each of the four regions I–IV in Figure 1. The third considers non-linear pricing, where prices can vary along three dimensions: the fixed fare, the per-mile fare, and a squared-distance fare. For each, I search across a set of multipliers to existing fares associated with each combination of origin, destination and time.[39] A description of each is outlined in Table 9. For each candidate set of new prices, I recompute origin-destination-specific demand, profits, and transitions, and I resolve the dynamic spatial equilibrium among taxis. This method uses estimated demand parameters to recompute both the level of demand in each location as well as the share of destinations demanded from within each location.

To account for the potential impact on consumers due to changing wait times, I calibrate waiting time elasticities to be -1.0, close to the estimates of Frechette et al. (2019) and Buchholz et al. (2020).[40] I compute a measure of waiting time as the mass of unmatched consumers in each period multiplied by the period length. Given these two measures I endogenize the demand response with respect to the percentage change in waiting times, which I compute as the percentage difference between the waiting time at baseline prices and the waiting time at any counterfactual price. I provide details of this procedure in Appendix A.11.1.

Within each flexible price regime, I numerically solve for an optimal configuration according to three different criteria: maximize total surplus, maximize consumer surplus, and maximize the total number of trips. The different criteria represent different planner objectives. In addition, I construct two benchmark counterfactuals in order to compare the new pricing regimes with two possible technological advances without re-pricing. One represents a frictionless matching technology, where nearby drivers are always matched to customers without searching. This technology is representative of modern app-based matching that matches taxis with consumers when they

[39] For example, if at the fare structure of $\$2.50 + \$2.00/mile$, a trip from location i to j costs \$10.00, a multiplier of 0.8 on trips from i to j would change this fare to \$8.00.

[40] Without waiting time elasticities, optimal prices would be driven very low as consumer surplus would grow faster than profits are lost under a fixed total supply, yet the probability of finding a taxi would also approach zero. Since the empirical evidence points to elastic responses, I do not solve for this pathological case. To measure the importance of the calibration, Appendix A.11.4 replicates the same analysis under alternative calibrated values.

Table 9: Description of Counterfactual Policies and Multipliers

Counterfactual Regime	**Multiplier Description**	**Example**
Location-Based Pricing	$\theta_k \cdot q_{ij}^t$ for $i \in$ Region k	$\theta_2 = 0.85 \Rightarrow$ 15% discounted baseline price q_{ij}^t for trips starting in Region II
Time-Based Pricing	$\theta_k \cdot q_{ij}^t$ for $t \in k^{th}$ element of {7-9a, 9-11a, 11a-2p, 2-4p}	$\theta_2 = 0.85 \Rightarrow$ 15% discounted baseline price q_{ij}^t for all trips during 9-11a
Non-Linear Pricing	$\theta_0 \cdot$ flag fare $+ \theta_1 \cdot$ dist. fare $+ \theta_2 \cdot$ dist.^{2}	$\theta_1 = 0.9, \theta_2 = 0.9, \theta_3 = -0.1 \Rightarrow$ new fare = \$1.80 + 2.25/mi. − 0.1/mi^2

This table details the three sets of tariff pricing rules considered in the counterfactual analysis. Prices are denoted q_{ij}^t and refer to the baseline fare price for a trip from i to j at time t, where the baseline price is set at August 2012 levels of \$2.00 fixed fare + \$2.50 per-mile.

are close to each other. The other technology is that of a social-planner as dispatcher, in which vacant cabs are directed to search in the areas where their expected contribution to total welfare is highest. This technology represents dynamically efficient search, whereas frictionless matching represents statically efficient search.

6.1 Results

Table 10 displays the dynamically efficient tariffs associated with location-, time- and distanced-based fares. Nearly all prices fall by around 10–20% in each regime. Even then, driver profits improve as utilization rates increase by 7–10%. Total welfare gains up to 4.0% and consumer welfare gains up to 9.3% are possible. The best regime offers \$193 thousand per day in welfare improvements or about \$0.91 per trip. Interestingly, different planner objectives within a price regime mostly coincide: under each of the three tariff structures, essentially the same set of optimal prices maximize both total surplus and consumer surplus. All regimes also improve taxi utilization rates, highlighting the role of flexible prices in allocating spare capacity to more productive areas. Each of these, however, gives a higher share of welfare to consumers by around 2–3%. Finally, matches rise by more than welfare, as lower average prices introduce more marginal consumers to the market.[41]

The final two rows of Table 10 contrast these results with a set of two benchmark counterfactuals representing different technology improvements. First is *Efficient Incentives* (EI) in which drivers' profit motives are replaced by search incentives that are socially optimal, holding fixed prices and matching technology. This scenario is akin to one in which a planner dispatches vacant cabs to

[41] The results corroborate theoretical insights of Schmalensee (1981) and Varian (1985) which find that a necessary condition for price discrimination to enhance social welfare is that it accompanies an increase in output.

locations with the highest social value. To compute the EI equilibrium, I replace drivers' profit functions in each location and at each time point with the marginal social welfare function.[42] By solving equilibrium, vacant drivers will allocate themselves according to socially efficient incentives. The second is *Matching Technology* (MT), where prices are equal to the baseline tariff but the matching technology is frictionless and given by $m(\lambda_i^t, v_i^t) = \min(\lambda_i^t, v_i^t)$. This case approximates a modern ride-share platform, where supply and demand in the same location are guaranteed to match, but taxis must still choose locations to search.[43] Consumer welfare benefits from this technology are somewhat larger than the benefits to optimal pricing and much better for taxis.

The pricing counterfactuals offer a combination of improved search incentives and more efficient trip pricing. Compared to the EI counterfactual, optimal pricing can attain about half of the consumer welfare gains. Since optimal pricing causes a drop in prices, taxi drivers do substantially better with the EI technology. Because under EI the market is still constrained by inefficient matching, the MT counterfactual illustrates even more impressive gains; frictionless matching generates predictably large benefits and provides a rationale for the success of modern ride-hail services.

The best performing tariff I study attains about 57% of the consumer benefits of EI and 42% of MT. Interestingly, MT generates only slightly more matches than the optimal tariff and EI even less; lower average prices under the new tariffs induce many more additional customers to enter the market despite lower wait times induced by EI and MT. It is noteworthy that the EI technology leads to slightly higher utilization than MT. Each of the benchmark technologies and all pricing counterfactuals are to some extent implementable in the real-world. However, pricing is simpler and does not require sophisticated tracking and dispatching systems.

6.2 Discussion: Comparing Tariff Changes with Real-time Pricing

The pricing counterfactuals in Table 10 are configured to average patterns of supply and demand. Implementing this type of price regime would not require any special technology; the regulator could simply post new tariffs that differ by time or location, both of which have been applied in various cities, such as a zone-based pricing system used in Washington, D.C. In contrast, a common feature of ride-hail platforms is to use real-time pricing (e.g., Uber's "Surge Pricing"). Real-time pricing re-adjusts prices in each period to accommodate unexpected shifts in supply or demand. However, conventional real-time pricing is not forward-looking. If it were, then my approach in the analysis above would apply. Nevertheless, better average pricing of the form indicated in Table 10 may enable the regulator to alleviate some of the need for additional real-time pricing, as supply and

[42] For example, if a location under consideration by a driver has 15 taxis, the profit to search in that location is the expected gain in social surplus by adding a 16th taxi, including both the matching friction as well as the value of all possible trips that could be generated from there.

[43] Note that this counterfactual does not simulate gains from other attributes of ride-sharing services such as the value of less waiting, the certainty of a match, app-based payments, etc.

Table 10: Efficient Pricing and Technology: Counterfactual Results

Type	Efficiency-optimized Multipliers θ_1	θ_2	θ_3	θ_4	Total Surplus (,000 USD)	Consumer Surplus (,000 USD)	Consumer Rent Share (percent)	Matches (,000)	Taxi Utilization (percent)
Baseline - 8/2012	1.00	1.00	1.00	1.00	5726.2	2452.6	42.8	211.3	42.2
Location-Based Pricing									
Max Total Surplus	0.83	0.87	0.72	1.25	5886.2 (+3.3 %)	2628.9 (+7.2 %)	44.7	257.3 (+23.0 %)	51.6
Max Cons. Surplus	0.83	0.86	0.72	1.25	5885.2 (+3.3 %)	2642.1 (+7.7 %)	44.9	257.6 (+23.1 %)	51.6
Max Matches	0.87	0.87	0.65	1.25	5849.0 (+2.7 %)	2604.5 (+6.2 %)	44.5	260.4 (+24.5 %)	51.9
Time-Based Pricing									
Max Total Surplus	0.88	0.90	0.84	0.81	5876.4 (+3.4 %)	2640.5 (+7.9 %)	44.9	246.0 (+17.8 %)	49.9
Max Cons. Surplus	0.88	0.90	0.84	0.81	5876.4 (+3.4 %)	2640.5 (+7.9 %)	44.9	246.0 (+17.8 %)	49.9
Max Matches	0.67	0.87	0.87	0.89	5781.0 (+1.7 %)	2544.9 (+4.0 %)	44.0	253.4 (+21.4 %)	49.8
Non-Linear Pricing									
Max Total Surplus	1.00	0.72	-0.25	.	5919.5 (+4.0 %)	2674.3 (+9.1 %)	45.2	242.5 (+16.0 %)	51.9
Max Cons. Surplus	1.00	0.71	-0.25	.	5919.4 (+4.0 %)	2679.5 (+9.3 %)	45.3	242.8 (+16.2 %)	52.0
Max Matches	0.65	1.24	0.20	.	5740.0 (+0.9 %)	2499.6 (+2.0 %)	43.5	258.5 (+23.7 %)	49.1
Technology Improvement	(at baseline prices)								
Efficient Incentives	.	.	.	.	6686.0 (+16.8 %)	2850.8 (+16.2 %)	42.6	247.3 (+17.1 %)	52.7
Matching Technology	.	.	.	.	6949.8 (+23.5 %)	2869.4 (+22.0 %)	41.3	262.7 (+24.4 %)	51.9

This table shows, for each weekday day-shift, the estimated change in total welfare (profits plus consumer surplus), consumer surplus, consumers' share of total surplus, total matches, and utilization rates across each counterfactual price policy. Each pricing policy shown is a rule that applies to four policy-specific multipliers on the baseline price p_{ijt} for every route, given by \$2.50 + \$2.00/mile. In location-based pricing, the multipliers $\theta_k(i)$ apply to p_{ijt} where $k(i) \in \{1, 2, 3, 4\}$ indexes regions r. In time-based pricing, the multipliers $\theta_k(t)$ apply to p_{ijt} where $k(t) \in \{1, 2, 3, 4\}$ indexes the time ranges of 7a–9a, 10a–11a, 12p–1p, 2p–4p. In non-linear pricing, the multipliers $\theta_k(i, j)$ apply to p_{ijt} where $k(i, j) \in \{1, 2, 3\}$ are coefficients that change existing tariffs according to $\theta_1 \cdot \textit{base fare} + \theta_2 \cdot \textit{fare per-mile} + \theta_3 \cdot \textit{miles}^2$. The final rows depict outcomes under two simulated technologies, computed at baseline prices.

demand will be more efficiently allocated across space and time, limiting the types of imbalances for which surge prices are designed to accommodate.

7 Conclusion

Supply and demand in the taxi market are uniquely shaped by space. Price regulations influence how taxis and their customers search for one another and how often they find each other. This paper models a dynamic spatial equilibrium in the search and matching process, showing how both supply and demand can be recovered from high-frequency trip data. Using data from New York, I estimate this model to recover the expected spatial and inter-temporal distribution of taxis and mean customer arrivals. Exploiting a change in regulated pricing, I estimate demand every 5 minutes across 39 neighborhoods and measure the distribution of search frictions across time and space. I show that total welfare attained in the New York market is \$5.7 million per day-shift on a typical weekday with about 43% of this surplus accruing to consumers.

The estimated model also allows me to recompute the equilibrium taxi supply, spatial matches, search frictions and welfare outcomes under alternative price schedules and a frictionless matching technology. I show that by optimally configuring tariffs to vary according to spatial regions, vacant taxi capacity is endogenously relocated where it is valued the most, providing up to 7.7% more welfare and 24% more trips. A more sophisticated tariff could offer different prices across a combination of location, time and distance. These counterfactual estimates suggest that additional gains might be possible in such a regime, although they would come at the expense of simplicity. The gains in matches due to optimal dynamic pricing are comparable to the gains due to a perfect static matching technology and superior to a setting in which drivers search according to efficient incentives, underscoring the importance of pricing even among modern ride-hail platforms.

References

Acemoglu, D. and M. K. Jensen (2015): "Robust comparative statics in large dynamic economies," *Journal of Political Economy*, 123, 587–640.

Allen, J., R. Clark, and J.-F. Houde (2014): "Search frictions and market power in negotiated price markets," Tech. rep., National Bureau of Economic Research.

Arcidiacono, P. and P. B. Ellickson (2011): "Practical methods for estimation of dynamic discrete choice models," *Annu. Rev. Econ.*, 3, 363–394.

Brancaccio, G., M. Kalouptsidi, and T. Papageorgiou (2019): "A guide to estimating matching functions in spatial models," *International Journal of Industrial Organization*, 102533.

——— (2020a): "Geography, Transportation, and Endogenous Trade Costs," *Econometrica*, 88, 657–691.

Brancaccio, G., M. Kalouptsidi, N. Rosaia, and T. Papageorgiou (2020b): "Efficiency in decentralized transport markets," Tech. rep., mimeo, Harvard University.

Brophy, T. (2013): "gpsmap: Routine for verifying and returning the attribute table of given decimal degree GPS coordinates," in *2013 Stata Conference*, Stata Users Group, 14.

Buchholz, N., L. Doval, J. Kastl, F. Matejka, and T. Salz (2020): "The Value of Time Across Space: Evidence from Auctioned Cab Rides," Working Paper.

Buchholz, N., M. Shum, and H. Xu (2017): "Flexible Work Hours and Dynamic Labor Supply: Evidence from Taxi Drivers," Working Paper.

Butters, G. R. (1977): "Equilibrium distributions of sales and advertising prices," *The Review of Economic Studies*, 465–491.

Cairns, R. D. and C. Liston-Heyes (1996): "Competition and regulation in the taxi industry," *Journal of Public Economics*, 59, 1–15.

Camerer, C., L. Babcock, G. Loewenstein, and R. Thaler (1997): "Labor supply of New York City cabdrivers: One day at a time," *The Quarterly Journal of Economics*, 112, 407–441.

Castillo, J. C. (2020): "Who Benefits from Surge Pricing?" Working Paper.

Castillo, J. C., D. Knoepfle, and G. Weyl (2017): "Surge Pricing Solves the Wild Goose Chase," Working Paper.

Crawford, V. P. and J. Meng (2011): "New york city cab drivers' labor supply revisited: Reference-dependent preferences with rational expectations targets for hours and income," *The American Economic Review*, 101, 1912–1932.

Diamond, P. A. (1981): "Mobility costs, frictional unemployment, and efficiency," *The Journal of Political Economy*, 798–812.

——— (1982a): "Aggregate demand management in search equilibrium," *The Journal of Political Economy*, 881–894.

——— (1982b): "Wage determination and efficiency in search equilibrium," *The Review of Economic Studies*, 49, 217–227.

Duffie, D., N. Gârleanu, and L. H. Pedersen (2002): "Securities lending, shorting, and pricing," *Journal of Financial Economics*, 66, 307–339.

——— (2005): "Over-the-Counter Markets," *Econometrica*, 73, 1815–1847.

Ericson, R. and A. Pakes (1995): "Markov-perfect industry dynamics: A framework for empirical work," *The Review of Economic Studies*, 62, 53–82.

Farber, H. S. (2005): "Is Tomorrow Another Day? The Labor Supply of New York City Cabdrivers," *The Journal of Political Economy*, 113, 46–82.

——— (2008): "Reference-dependent preferences and labor supply: The case of New York City taxi drivers," *The American Economic Review*, 98, 1069–1082.

Fershtman, C. and A. Pakes (2012): "Dynamic games with asymmetric information: A framework for empirical work," *The Quarterly Journal of Economics*, 127, 1611–1661.

Flath, D. (2006): "Taxicab regulation in Japan," *Journal of the Japanese and International Economies*, 20, 288–304.

Frechette, G. R., A. Lizzeri, and T. Salz (2019): "Frictions in a competitive, regulated market: Evidence from taxis," *American Economic Review*, 109, 2954–92.

Gallick, E. C. and D. E. Sisk (1987): "Reconsideration of Taxi Regulation," *JL Econ. & Org.*, 3, 117.

Gavazza, A. (2011): "The role of trading frictions in real asset markets," *The American Economic Review*, 101, 1106–1143.

Häckner, J. and S. Nyberg (1995): "Deregulating taxi services: a word of caution," *Journal of Transport Economics and Policy*, 195–207.

Hall, J., C. Kendrick, and C. Nosko (2015): "The effects of Uber?s surge pricing: A case study," *The University of Chicago Booth School of Business*.

Hall, R. E. (1979): "A theory of the natural unemployment rate and the duration of employment," *Journal of monetary economics*, 5, 153–169.

Hong, H. and M. Shum (2010): "Pairwise-difference estimation of a dynamic optimization model," *The Review of Economic Studies*, 77, 273–304.

Hopenhayn, H. A. (1992): "Entry, exit, and firm dynamics in long run equilibrium," *Econometrica: Journal of the Econometric Society*, 1127–1150.

Kiyotaki, N. and R. Wright (1989): "On money as a medium of exchange," *Journal of Political economy*, 97, 927–954.

——— (1993): "A search-theoretic approach to monetary economics," *The American Economic Review*, 63–77.

Kreindler, G. E. (2020): "The welfare effect of road congestion pricing: Experimental evidence and equilibrium implications," Tech. rep., mimeo, Harvard University.

Lagos, R. (2000): "An Alternative Approach to Search Frictions," *The Journal of Political Economy*, 108, 851–873.

——— (2003): "An analysis of the market for taxicab rides in New York City," *International Economic Review*, 44, 423–434.

Light, B. and G. Y. Weintraub (2021): "Mean field equilibrium: uniqueness, existence, and comparative statics," *Operations Research*.

Melitz, M. and C. James (2007): "The Dynamics of Firm-Level Adjustment to Trade," in *The Organization of Firms in a Global Economy*, ed. by ed. E. Helpman, D. Marin, and T. Verdier, Harvard University Press.

Mortensen, D. T. (1982a): "The matching process as a noncooperative bargaining game," in *The economics of information and uncertainty*, University of Chicago Press, 233–258.

——— (1982b): "Property rights and efficiency in mating, racing, and related games," *The American Economic Review*, 968–979.

——— (1986): "Job search and labor market analysis," *Handbook of labor economics*, 2, 849–919.

——— (1988): "Matching: finding a partner for life or otherwise," *American Journal of Sociology*, S215–S240.

Mortensen, D. T. and C. A. Pissarides (1999): "New developments in models of search in the labor market," *Handbook of labor economics*, 3, 2567–2627.

Petrongolo, B. and C. A. Pissarides (2001): "Looking into the black box: A survey of the matching function," *Journal of Economic literature*, 390–431.

Pissarides, C. A. (1984): "Search intensity, job advertising, and efficiency," *Journal of Labor Economics*, 128–143.

——— (1985): "Short-run equilibrium dynamics of unemployment, vacancies, and real wages," *The American Economic Review*, 676–690.

Rogerson, R., R. Shimer, and R. Wright (2005): "Search-theoretic models of the labor market: A survey," *Journal of economic literature*, 43, 959–988.

Rosaia, N. (2020): "Competing Platforms and Transport Equilibrium: Evidence from New York City," Tech. rep., mimeo, Harvard University.

Rust, J. (2016): "Dynamic programming," *The New Palgrave Dictionary of Economics*, 1–26.

Schaller, B. (2007): "Entry controls in taxi regulation: Implications of US and Canadian experience for taxi regulation and deregulation," *Transport Policy*, 14, 490–506.

Schmalensee, R. (1981): "Output and welfare implications of monopolistic third-degree price discrimination," *The American Economic Review*, 71, 242–247.

Schrieber, C. (1975): "The Economic Reasons for Price and Entry Regulation of Taxicabs," *Journal of Transport Economics and Policy*, 9, 268–79.

Small, K. A. (2012): "Valuation of travel time," *Economics of Transportation*, 1, 2 – 14.

Stokey, N. L. and R. E. Lucas (1989): *Recursive methods in economic dynamics*, Harvard University Press.

Thakral, N. and L. T. Tô (2017): "Daily Labor Supply and Adaptive Reference Points," Tech. rep., Working Paper.

Varian, H. R. (1985): "Price discrimination and social welfare," *The American Economic Review*, 75, 870–875.

Weintraub, G. Y., C. L. Benkard, P. Jeziorski, and B. Van Roy (2008a): "Nonstationary Oblivious Equilibrium," *Manuscript, Columbia University*.

Weintraub, G. Y., C. L. Benkard, and B. Van Roy (2008b): "Markov perfect industry dynamics with many firms," *Econometrica*, 76, 1375–1411.

Winston, C. and C. Shirley (1998): *Alternate route: Toward efficient urban transportation*, Brookings Institution Press.

A Appendix

A.1 Data Cleaning

Taxi trip and fare data are subject to some errors from usage or technology flaws. I first drop any apparently erroneous observations (e.g. well outside of the New York Area). Next, I drop observations outside of the locations of interest, Manhattan and the two airports. This section describes how data are cleaned and provides some related statistics.

Data Cleaning Routine

1. Begin with merged trip and fare data from August 2012 to September 2012.
2. Drop observations outside of USA boundaries.
3. Drop observations outside of the New York area.
4. Drop duplicates in terms of taxi driver ID and date-time of pickup.
5. Drop observations outside of Manhattan (bounded above by 125th st.) or either airport.
6. Drop observations that cannot be mapped to any of the 39 locations in Figure 1.

Table A1 shows the incidence of each cleaning criterion.

Table A1: Data Cleaning Summary

Procedure	**Criterion Applied**	**Obs. Change**
	1. Initial data	28,927,944
Drop Errors	2. Obs. outside USA	-749,623
	3. Obs. outside NYC	-5,298
	4. Drop duplicates	-57
Drop Unusable Data	5. Keep manhattan + airports	-3,622,803
	6. Un-mapped data	-117,249

Final Data Set: 24,432,914 observations

This table summarizes the data cleaning routine for TLC data from 8/1/2012-9/30/2012.

A.2 Map Preparation

I generate the 39 spatial locations shown in Figure 1 by uniting census tracts, representing 98% of all taxi ride originations. While there is some arbitrariness involved in their exact specification, the number of locations used is a compromise between tradeoffs; more locations give a richer map of

spatial choice behavior, but impose greater requirements on both data and computation. Because of the sparsity of data in the other boroughs, I focus on the set of locations falling within Manhattan below 125th street, three nearby areas within Brooklyn and Queens, and the two New York City airports, Laguardia and J.F.K.

The following graphics show how I convert raw GPS data points into locations.[44] I begin with New York census tracts, 425 of which cover the locations of interest. From these, I examine taxi activity, and group census tracts into areas with clusters of activity. Figure A1 shows the origin of each trip in a 10-percent sample of TLC data. It can be seen that trip origins are most heavily concentrated around major streets, particularly north-south and diagonal thoroughfares in the north, with more scattered origin points in Lower Manhattan and Midtown Manhattan. The densest neighborhoods are clearly those in Midtown. I have grouped census tracts to form locations in a way that attempts to minimize the number of location boundaries that overlap clusters of activity, for example the clusters around a busy transit station.

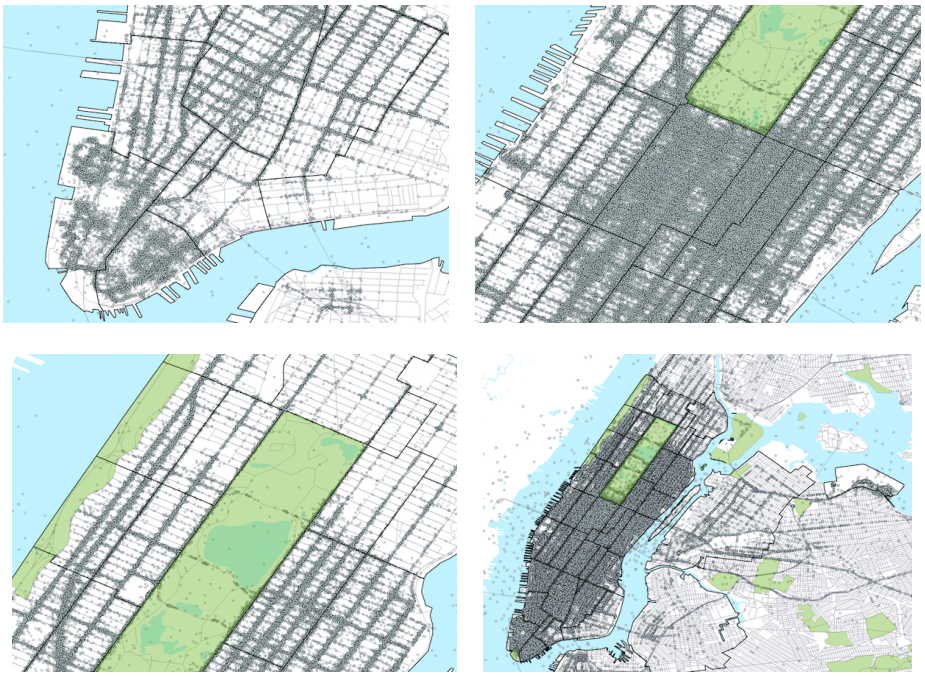

Figure A1: Mapping GPS points to Locations

This figure shows TLC data for a 10 percent sample of taxi trips taken in August 2012. Each dot on the map is the GPS origin of a trip.

[44] This association is achieved via the point-in-polygon matching procedure outlined in Brophy (2013).

A.3 Additional Summary Statistics

This sub-section provides additional descriptive information about taxi trips. Table A2 decomposes the trip and fare summary statistics by month, before and after the fare change.

Table A2: Taxi Trip and Fare Summary Statistics by Month

Sample	Rate Type	Variable	Obs.	10%ile	Mean	90%ile	S.D.
Weekdays, Day-Shift, Manhattan & Boro. (Aug. 2012)	Standard Fares	Total Fare ($)	4,299,474	4.50	9.20	15.7	5.46
		Dist. Fare ($)	4,299,474	1.04	4.19	8.96	4.66
		Flag Fare ($)	4,299,474	2.50	2.5	2.5	0
		Distance (mi.)	4,299,474	0.72	2.29	4.68	2.34
		Trip Time (min.)	4,299,474	4.00	12.24	22.48	7.95
	JFK Fares	Total Fare ($)	81,493	45	45	45	0.75
		Distance (mi.)	81,493	4.0	16.28	20.94	5.91
		Trip Time (min.)	81,493	28.00	46.01	66.00	18.44
Weekdays, Day-Shift, Manhattan & Boro. (Sep. 2012)	Standard Fares	Total Fare ($)	3,823,041	5.00	11.23	19.70	7.15
		Dist. Fare ($)	3,823,041	1.20	5.17	11.00	5.89
		Flag Fare ($)	3,823,041	2.50	2.5	2.5	0
		Distance (mi.)	3,823,041	0.70	2.27	4.65	2.38
		Trip Time (min.)	3,823,041	4.12	13.30	25.0	9.01
	JFK Fares	Total Fare ($)	82,244	52.00	51.56	52.00	1.96
		Distance (mi.)	82,244	9.11	16.54	20.98	5.63
		Trip Time (min.)	82,244	28.00	46.69	68.75	18.35

Taxi trip and fare data come from New York Taxi and Limousine Commission (TLC). This table provides statistics related to individual taxi trips taken in New York City in the months of August 2012 and September 2012 for two fare types. The first is the standard metered fare (TLC rate code 1), in which standard fares apply. The second is a trip to or from JFK airport (TLC rate code 2). Total Fare and Distance data are reported for each ride. While not reported directly or separated from waiting costs, I predict distance and flag fares using the prevailing fare structure on the day of travel and the distance travelled.

Table A3 summarizes how cabs move around space. Panel (a) aggregates all passenger trips into Regions and all times of day to display the density of employed-taxi transitions between regions. This matrix represents customer preferences for travel. At the end of a trip, taxis become vacant in these new regions. Panel (b) displays the observed location of a matched taxi, at the start of a ride, conditional on the last observed location of the same taxi, at the previous drop-off location. Thus Panel (b) reveals the transition of vacant cabs, though not accounting for period-by-period choices – only the eventual location of the next pickup. As I will show, an equilibrium estimate of drivers' period-by-period spatial choices closely mirrors the pattern of Panel (b), but with higher frequency weights put on same-location transitions. The difference occurs because drivers search on average for 2.5 periods before finding a passenger. The ride-to-ride transitions are therefore more dispersed.

Table A3: Observed Pickup and Drop-off Activity by Region

Origin \ Destination	*Region I*	*Region II*	*Region III*	*Region IV*	*Region V*
Region I	0.357	0.152	0.060	0.230	0.102
Region II	0.484	0.623	0.444	0.251	0.295
Region III	0.102	0.185	0.471	0.144	0.103
Region IV	0.035	0.012	0.010	0.332	0.102
Region V	0.022	0.027	0.015	0.042	0.398

(a) Passenger Trips

Origin \ Destination	*Region I*	*Region II*	*Region III*	*Region IV*	*Region V*
Region I	0.762	0.061	0.014	0.221	0.062
Region II	0.183	0.775	0.131	0.117	0.131
Region III	0.029	0.141	0.834	0.149	0.186
Region IV	0.010	0.007	0.007	0.371	0.091
Region V	0.015	0.016	0.014	0.141	0.531

(b) Vacant Transitions

This table summarizes transitions in the TLC data. Data in the table are aggregated to the regions from Figure 1. Panel (a) depicts the transition density of taxi-passenger matches and Panel (b) depicts the transition of vacant taxis between each drop-off and the same driver's subsequent pickup.

A.4 Additional Detail on September 2012 Fare Hike

Section 2.3 highlights the impact of the September 2012 fare hike on average fares and total trips by trip distance. In this subsection I show the impact on trips by route instead of distance. Table A4 splits all trips into origins and destinations across the five aggregate regions depicted in Figure 1. This table shows that the average increase in fares paid following the fare hike varied between about 15% to 23%. The lowest increase occurred across airport routes, where the JFK flat-fare only increased by 15%, and in shorter routes in which origin and destination regions were the same. The decline in matches across routes follows a similar but less consistent pattern. Since matches are formed by changes in both supply and demand, these patterns are difficult to predict in the absence of an equilibrium model.

Table A4: Route-Specific Effects of the Fare Hike

Origin \ Destination	*Region I*	*Region II*	*Region III*	*Region IV*	*Region V*
Region I	0.149	0.183	0.204	0.177	0.160
Region II	0.184	0.159	0.211	0.211	0.164
Region III	0.221	0.231	0.181	0.224	0.161
Region IV	0.157	0.186	0.207	0.167	0.174
Region V	0.160	0.168	0.161	0.202	0.085

(a) Average Fare Response

Origin \ Destination	*Region I*	*Region II*	*Region III*	*Region IV*	*Region V*
Region I	−0.129	−0.173	−0.112	−0.123	−0.140
Region II	−0.157	−0.225	−0.178	−0.180	−0.130
Region III	−0.185	−0.222	0.002	−0.226	−0.217
Region IV	−0.136	−0.233	−0.104	−0.111	−0.203
Region V	−0.096	−0.108	−0.194	−0.213	−0.397

(b) Average Trip Response

This table shows the mean change in log fares and log number of trips following the September 4, 2012 fare hike. Fare calculation includes base fares, taxes, surcharges and imputed tips. Data in the table are aggregated to the regions from Figure 1. Panel (a) depicts the impact on average fares and Panel (b) depicts the impact on average number of trips by location.

A.5 Medallion Counts

Figure A2 shows the unique number of medallions observed each day of August and September 2012 in the TLC data during weekdays during the day shift. The mean across all days is 11,911.88.

It should be noted however, that about 2% of trips occur outside of the 39 locations defined in this paper during this period. This implies that approximately 11,673 medallions are active within the locations, with some additional diminishment in reality due to breaks, refueling, etc. The second point of this figure is that the medallion counts seem fairly stable between price changes, lending support for the assumption that this overall level remains constant. The drop on September 3rd seems to reflect the extra servicing of metering equipment just prior to the tariff change on September 4th.

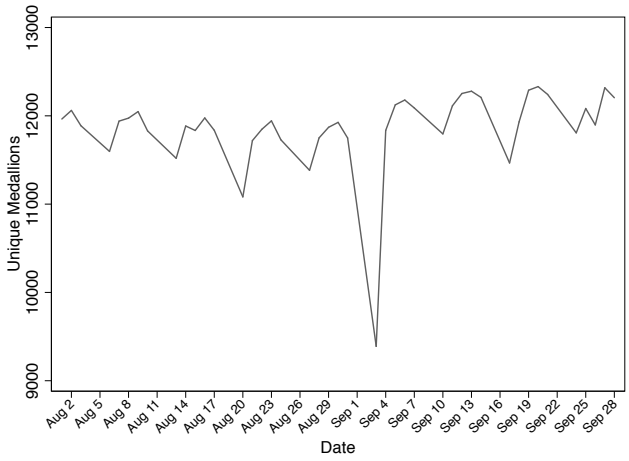

Figure A2: Medallions per day, Aug-Sep 2012

This figure depicts the unique number of medallions observed each day of August and September 2012 in the TLC data during weekdays during the day-shift.

Figure A3 illustrates the time-of-day appearance of medallions by showing the number of active taxis by hour beginning at 6am. To compute this, I first calculate the hours in which a taxi is on a shift by using the shift definition common in the literature. This definition specifies that a driver is on a shift when he shows up in the data (i.e., a ride is given by the driver) and remains on shift until a gap of five or more hours between observed rides occurs. Next, I count how many taxis are working a shift in each hour and plot this count by hour. Note that levels shown will be smaller than the total medallion count of 13,237. One reason is that a driver will not appear immediately upon starting a shift, as it takes time to find passengers. As a result there may be significant downward bias in the mornings.

A.6 Details on State Transitions

The combined set of transitions forms an aggregate transition kernel that defines the law-of-motion, given by $Q(\mathcal{S}^{t+1}|\mathcal{S}^t) = Q^{employed}(\boldsymbol{e}_i^{t+1}|\boldsymbol{e}_i^t, \boldsymbol{M}^t, \boldsymbol{m}^t) + Q^{vacant}(\boldsymbol{v}_i^{t+1}|\boldsymbol{v}_i^t, \sigma^t)$. Here I use addition in-

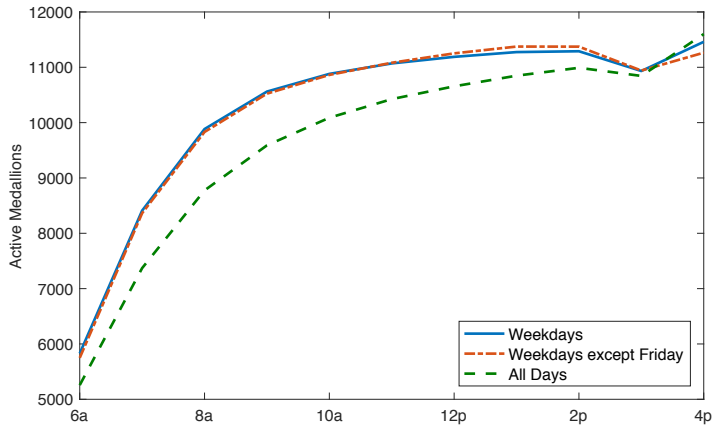

Figure A3: Total medallion activity by hour

This figure is derived from August 2012 TLC trip data. It shows the number of unique medallions present in the data by hour-of-day, where presence is determined by finding the first- and last-appearance times within the day-shift, and counting each taxi as *active* in the hours between (inclusive of end-points). It approximates the total number of taxis working during the day shift, by hour, averaged across each day in the data set. Note that earlier hours will be systematically downward biased because drivers who begin a shift are not observed until finding their first passenger.

stead of union notation to signify that the transitions of both employed and vacant cabs lead to new stocks of vacant cabs.

Let the following objects be defined:

$\boldsymbol{e}^t$ be the $(L+K)\times 1$ vector of employed cabs at the start of period t, where L is the total number of search locations and K is the total number of positions between locations (e.g., if a route takes 4 periods to travel, there is a pickup-location i, 2 in-between positions, and a drop-off location j). $\boldsymbol{m}^t$ is the $(L+K)\times 1$ vector of matches in period t, where the first L entries are the matches in each location and the next K entries are zeros (as no matches occur while cabs are employed and in-transit. $\boldsymbol{M}^t$ be the $(L+K)\times(L+K)$ vector of one-period transition probabilities of customers from all locations {1,...,L} and all in-between positions {1,...,K}. The number of in-between positions is based on the mean number of periods it takes to travel from any locations i to j, rounded to the nearest period (e.g., an average 16-minute trip would be considered 3.2 periods, and then rounded to be 3 periods, with a single in-between position). $\boldsymbol{m}^{t-\tau_{ji}}$ describes how many drop-offs will occur in period t, which is the number of matches made in each pick-up location in τ_{ji} prior periods, and transition matrix $\boldsymbol{M}^{t-\tau ji}$ re-distributes those earlier matches to locations at time t.

Given these objects, we can write the state transitions of employed cabs as follows, reflecting

the transitions of new matches and already-employed taxis at time t, minus the time t drop-offs:

$$\boldsymbol{e}^{t+1} = \left((\boldsymbol{e}^t + \boldsymbol{m}^t) \times \boldsymbol{M}^t\right) - \left(\boldsymbol{m}^{t-\tau_{ji}} \times \boldsymbol{M}^{t-\tau_{ji}}\right). \tag{16}$$

Next, I define the state transitions of vacant taxis. Let $\boldsymbol{v}^t$ be the $(L+K) \times 1$ vector of vacant taxis in all search locations and in-between locations $\{1, ..., (L+K)\}$. Note that there *may* be taxis in the in-between locations. For example, driving vacant to the airport may take more than one period. Let $\boldsymbol{v}^t$ be the $(L+K) \times (L+K)$ vector of one-period transition probabilities of vacant taxis from all locations {1,...,L} and all in-between positions {1,...,K}. Then the state transitions of vacant cabs is given by the vector of vacant cabs at the start of period t minus the period t matches, multiplied by the policy functions in each period:

$$\boldsymbol{v}^{t+1} = (\boldsymbol{v}^t - \boldsymbol{m}^t) \times \boldsymbol{\sigma}^t. \tag{17}$$

Summing these two transition formulas defines the state transitions from t to $t+1$.

A.7 Proofs

Proof of Proposition 3.1

Part (i): Equilibrium Existence

Proof. In the last period in which actions may be taken, t=T-1, policy functions are simply determined by the payoffs attributable to search in the final period. The sum of policies among agents in a particular location are summarized by the following

$$\sigma_{ij}^{T-1} \equiv P_i^{T-1}[j_a|\mathcal{S}^{T-1}] = \frac{exp\left(p_j(\lambda_j^T, v_j^T) \cdot \sum_l \Pi_{jl}/\sigma_\varepsilon - c_{ij}\right)}{\sum_k exp\left(p_k(\lambda_k^T, v_k^T) \cdot \sum_l \Pi_{kl}/\sigma_\varepsilon - c_{ik}\right)}. \tag{18}$$

Further note that the final period state v_j^T can be described by $v_j^T = \sum_i (v_i^{T-1} - m_i^{T-1}) \cdot \sigma_{ij}^{T-1} + \left(\sum_{i,\tau} m_i^{T-\tau_{ij}} M_{ij}^{T-\tau_{ij}}\right)$ from the definition of the transition kernel (see Section A.6). Let $\boldsymbol{\sigma^{T-1}} = \sigma_{ij}^{T-1}$ for all $i \in \{1, ..., L\}$ and all $j \in \{1, ..., L\}$. In prior periods, policies are similarly defined except for the inclusion of continuation values, which are bounded below by zero and above by the maximum fare revenue attainable in the remaining periods up to T. For each period let $F(\boldsymbol{\sigma^t})$ define the above mapping between the vector $\boldsymbol{\sigma}^t \in \mathbb{S}^{L \times L}$ to itself, where $\mathbb{S}^n$ denotes the $n-$dimensional unit ball. Direct application of Brouwer's Fixed-Point theorem implies the existence of a fixed point in F, which by repeated application for $t = 1, ..., T$ implies that the equilibrium $\hat{\boldsymbol{\sigma}}^{\boldsymbol{t}}$ for $t = 1, ..., T$ exists. □

Part (ii): Equilibrium Uniqueness

Proof. To show that the fixed point defining equilibrium is unique, suppose there are two such equilibria given by $\boldsymbol{\sigma}_1^{T-1}$ and $\boldsymbol{\sigma}_2^{T-1}$. Without loss of generality this implies that there exists some i, j for which $\sigma_{1,ij}^{T-1} > \sigma_{2,ij}^{T-1}$. Thus the ratio defined in equation 18 is greater for equilibrium 1. Since all objects indexed by i in this ratio are taken to be exogenous and fixed (e.g., c_{ij}), this further implies that $\sigma_{1,ij}^{T-1} > \sigma_{2,ij}^{T-1}$ for all i. In turn equation 17 defining vacant state transitions implies that v_j^T is higher under equilibrium 1 than in equilibrium 2. Since $p_j(\lambda_j^T, v_j^T)$ is decreasing in v_j^T, and since $\sum v_j^T = \bar{v}$ (i.e. the total number of taxis in the city is exogenous and fixed across equilibria), the following must hold:

$$\sum_k exp\left(p_k(\lambda_k^T, v_{1,k}^T) \cdot \sum_l \Pi_{kl}/\sigma_\varepsilon - c_{ik}\right) < \sum_k exp\left(p_k(\lambda_k^T, v_{2,k}^T) \cdot \sum_l \Pi_{kl}/\sigma_\varepsilon - c_{ik}\right).$$

However, since for all i, $\sum_k \sigma_{ik} = 1$ by construction, for some $l \neq j$ we have $\sigma_{1,il}^{T-1} < \sigma_{2,il}^{T-1}$. By the same logic as above, equation 18 then implies that $p_l(1) > p_l(2)$. Thus, it must be that

$$\sum_k exp\left(p_k(\lambda_k^T, v_{1,k}^T) \cdot \sum_l \Pi_{kl}/\sigma_\varepsilon - c_{ik}\right) > \sum_k exp\left(p_k(\lambda_k^T, v_{2,k}^T) \cdot \sum_l \Pi_{kl}/\sigma_\varepsilon - c_{ik}\right).$$

This implies a contradiction, so there cannot exist two equilibria to this system. This proves that policies $\sigma^{T-1}(\mathcal{S}^{T-1})$ and therefore also values $V(S^T)$ are unique.

To show that uniqueness of values and policies in period $t+1$ implies uniqueness in period t, I first show that two conditions hold.

Condition 1: Flow payoffs defined by equation 6 are bounded, continuous, and strictly concave with respect to probabilities over actions σ_i^t.

To show this, I first re-write the choice-specific value functions (8). For exposition it will be convenient to re-write current location i and choice-location k as arguments instead of subscripts.

$$W^t(i,k,\mathcal{S}) = p(k,\mathcal{S}) \cdot \bar{\pi} + (1 - p(k,\mathcal{S})) \cdot (-c(i,k)) + \epsilon(a,k) + \left(p(k,\mathcal{S}) \cdot V^{t+\tau(k,k')}(k',\mathcal{S}) + (1 - p(k,\mathcal{S})) \cdot \arg\max_{\ell \in A(k)} W^{t+\tau(k,\ell)}(k,\ell,\mathcal{S})\right), \quad (19)$$

Where $\bar{\pi}(k) = \sum_j M_{kj}^t \Pi_{kj}$. The above expression explicitly separates period payoff functions from continuation values. To demonstrate concavity of the former, denote period payoffs as follows:

$$F(i,k,\mathcal{S}) = p(k,\mathcal{S}) \cdot \bar{\pi}(k) + (1 - p(k,\mathcal{S})) \cdot (-c(i,k)) + \epsilon(a,k).$$

Concavity implies that for $\gamma \in (0,1)$ and $k, k' \in A(i)$, that

$$F(i, \gamma k + (1-\gamma)k', \mathcal{S}) > \gamma F(i,k,\mathcal{S}) + (1-\gamma)F(i,k',\mathcal{S}).$$

Since profits $\bar{\pi}(k) > 0$ and fuel costs $-c(i,j) < 0$, and since location choice k only indexes a discrete point of $\bar{\pi}, c(i,k)$, and $\epsilon(a,k)$, it is sufficient to show that $p(k,\mathcal{S})$ is concave. Let $v(k)$ be the k-th element of the state $\mathcal{S}$ and $\hat{\lambda}(k)$ an exogenous parameter for location k. Then

$$p(k,\mathcal{S}) = 1 - \exp\left(\frac{\hat{\lambda}(k)}{v(k)}\right).$$

Thus, concavity of $p(k,\mathcal{S})$ follows from the convexity of $-p(\cdot,\cdot)$ via the convexity of $\exp(\cdot)$.

Condition 2: Feasibility constraints $\Gamma(\mathcal{S})$ on vacant state transitions are nonempty, compact and convex.

$\Gamma(\mathcal{S}^t)$ represents the constraint set of possible actions to be taken by drivers. Constraints are defined to be the set of locations A(i) adjacent to drivers in location i. Non-emptiness follows from the adjacency of each location with itself. Compactness follows from the finite measure of agents choosing over a finite set of adjacent locations. To show that $\Gamma(\mathcal{S})$ is convex, let $s_1 \in \Gamma(\mathcal{S}_1)$ and $s_2 \in \Gamma(\mathcal{S}_2)$. s_j is a feasible allocation of vacant taxis starting from $\mathcal{S}_j$. Given that vacant taxis are non-atomic, it follows that for any $a > 0$, $a \cdot s_j \in \Gamma(a \cdot \mathcal{S}_j)$. Further, $(s_j + s_k) \in \Gamma(\mathcal{S}_j + \mathcal{S}_k)$ as one can label drivers belonging to either set and independently assign feasible allocations according to $\Gamma(\cdot)$. Therefore it follows that $(a \cdot s_j + (1-a) \cdot s_k) \in \Gamma(a \cdot \mathcal{S}_j + (1-a) \cdot \mathcal{S}_k)$.

Together these conditions imply that the value functions defined by equation 6 are strictly concave (c.f., Theorem 4.8 in Stokey and Lucas (1989)), and therefore since best response functions defined by equation 9 are single-valued, there is a unique solution to the driver's problem in period $t-1$. We may now implement backwards induction (c.f., Rust (2016)): substitute the recovered $V_i^T(S^T)$ into the set of equations defining optimal policies at T-2 and repeat the above exercise to recover unique $V_i^{T-1}(S^{T-1})$ and iterate until period 1, in which S^1 is exogenous and known to drivers.[45] □

[45] More general results relating to equilibrium existence and uniqueness in large-scale games with a continuum of agents may be found in Acemoglu and Jensen (2015) and Light and Weintraub (2021).

A.8 Computational Details

A.8.1 Taxi Equilibrium Algorithm

The algorithm that I implement takes as inputs all model primitives, parameters, and an initial state. It returns the equilibrium state and policy functions for each location and each time period. Equilibrium states constitute a $L \times T$ matrix (i.e., how many taxis are in each location in each period), and equilibrium policy functions constitute a $L \times L \times T$ matrix (i.e., the probability of vacant taxi transition from any location $i \in \{1, ..., L\}$ to any location $j \in \{1, ..., L\}$ in each period). The algorithm uses backwards iteration to solve for continuation values and forward iteration to generate transition paths. Each component repeats, updating the state and policy vectors in each iteration. The process terminates when all policies and continuation values converge to a fixed point. The algorithm is described below.

Algorithm 1 Taxi Equilibrium Algorithm

Input empirical matches $\{\tilde{m}_{ij}^t\}$ and $\tilde{\mathbf{m}} = \{\sum_j \tilde{m}_{ij}^t\}$
Fix parameter value σ_ε.
Set counter $k = 0$
Input initial and future states guess $\mathcal{S}_0^t$ for $t = 1, ..., T$.
repeat
  for $t = T$ to 1 **do** ▷ Backwards Iteration
    Compute $V_i^t(\mathcal{S}_k^t | \tilde{\mathbf{m}}^\mathbf{t})$ for all i
  end for
  for $t = 1$ to $T - 1$ **do** ▷ Fwd. Iteration to T for each step back
    Derive choice-specific value functions $W_i^t(j, \mathcal{S}^t)$ for all t, i, j per equation 8
    Find policy fcts. $\sigma_k^t(W_k^{t+1})$ per equation 7
    Given $\mathcal{S}_k^t$ compute transition to $\mathcal{S}_k^{t+1}$ per equations 16 and 17.
  end for
  Update next period state $S_{k+1}^{t+1} \leftarrow \tilde{\mathcal{S}}^{t+1}$
  Update next period continuation values as $V^{t+1}(\mathcal{S}_{k+1}^{t+1}, \tilde{\mathbf{m}}^t)$
  $k \leftarrow k + 1$
until $|V_k^t - V_{k-1}^t| \leq \epsilon \quad \forall t$

The Taxi Equilibrium Algorithm begins with an initial guess of the state vector $\boldsymbol{\mathcal{S}}_0 = \{\mathcal{S}^t\}$ for all t. With $\boldsymbol{\mathcal{S}}_0$ as well as observations of the empirical distributions of taxi-passenger matches, $\tilde{\mathbf{m}}$, I can compute value functions $V_i^t(\mathcal{S}_0; \tilde{\mathbf{m}})$ for each i and t via backwards induction, beginning at period T.[46]Next, using the value functions, I compute choice-specific value functions and optimal

[46]Note this process requires integrating over future period states and shocks. State transitions are deterministic and thus the first integral is trivial. To integrate over driver-specific shocks $\varepsilon_{j,a}$ I rely on the fact that for discrete-choice logit models there is a closed form expression for the conditional expectation of unobservables given by $E[\varepsilon|j, \mathcal{S}] = \gamma_0 - \sum_j \log(\sigma_i(j|\mathcal{S}) \cdot \sigma_i(j|\mathcal{S}))$ where γ_0 is Euler's constant. See e.g., Arcidiacono and Ellickson (2011).

policies as in equation 9. Next, I use the computed policy functions and, starting at time $t = 1$ at $\mathcal{S}_0^1$, I forward simulate the optimal transition paths and update the initial state for $t = 2, ..., T$, resulting in a new guess of the state, $\mathcal{S}_1$. With $\mathcal{S}_1$, I again combine the same observations $\tilde{\mathbf{m}}$ to update value functions $V_i^t(\mathcal{S}_1; \tilde{\mathbf{m}})$. This process repeats until value and policy functions converge.

A.8.2 Initial conditions

Recall that $\mathcal{S}_0^t$ is a state vector of the number of vacant taxis in each location at time t. The initial guess of the state in each period, $\mathcal{S}_0^t$, is assigned by allocating the exogenous total number of taxis according to the empirical distribution of matches. As the algorithm runs, each vector $\mathcal{S}_0^t$ for $t \geq 2$ is updated as $t-1$ transitions are computed given the $t-1$ initial state and value functions for $t, t+1, ..., T$. Only one term, $\mathcal{S}_0^1$ remains exogenously chosen.

To mitigate any issues related to this remaining first-period exogenous initial state, I define $t = 1$ as 6:00am. In this period, the assumption that all available cabs are actively searching or with customers is less credible.[47] Nevertheless, by starting the equilibrium algorithm at 6:00am, a wide range of initial conditions quickly wash out within the first hour. This is verified by setting alternative initial conditions and comparing equilibrium levels of taxi supply across locations. As results are reported starting at 7:00am, the spatial distribution of taxis reaches an equilibrium mostly unaffected by the initial state assumption. Table A5 shows the impact of more extreme initial condition assumptions on the equilibrium supply of taxis under increasingly heterogeneous starting points. The baseline case, as described above, is compared with (1) a uniform initial distribution and (2) a distribution in which all initial vacant cabs are distributed at *edge* locations: those locations adjacent to the boundaries of the map.[48] The latter *edge* distribution is meant to simulate the case in which taxis start the day by driving from garages where they are stored. The locations of these garages are not available in my data, so this condition serves as a check on any misspecification due to unobserved initial conditions, where all taxis are stored in outer boroughs. In both cases, the equilibrium supply of taxis is very close to the baseline, with average percentage differences across all i, t pairs no worse than 2.1% and average level differences no worse than 4.2 vacant taxis.

[47] Recall that the data do not allow for distinguishing whether fewer matches in the morning are due to low supply or demand; and thus it is impossible to say how many cabs are actually on the road at any point.

[48] Boundary locations are all peripheral locations with adjacent access to the outer boroughs and New Jersey. This includes all locations in Manhattan with bridges and those bordering 125th street, all Brooklyn and Queens locations, and each Airport.

Table A5: Alternative Initial Conditions

Initial Condition	$\triangle v_i^t$ (mean)	$\%\triangle v_i^t$ (mean)
Baseline	0.0	0.0
Uniform	4.228	0.020
Edge	-3.839	-0.021

This table shows the change in taxis' spatial equilibrium distribution given changes in initial conditions. *Baseline* is the initial condition used throughout the paper, as described above. *Uniform* imposes an initial distribution that is uniform across all locations at 6am. *Edge* imposes an initial distribution that uniformly puts all vacant taxis across edge locations: all peripheral locations with adjacent access to the outer boroughs and New Jersey.

A.9 Estimation Details

A.9.1 Details on Estimating σ_ε

I estimate σ_ε for each of August 2012 and September 2012. These are obtained numerically through the use of a nonlinear program solver. In order to demonstrate how this estimate relates to the underlying moments, I conducted a grid-search analogue in order to evaluate the impact of this parameter on the GMM criterion function. Figure A4 displays the criterion value for the August σ_ε parameter and shows that this function is relatively well-behaved despite some visible noise due to simulation error.

The grid in this figure displays objective function values for σ_ε in the range of 1.2 to 4, in increments of 0.01. For values of σ_ε below this range, driver behavior becomes increasingly dictated by the observable profit function compared with any unobservables. This creates problems with convergence in the underlying value function iteration needed to solve for equilibrium by introducing more rigid cycling in each iteration. Fortunately, the criterion function is well-behaved enough that an estimate of σ_ε can be obtained.

A.9.2 Details on Estimating α_r

The variance of matches The matching function given in 3 describes the number of average number of matches produced in an area with v_i^t taxis and demand parameter λ_i^t. Estimating α will require computing the variance in matches produced by the daily draws u_i^t from each i,t-specific Poisson distribution. To compute this, I first determine the day-specific matching function $m_i^d(u_i^t, v_i^t)$ that would give rise to the equation 3. This function is given by

$$m(u_i^t, v_i^t; \alpha_r) = v_i^t \left(1 - \left(1 - \frac{1}{\alpha_r v_i^t}\right)^{u_i^t}\right). \tag{20}$$

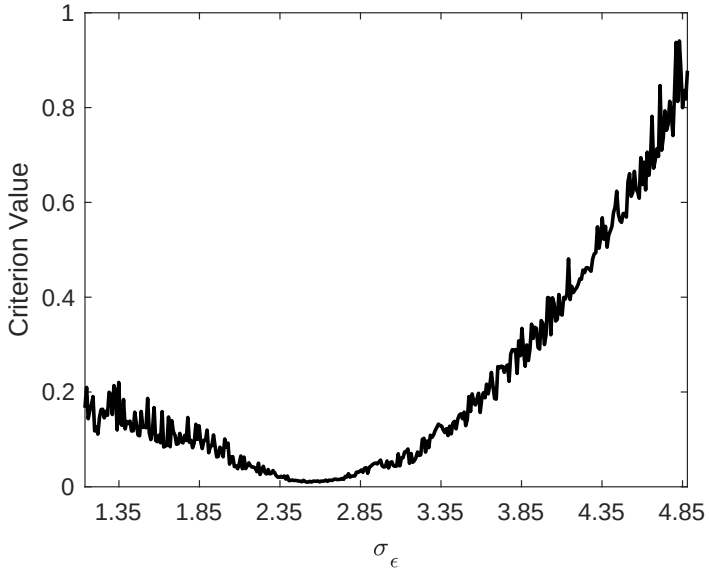

Figure A4: Criterion Values for σ_ε

Let $\rho = \left(1 - \frac{1}{\alpha_r v_i^t}\right)$. From here we can integrate equation 20 over the distribution of u_i^t.

$$\begin{aligned}
E[m_i|v_i^t, \lambda_i^t] &= v_i^t \sum_{k=0}^{\infty} \left(1 - \left(1 - \frac{1}{\alpha_r v_i^t}\right)^k\right) f_{\lambda_i^t}(k) \\
&= v_i^t - v_i^t \sum_{k=0}^{\infty} \rho^k f_{\lambda_i^t}(k) \\
&= v_i^t - v_i^t \sum_{k=0}^{\infty} \frac{\rho^k (\lambda_i^t)^k e^{-\lambda_i^t}}{k!} \\
&= v_i^t - v_i^t \frac{e^{-\lambda_i^t}}{e^{-\rho\lambda_i^t}} \sum_{k=0}^{\infty} \frac{(\rho\lambda_i^t)^k e^{-\rho\lambda_i^t}}{k!} \\
&= v_i^t - v_i^t \cdot e^{-\lambda_i^t(1-\rho)} \\
&= v_i^t (1 - e^{-\frac{\lambda_i^t}{\alpha_r v_i^t}}).
\end{aligned}$$

The second to last equation follows as integrating the probability mass function of the Poisson distribution over its entire support is equal to one. I now repeat the exercise to compute the variance of matches implied by the stochastic process governing $\{u_i^t\}$ as $E[m_i^2|v_i^t, \lambda_i^t] - E[m_i|v_i^t, \lambda_i^t]^2$. First,

following directly from equation 20, we have

$$\begin{aligned} E[m_i|v_i^t,\lambda_i^t]^2 &= (v_i^t)^2(1-e^{-\frac{\lambda_i^t}{\alpha_r v_i^t}})^2 \\ &= (v_i^t)^2(1-2e^{-\frac{\lambda_i^t}{\alpha_r v_i^t}}+e^{-\frac{2\lambda_i^t}{\alpha_r v_i^t}}), \end{aligned}$$

and second,

$$\begin{aligned} E[m_i^2|v_i^t,\lambda_i^t] &= v^2\sum_{k=0}^{\infty}\left(1-\left(1-\frac{1}{\alpha_r v_i^t}\right)^k\right)^2 f_{\lambda_i^t}(k) \\ &= v^2\sum_{k=0}^{\infty}\left(1-\rho^k\right)^2 f_{\lambda_i^t}(k) \\ &= v^2\sum_{k=0}^{\infty}\left(1-2\rho^k+\rho^{2k}\right) f_{\lambda_i^t}(k) \\ &= v^2\left(1-2\sum_{k=0}^{\infty}\rho^k f_{\lambda_i^t}+\sum_{k=0}^{\infty}\rho^{2k} f_{\lambda_i^t}(k)\right) \\ &= v^2\left(1-2e^{-\frac{\lambda_i^t}{\alpha_r v_i^t}}+\frac{e^{-\lambda_i^t}}{e^{-\rho^2\lambda_i^t}}\sum_{k=0}^{\infty}\frac{(\rho^2\lambda_i^t)^k e^{-\rho^2\lambda_i^t}}{k!}\right) \\ &= v^2\left(1-2e^{-\frac{\lambda_i^t}{\alpha_r v_i^t}}+e^{-\lambda_i^t(1-\rho^2)}\right) \\ &= v^2\left(1-2e^{-\frac{\lambda_i^t}{\alpha_r v_i^t}}+e^{-2\frac{\lambda}{\alpha v}+\frac{\lambda}{\alpha^2 v^2}}\right). \end{aligned}$$

Putting these terms together gives,

$$\begin{aligned} Var[m_i|v_i^t,\lambda_i^t] &= E[m_i^2|v_i^t,\lambda_i^t]-E[m_i|v_i^t,\lambda_i^t]^2 && (21) \\ &= \left(v_i^t\right)^2\left(e^{-2\frac{\lambda_i^t}{\alpha_r v_i^t}+\frac{\lambda_i^t}{\alpha_r^2 v_i^2}}-e^{-2\frac{\lambda_i^t}{\alpha_r v_i^t}}\right) && (22) \\ &= \left(v_i^t\right)^2 e^{-2\frac{\lambda_{it}}{\alpha_r}\frac{1}{v_{it}}}\left(e^{\frac{\lambda_{it}}{\alpha_r^2}\frac{1}{v_{it}^{*2}}}-1\right). && (23) \end{aligned}$$

Accounting for the variance of v_i^t Equation 21 is derived under Assumption 3 that the variance of v_i^t in each region r is zero. To motivate this assumption, Table A6 compares the outcome of

two simulation exercises. First is a simulation over one month of the market, in which demand is drawn in each i, t from the corresponding λ_i^t parameters. This process generates some variance in the distribution of taxis. From this simulation the variance of matches across days of the month are computed. Second, a second simulation is computed that is identical except imposes that the level of taxis is fixed at the equilibrium forecast generated by the model. In essence this shuts down the possibility that any variance in matches is attributable to variance in taxis. Finally, the table reports the theoretical variance in matches via equation 21. This comparison shows that the variances are for the most part not statistically distinguishable from one another.

Table A6: Simulated Variance Comparison

Description	**Region**			
	Lower Manhattan	*Midtown Manhattan*	*Uptown Manhattan*	*Brooklyn/Queens*
Simulated $Var(m_i^t)$	16.553	37.297	18.350	1.926
	(0.446)	(1.048)	(0.335)	(0.086)
Simulated $Var(m_i^t)$ (Fixed v_i^t)	15.2646	35.2556	17.8758	1.8484
	(0.375)	(0.753)	(0.324)	(0.089)
Theoretical $Var(m_i^t)$ (Fixed v_i^t)	14.801	34.378	17.869	1.939

95% C.I. in parentheses

This table shows the variance of matches in New York Regions I-IV, generated under two sets of simulations of one month of data each. 95% Confidence intervals are reported. Confidence intervals are based on standard deviations of variance estimates produced by replicating each simulation 150 times and computing standard errors for each variance measure.

The result that the variance of taxis has little apparent bearing on the variance of matches is not surprising, as taxis most often outnumber customers across the city. Even with some degree of search frictions, this discrepancy implies that variation in taxis will have less impact than variation in demand. Figure A5 Panel (a) shows the ratio of taxi shows simulated ratio of variation in taxis to demand across regions. Panel (b) shows the ratio of taxis in levels to that of demand across regions. While there are many reversals (see detailed estimates in Figure A7), the average ratio of taxis-to-customers across regions is between 3-10 throughout most of the day.

Together these results suggest that the variance of taxis can be regarded as negligible with respect to their impact on the overall variance of matches used to identify the efficiency parameters α_r.

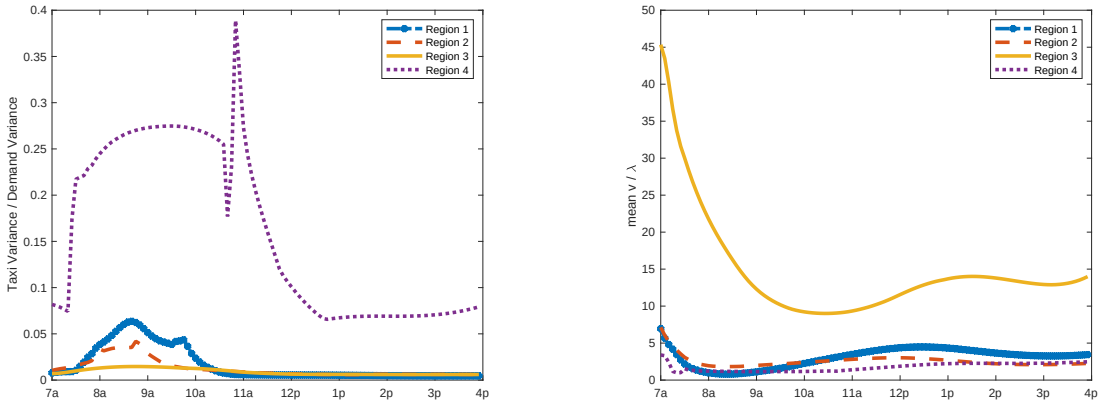

(a) Variance Ratios

(b) Level Ratios

Figure A5: Equilibrium Variance and Level Ratios of Supply and Demand

A.10 Detailed Estimation Results

A.10.1 Aggregate Supply and Demand by Time-of-day

Figure A6 shows aggregate supply and demand results, summing all 39 locations into the five regions corresponding to Figure 1. The results above demonstrate that the while taxi supply maintains some coverage across all locations throughout the day, there are intra-day trends in spatial availability and demand. Spatial mismatch is evident, as the relative proportions of supply and demand are not the same across each region.

A.10.2 Supply and Demand by Location

Figures A7 and A8 show detailed results of supply and demand in all locations. Note that location numbers 1-34 roughly track from South to North in Manhattan, locations 35-37 track South to North from Brooklyn to Queens, location 38 is LaGuardia airport and location 39 is JFK airport. We see that most locations have a surplus of taxis except for a few areas of very high demand. Lower Manhattan, parts of Midtown Manhattan and far North-east Manhattan all demonstrate particularly large constraints in the ratio of vacant taxis to demand. All locations demonstrate some search frictions on both sides of the market, but we see here that the impact is felt more on the taxi side.

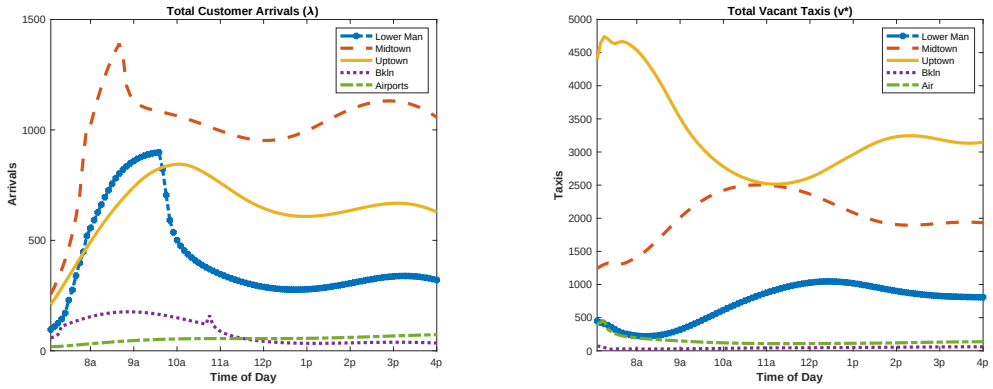

(a) Total Customer Arrivals (λ) (b) Total Vacant Taxis ($\mathcal{S}^*$)

Figure A6: Equilibrium Vacant Taxis: Weekdays 7a-4p, 9/2012 (Five Region Aggregates)

This figure depicts the equilibrium spatial distribution of taxis and mean arrival of customers across the Five Regions shown in Figure 1. Results across all 39 locations are summed to these five areas. Results are depicted for the weekday taxi drivers' day shift, from 7a-4p in September 2012.

A.10.3 Transitions

Table A7 shows the five-region average per-period transition matrix of vacant taxis in Panel (a) and of all taxis, vacant and employed, in Panel (b). Comparing these two transitions shows how the spatial distribution of taxi supply is driven by customer destination preferences versus taxis' search behavior. For example vacant taxis are much less likely to leave from their current location than an average taxi, vacant or not. The movement of vacant taxis also mirrors that shown in Table A3, Panel (b), which depicts the transitions from drop-off location to next pickup location. The fact that Table A7 shows slightly more dispersion (i.e. more weight on the off-diagonal elements) is natural: it reflects that the average time from drop-off to the next pickup is longer than a period (12 minutes 39 seconds, or about 2.5 periods).

A.10.4 Value Functions

Figure A9 shows the evolution of value functions by time of day. Each series is the value for a single location. The high correlation between each value function reflects the equilibrium result that drivers' policy functions ensure that there is no spatial arbitrage possible. The remaining differences between each location's value is due to the transportation cost that prevents perfect cross-location arbitrage. As the day reaches its 4pm end, the value of search in each location systematically drops to zero.

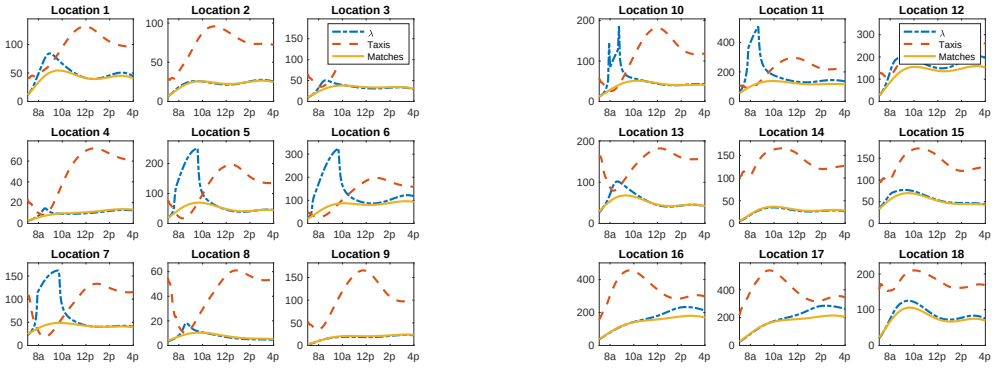

Figure A7: Detailed Estimates of v_i^t and λ_i^t (1)

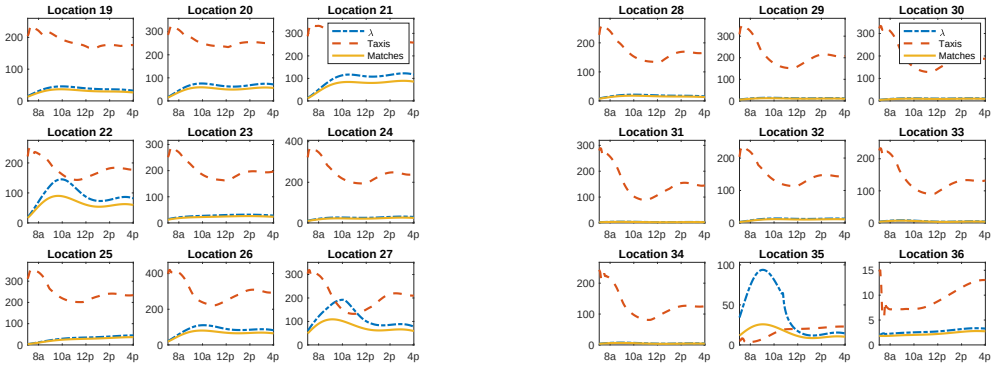

Figure A8: Detailed Estimates of v_i^t and λ_i^t (2)

Table A7: Equilibrium Capacity Flows

		Destination				
		Region I	*Region II*	*Region III*	*Region IV*	*Region V*
Origin	*Region I*	0.707	0.137	0.000	0.454	0.088
	Region II	0.274	0.607	0.086	0.000	0.171
	Region III	0.000	0.248	0.901	0.000	0.363
	Region IV	0.011	0.000	0.000	0.361	0.072
	Region V	0.009	0.008	0.013	0.186	0.307

(a) Vacant Taxis

		Destination				
		Region I	*Region II*	*Region III*	*Region IV*	*Region V*
Origin	*Region I*	0.514	0.133	0.011	0.286	0.070
	Region II	0.391	0.603	0.142	0.139	0.145
	Region III	0.054	0.239	0.832	0.083	0.342
	Region IV	0.023	0.006	0.002	0.414	0.083
	Region V	0.018	0.019	0.013	0.078	0.361

(b) All Taxis

Data in the table are aggregated across day-shift hours and regions as described in Figure 1. Panel (a) depicts the transition density of vacant taxis in each period and Panel (b) depicts the transition of vacant taxis between each drop-off and the same driver's subsequent pickup.

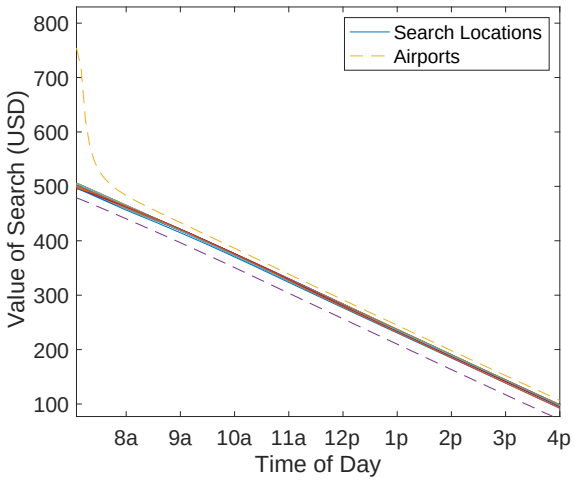

Figure A9: Equilibrium Value Functions

This figure depicts the equilibrium value functions for all 39 locations, by time of day, estimated from August 2012 data. Each line depicts a separate location. The highest-valued function is that of LGA airport and the least-valued function is that of JFK airport. All other locations' values fall in-between. Values do not include any medallion leasing fees.

A.10.5 Model Fit

The primary moments used in this study are the spatial and inter-temporal patterns of taxi-passenger matches. Here I describe and analyze the model fit.

Since taxis' dynamic spatial equilibrium is computed by the inversion procedure described in Section 4.2, this part of the model fits the taxi-passenger matches data perfectly by construction. In other words, given estimated parameters, the model would generate a set of equilibrium matches across periods and location that perfectly line up with the data.

For the model to generate counterfactuals and welfare estimates, I rely on the estimation of demand elasticities. The ability of the model to fit data thus rests on the fit associated with the demand model as well as the subsequent computation of equilibrium. Figure A10 shows the predicted and actual spatial heterogeneity of demand and matches respectively. Each comparison involves an aggregation over 164,268 (39 x 39 x 108) predictions of λ_i^t at observed prices. Demand fits quite well across time and space. Lower Manhattan demand is under-predicted in the morning while Uptown demand is over-predicted, but the ordering across regions and broad time trajectories lines up well.

Computing equilibrium matches requires demand predictions as inputs. The model uses all demand estimates to compute equilibrium supply in each location and time, which leads to 4,212

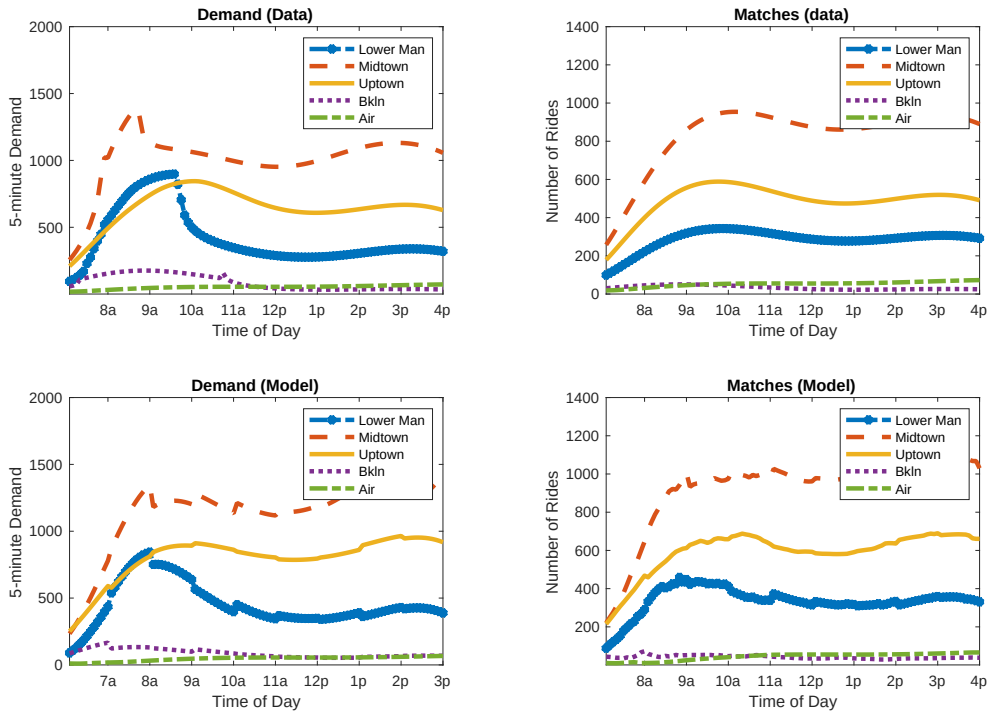

(a) Fit of Demand Model (b) Fit of Equilibrium Matches

Figure A10: Model Fit by Aggregate Regions and Time

This figure demonstrates model fit across demand and matches. The left panel shows the fit of the demand model. The right panel shows the fit of the equilibrium model to the total number of matches. Each series displayed aggregates origin-destination-specific series into five origin-based regions as shown on Figure 1.

(38 x 108) predictions on matches. Since taxi supply is increasing in demand for any location and time, any bias in demand will be exacerbated in computing matches for two reasons. First, demand is most often the short side of the market, so that an additional unit of demand leads to almost one additional match. Second, in equilibrium taxi drivers' search in a location increases with demand in that location, which implies that matches will increase with demand from both a direct and indirect effect. Nevertheless, the model is able to fairly-well reproduce a complex system of spatial and inter-temporal patterns of matches.

A.10.6 Impact of the Aggregate Supply Assumption

Estimation results are ultimately premised on the assumption that 11,500 taxis are in operation over the day. While the true number of taxis in operation in any period is unobserved, I derive this number based on an analysis presented in Section A.5. However, per Figure A3 the number may be lower in the morning hours, particularly before 10am. To investigate the relevance of this assumption I re-compute measures of equilibrium frictions under the assumption that only 9,000 taxis are in operation. Under this 21% drop in taxi supply, total demand through the day is estimated to be 4.85% lower, per-period unserved trips are 20.5% lower and per-period vacant taxis are 25% lower. While 9,000 is clearly very low compared to observable taxi activity after about 8am, it nevertheless suggests that friction results will scale roughly with the number of vacant taxis assumed to be in the market. In addition, Section A.11.3 computes all policy experiments below from a more limited time frame of 10am-4pm and finds very similar results.

A.11 Details on Counterfactual Results

A.11.1 Welfare Calculation

Consumer welfare is computed by integrating under the the estimated CES demand curves in each origin, destination, time pair (i.e., each i, j, t). The integral can be computed analytically as follows:

$$W_{ijt}(m_{ij}^t, \hat{\lambda}_{ij}^t, \pi_{ij}^t, \boldsymbol{\beta}) = \underbrace{\frac{m_{ij}^t(\hat{\lambda}_{ij}^t, v_i^t(\hat{\boldsymbol{\lambda}}))}{\hat{\lambda}_{ij}^t(\pi_{ij}^t)}}_{\text{frac. successful matches}} \cdot \underbrace{\left(\frac{\beta_{1,s,\iota}}{\beta_{1,s,\iota}+1} \cdot e^{-\frac{\beta_{0,i,t,s,\iota}}{\beta_{1,s,\iota}}} \cdot \hat{\lambda}_{ijt}(\pi_{ij}^t)^{\beta_{1,s,\iota}^{-1}+1} - \hat{\lambda}_{ijt}(\pi_{ij}^t) \cdot \pi_{ij}^t \right)}_{\text{total available surplus at price } \pi_{ij}^t}, \quad (24)$$

where $\beta_{0,i,t,s,\iota}$ and $\beta_{1,s,\iota}$ are the estimated demand parameters, $\hat{\lambda}_{ijt}$ is the predicted level of demand given price π_{ij}^t, and $v_i^t(\hat{\boldsymbol{\lambda}})$ is the equilibrium mass of taxis in each location (a function of the distribution of demand across locations and time). In counterfactuals I incorporate waiting time elasticities into this calculation. To do this I augment equation 1 as follows:

$$ln(\lambda_{ij}^t(\pi_{ij}^t)) = \beta_{0,i,t,s,\iota} + \beta_{1,s,\iota} ln(\pi_{ij}^t) + \beta_{2,i,t} \Delta w_{i,j,t} + \eta_{i,t,s,\iota}, \quad (25)$$

where $\Delta w_{i,j,t}$, is the percentage change in the consumer waiting time measure between the baseline case and the counterfactual waiting time evaluated as if there were no waiting time elasticity. To create the variable $\Delta w_{i,j,t}$ I first predict demand and compute equilibrium once with no waiting time elasticity, then I generate the predicted change in waiting times, and then I re-compute

demand with the calibrated waiting time elasticity $\beta_{2,i,t} = -1$ and again re-compute equilibrium. After the second round is complete, I evaluate welfare. This is a computationally intensive process, so I do not conduct additional iterations. However, after many trials adding one additional iteration the differences in outcomes seem to be very small.

Finally taxi profits are computed as follows:

$$W_{ijt}^{\text{taxi}}(m_{ij}^t, \hat{\lambda}_{ij}^t, \pi_{ij}^t, c_{ij}) = \underbrace{\frac{m_{ij}^t(\hat{\lambda}_{ij}^t, v_i^t(\hat{\boldsymbol{\lambda}}))}{\hat{\lambda}_{ij}^t(\pi_{ij}^t)}}_{\text{frac. successful matches}} \underbrace{\left(\hat{\lambda}_{ijt}(\pi_{ij}^t) \cdot \left(\pi_{ij}^t - c_{ij}\right)\right)}_{\text{trip revenues at price } \pi_{ij}^t}, \tag{26}$$

where c_{ij} is the fuel cost for a trip from i to j.

A.11.2 Spatial Impact of Counterfactuals

Figure A12 maps the per-period average impact of each welfare-optimized price counterfactual across space. While matches improve everywhere, they particularly improve in centralized, high-density locations. Welfare falls in some regions as lower prices induce new marginal consumers into the market with lower trip valuations. By virtue of random matching, some of these marginal consumers receive trips over the infra-marginal, higher-valuation consumers.

Figure A13 maps the per-period average impact of each benchmark technology counterfactual across space. In contrast to Figure A12 it shows that welfare improves more uniformly when technologies enable better matching to high valuation consumers.

A.11.3 Robustness to Omitting the Early Morning

Figures A2 and A3 suggest that, despite a consistent daily participation rate of drivers, many fewer matches occur in the period between 7a-9a. One concern is that the total supply of vacant taxis is unobservably low during this early period, as only the time of the first passenger match is observed and not the drivers' actual start times. By assuming supply to be fixed at 11,500 through the day, the model may attribute low match rates in the morning to low demand instead of low supply. Table A8 demonstrates that counterfactual results are robust to omitting the first two hours of the day. It shows that optimal pricing patterns are very similar to those discussed in Section 6 and displayed in Table 10; all optimized pricing policies lower average prices, increase matches by around 20-30% and increase utilization rates by about 7-10%.

A.11.4 Robustness to Alternative Waiting Time Elasticities

On the basis of empirical evidence from recent work, I calibrate a waiting time elasticity equal to -1.0. In this section I re-compute the main counterfactual results under different calibrated elasticity

Table A8: Efficient Pricing and Matching Technology: Counterfactual Results

Price Type	**Efficiency-optimized Multipliers**				**Total Surplus**	**Consumer Surplus**	**Consumer Rent Share**	**Matches**	**Taxi Utilization**
	θ_1	θ_2	θ_3	θ_4	(,000 USD)	(,000 USD)	(percent)	(,000)	(percent)
Baseline - 8/2012	1.00	1.00	1.00	1.00	5661.6	2425.3	42.8	176.3	45.3
Location-Based Pricing									
Max Total Surplus	0.84	0.94	0.82	1.24	4255.1 (+3.8 %)	1935.6 (+8.9 %)	45.5	198.0 (+12.3 %)	49.9
Max Cons. Surplus	0.84	0.94	0.82	1.24	4255.1 (+3.8 %)	1935.6 (+8.9 %)	45.5	198.0 (+12.3 %)	49.9
Max Matches	0.89	0.95	0.75	1.20	4238.9 (+3.5 %)	1919.4 (+7.9 %)	45.3	200.9 (+14.0 %)	50.6
Time-Based Pricing									
Max Total Surplus	.	0.94	0.89	0.94	4243.0 (+3.6 %)	1923.4 (+8.2 %)	45.3	189.2 (+7.3 %)	48.1
Max Cons. Surplus	.	0.94	0.89	0.94	4243.0 (+3.6 %)	1923.4 (+8.2 %)	45.3	189.2 (+7.3 %)	48.1
Max Matches	.	0.81	0.89	0.97	4185.1 (+2.1 %)	1865.7 (+4.9 %)	44.6	194.7 (+10.4 %)	49.2
Non-Linear Pricing									
Max Total Surplus	0.99	0.98	-0.20	.	4249.4 (+3.6 %)	1928.3 (+8.4 %)	45.4	187.0 (+6.1 %)	49.0
Max Cons. Surplus	0.99	0.98	-0.20	.	4249.4 (+3.6 %)	1928.3 (+8.4 %)	45.4	187.0 (+6.1 %)	49.0
Max Matches	0.81	1.01	0.25	.	4178.8 (+1.9 %)	1857.5 (+4.4 %)	44.5	195.8 (+11.1 %)	47.4
Technology Improvement	(at baseline prices)								
Efficient Incentives	.	.	.	.	6686.0 (+18.1 %)	2850.8 (+17.5 %)	42.6	207.5 (+17.7 %)	51.7
Matching Technology	.	.	.	.	7423.7 (+31.1 %)	2949.0 (+21.6 %)	39.7	248.3 (+40.8 %)	62.7

This table shows, for each weekday period from 10a-4p, the estimated change in total welfare (profits plus consumer surplus), consumer surplus, the consumer surplus share of total surplus, total matches, and utilization rates across each counterfactual price policy. Each pricing policy shown is a rule that applies to four policy-specific multipliers on the baseline price p_{ijt} for every route, given by \$2.50 + \$2.00/mile. In location-based pricing, the multipliers $\theta_k(i)$ apply to p_{ijt} where $k(i) \in \{1, 2, 3, 4\}$ indexes the region of location i according to Figure 1. In time-based pricing, the multipliers $\theta_k(t)$ apply to p_{ijt} where $k(t) \in \{1, 2, 3, 4\}$ respectively indexes the time ranges of 7a-9a (omitted here by construction), 10a-11a, 12p-1p, 2p-4p. In non-linear pricing, the multipliers $\theta_k(i, j)$ apply to p_{ijt} where $k(i, j) \in \{1, 2, 3\}$ are coefficients which change existing tariffs according to $\theta_1 \cdot \textit{base fare} + \theta_2 \cdot \textit{fare per-mile} + \theta_3 \cdot \textit{fare per-mile}^2$. The final row depicts equilibrium outcomes under a simulated matching technology in which the matching function takes the form $m_i^t = \min(\lambda_i^t, v_i^t)$. This last counterfactual is computed at baseline prices.

values of -1.2 and -0.8. Tables A9 and A10 summarize the results. They imply that the qualitative findings are robust: from an efficiency perspective, overall prices in Manhattan are too high. More granularly, lower and upper Manhattan locations are optimally lower priced than Midtown and Brooklyn, the afternoon hours should be priced slightly lower than the morning hours, and some small convexity in the distance price is optimal. Changing the waiting time elasticity impacts how much price decrease is optimal. This result is intuitive; the less responsive consumers are to waiting relative to their price elasticity, the more they will tolerate higher waiting times in exchange for lower prices.

Table A9: Efficient Pricing and Matching Technology: Counterfactual Results

Price Type	Efficiency-optimized Multipliers				Total Surplus	Consumer Surplus	Consumer Rent Share	Matches	Taxi Utilization
	θ_1	θ_2	θ_3	θ_4	(,000 USD)	(,000 USD)	(percent)	(,000)	(percent)
Baseline - 8/2012	1.00	1.00	1.00	1.00	5726.2	2452.6	42.8	211.3	42.2
Location-Based Pricing									
Max Total Surplus	0.73	0.87	0.65	1.00	5967.9 (+5.0 %)	2718.0 (+11.0 %)	45.5	219.7 (+24.6 %)	54.9
Max Cons. Surplus	0.71	0.87	0.65	0.99	5966.6 (+5.0 %)	2728.4 (+11.4 %)	45.7	219.8 (+24.7 %)	54.9
Max Matches	0.82	0.83	0.65	0.65	5957.9 (+4.8 %)	2721.2 (+11.1 %)	45.7	221.4 (+25.6 %)	55.2
Time-Based Pricing									
Max Total Surplus	0.84	0.90	0.74	0.83	5893.3 (+3.7 %)	2656.9 (+8.5 %)	45.1	206.8 (+17.3 %)	52.4
Max Cons. Surplus	0.82	0.89	0.75	0.83	5893.3 (+3.7 %)	2657.0 (+8.5 %)	45.1	207.1 (+17.5 %)	52.4
Max Matches	0.85	0.77	0.78	0.87	5845.5 (+2.8 %)	2608.5 (+6.5 %)	44.6	209.6 (+18.9 %)	52.6
Non-Linear Pricing									
Max Total Surplus	0.86	1.04	-0.24	.	5950.3 (+4.6 %)	2673.1 (+9.1 %)	44.9	204.3 (+15.9 %)	53.1
Max Cons. Surplus	0.83	1.06	-0.25	.	5946.2 (+4.6 %)	2708.5 (+10.6 %)	45.5	207.4 (+17.6 %)	53.7
Max Matches	0.66	0.99	0.25	.	5788.6 (+1.8 %)	2551.0 (+4.1 %)	44.1	220.1 (+24.8 %)	51.9
Technology Improvement	(at baseline prices)								
Efficient Incentives	.	.	.	.	6551.8 (+15.7 %)	2791.2 (+15.1 %)	42.6	242.5 (+16.1 %)	51.6
Matching Technology	.	.	.	.	7580.3 (+32.4 %)	2883.2 (+17.6 %)	38.0	247.4 (+17.1 %)	62.7

This table replicates Table 10 except with a waiting time elasticity of demand set to -0.8.

Table A10: Efficient Pricing and Matching Technology: Counterfactual Results

Price Type	Efficiency-optimized Multipliers				Total Surplus	Consumer Surplus	Consumer Rent Share	Matches	Taxi Utilization
	θ_1	θ_2	θ_3	θ_4	(,000 USD)	(,000 USD)	(percent)	(,000)	(percent)
Baseline - 8/2012	1.00	1.00	1.00	1.00	5726.2	2452.6	42.8	211.3	42.2
Location-Based Pricing									
Max Total Surplus	0.91	0.89	0.86	1.25	5852.4 (+2.9 %)	2558.2 (+4.5 %)	43.7	192.7 (+9.3 %)	49.1
Max Cons. Surplus	0.90	0.86	0.86	1.25	5844.6 (+2.8 %)	2608.2 (+6.5 %)	44.6	192.4 (+9.1 %)	49.0
Max Matches	0.91	0.92	0.71	1.03	5748.0 (+1.1 %)	2511.7 (+2.6 %)	43.7	199.4 (+13.1 %)	50.5
Time-Based Pricing									
Max Total Surplus	0.79	0.97	0.89	0.86	5829.1 (+2.5 %)	2591.0 (+5.8 %)	44.4	190.3 (+8.0 %)	48.6
Max Cons. Surplus	0.82	0.96	0.89	0.86	5828.3 (+2.5 %)	2591.9 (+5.8 %)	44.5	190.3 (+8.0 %)	48.6
Max Matches	0.88	0.84	0.86	0.93	5786.1 (+1.8 %)	2549.3 (+4.1 %)	44.1	191.9 (+8.9 %)	48.9
Non-Linear Pricing									
Max Total Surplus	1.00	0.89	-0.28	.	5910.8 (+3.8 %)	2664.5 (+8.7 %)	45.1	187.9 (+6.5 %)	50.6
Max Cons. Surplus	1.00	0.88	-0.28	.	5910.8 (+3.8 %)	2669.3 (+8.9 %)	45.2	188.1 (+6.6 %)	50.6
Max Matches	0.69	1.23	0.25	.	5726.7 (+0.6 %)	2485.5 (+1.4 %)	43.4	198.9 (+12.7 %)	47.6
Technology Improvement	(at baseline prices)								
Efficient Incentives	.	.	.	.	6812.0 (+20.3 %)	2906.9 (+19.9 %)	42.7	251.9 (+20.6 %)	53.6
Matching Technology	.	.	.	.	7642.7 (+33.5 %)	2822.7 (+15.1 %)	36.9	254.6 (+20.5 %)	64.5

This table replicates Table 10 except with a waiting time elasticity of demand set to -1.2.

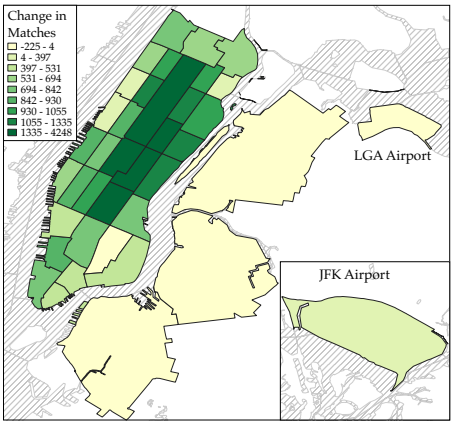

(a) Δ in Matches: Location Pricing

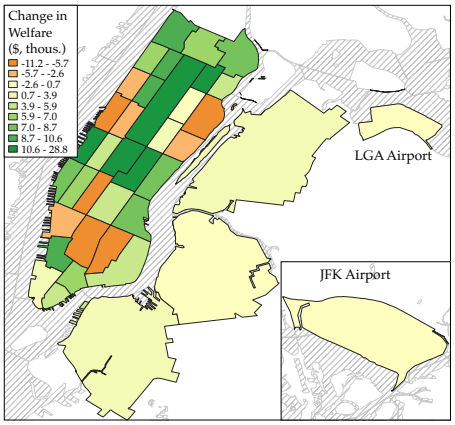

(b) Δ in Welfare: Location Pricing

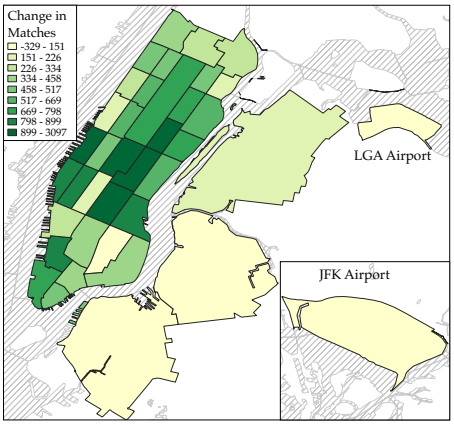

(c) Δ in Matching: Time Pricing

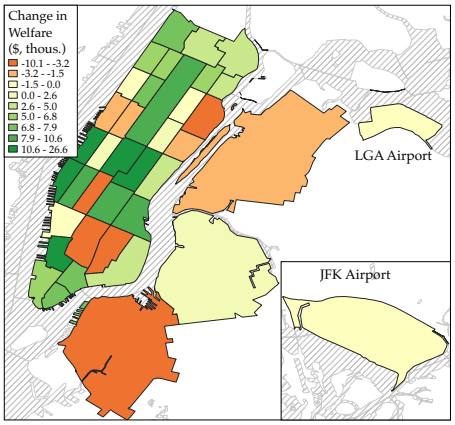

(d) Δ in Welfare: Time Pricing

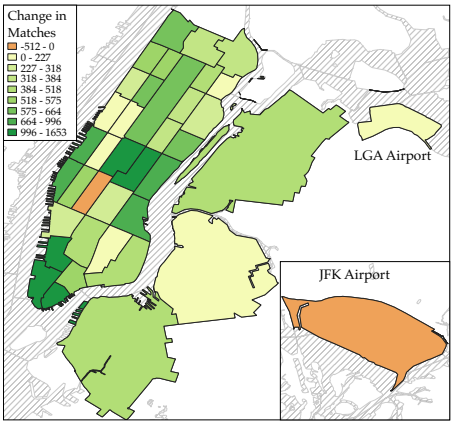

(e) Δ in Matching: Non-linear Tariffs

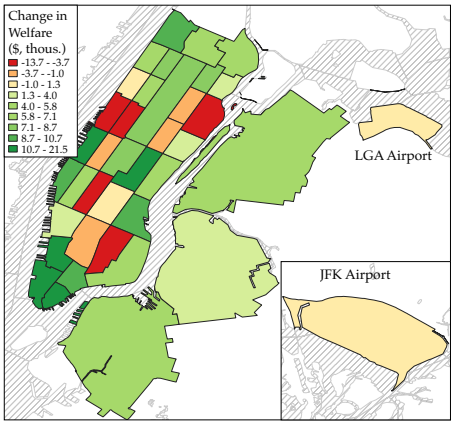

(f) Δ in Welfare: Non-linear Tariffs

Figure A11: Spatial Impact of Counterfactual Equilibria (con't.)

This figure shows the impact of each counterfactual on matches and welfare, averaged across the day-shift hours of a weekday, on each of the 39 locations. The left-hand side depicts the period-by-period average change in matches against the predicted baseline equilibrium of August 2012. The right-hand side depicts the changes in welfare.

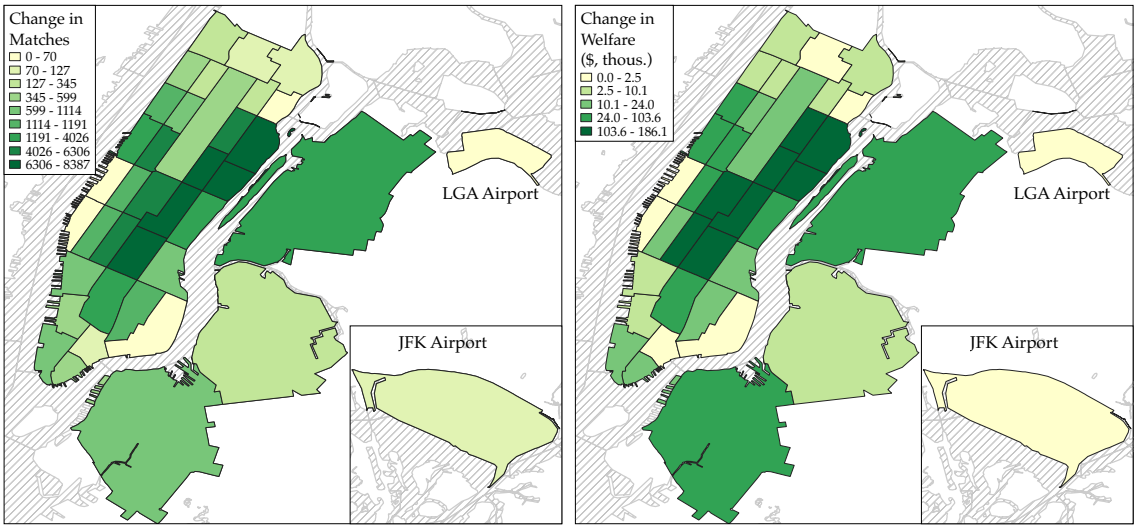

(a) Δ in Matches: Static Matching

(b) Δ in Welfare: Static Matching

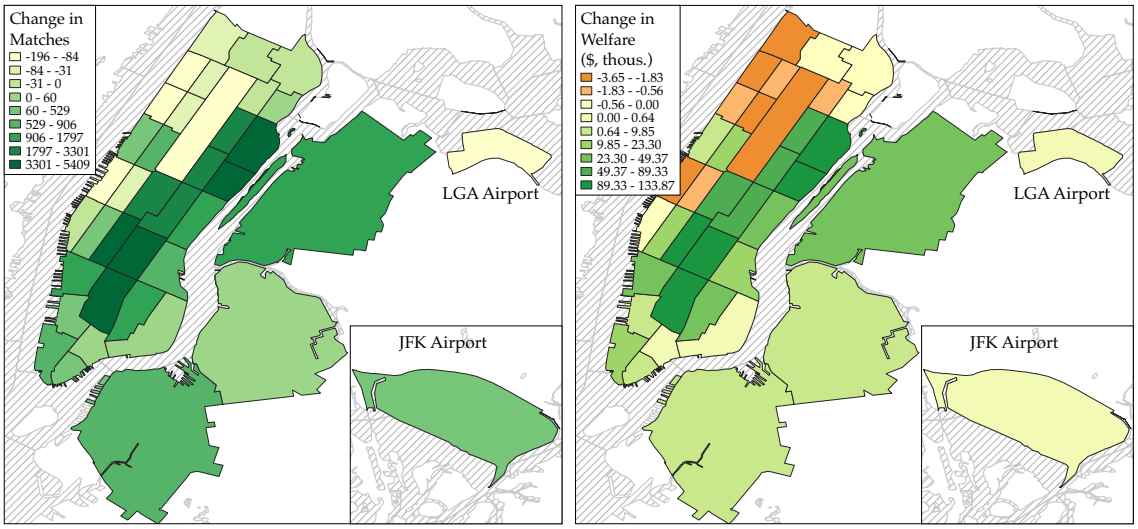

(c) Δ in Matching: Dynamic Incentives

(d) Δ in Welfare: Dynamic Incentives

Figure A12: Counterfactual Equilibrium Mapped

This figure shows the impact of each counterfactual on matches and welfare, averaged across the day-shift hours of a weekday, on each of the 39 locations. The left-hand side depicts the period-by-period average change in matches against the predicted baseline equilibrium of August 2012. The right-hand side depicts the changes in welfare.